ON THE PRACTICAL IMPLEMENTATION OF COMPRESSIVE SENSING TO ULTRAWIDEBAND CHANNELS

By

Mohammad Tamim Alkhodary

ID: 200806080

A Thesis Presented to the

DEANSHIP OF GRADUATE STUDIES

in Partial Fulfillment of the Requirements

for the degree of

MASTER OF SCIENCE

In

Telecommunication Engineering

KING FAHD UNIVERSITY OF PETROLEUM & MINERALS
Dhahran, Saudi Arabia

December, 2011

ON THE PRACTICAL IMPLEMENTATION OF COMPRESSIVE SENSING TO ULTRAWIDEBAND CHANNELS

BY

MOHAMMAD TAMIM ALKHODARY

A Thesis Presented to the
DEANSHIP OF GRADUATE STUDIES

KING FAHD UNIVERSITY OF PETROLEUM & MINERALS

DHAHRAN, SAUDI ARABIA

In Partial Fulfillment of the
Requirements for the Degree of

MASTER OF SCIENCE

In

TELECOMMUNICATION ENGINEERING

December 2011

KING FAHD UNIVERSITY OF PETROLEUM & MINERALS
DHAHRAN, SAUDI ARABIA
DEANSHIP OF GRADUATE STUDIES

This thesis, written by MOHAMMAD TAMIM ALKHODARY under the direction of his thesis advisor and approved by his thesis committee, has been presented to and accepted by the Dean of Graduate Studies, in partial fulfilment of the requirements for the degree of MASTER OF SCIENCE in TELECOMMUNICATION ENGINEERING.

Thesis Committee

Dr. Ali H. Muqaibel (Advisor)

Dr. Tareq Y. Al-Naffouri (Member)

Dr. Salam Adel Zummo (Member)

Dr. Ali Ahmed Al-Shaikhi
Department Chairman

Dr. Salam Adel Zummo
Dean of Graduate Studies

2/1/12

Date

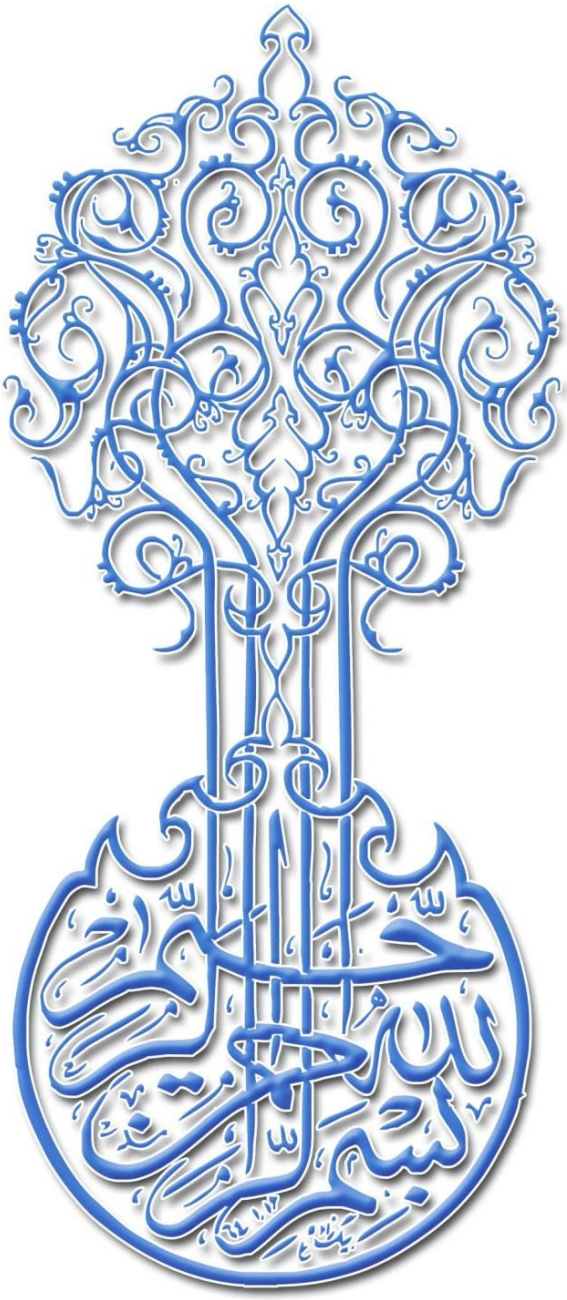
بسم الله الرحمن الرحيم

To my Beloved Mother, Ahlam Alitr

To my Beloved Father, Tamim Alkhodary

To my Sisters

ACKNOWLEDGMENTS

In the name of Allah, the Most Gracious, the Most Merciful

All praise is due to ALMIGHTY ALLAH; to whom belongs the dominion of Heaven and Earth. Peace and mercy be upon His Prophet who showed us the way of peace and real success in our lives and hereafter.

First and foremost, my thanks are due to ALMIGHTY ALLAH who blessed me with essential knowledge and patience to carry out this challenging work.

Secondly, I must acknowledge the continuous motivation and prayers of my beloved parents who have always been there to help me achieve major milestones in my life. I will never be able to reward in the slightest their endless support at every stage of my life. Dear Mother, I wish I could tell you how much you mean to me, but I can't find enough words to say how much I admire, appreciate, and feel thankful to you for everything you have done. Father you mean so numerous things to me: an understanding heart, a source of strength and support, a constant readiness to help in a kind thoughtful wise and patient way. A Father means so many things when he is a man like you.

I also acknowledge the love and the encouragement of my sisters and brothers who have helped me immensely in pursuing my studies despite being far away from them.

I would like to offer my indebtedness and sincere appreciation to my advisor Dr. Ali Muqaibel. No words of thanks would be sufficient for his guidance, advice and support.

During the course of research, he was always available and ready even on holidays, or at his break hours.

Special thanks are due to my thesis committee members, Dr. Tareq Y. Al-Naffouri and Dr. Salam Adel Zummo for all their cooperation and advice.

I would also express my deep gratitude to Dr. Maan Kousa, Dr. Amine Nehari, and Dr. Abdurrahman Al-Qussear, who generously supported me from the beginning of my study in KFUPM.

I am greatly indebted to my friends Mr. Hamid Alaidaruse, Mr. Ebrahim Al-Safadi, Dr.Yousef Elarian, and Mr. Sadiq Owodunni, for their valuable time spent to support me with many memorable moments. I extend my thanks and appreciation to all of my friends who helped me in one way or the other; I was indeed honored to know them.

I would like to acknowledge the support provided by the Deanship of Scientific Research (DSR) at King Fahd University of Petroleum & Minerals (KFUPM) for funding this work through project No. SB111007.

Finally, I wish to acknowledge King Fahd University of Petroleum and Minerals for providing the various facilities, support and resources utilized in the preparation of this thesis.

Mohammad Tamim Alkhodary

TABLE OF CONTENTS

LIST OF TABLES

LIST OF FIGURESP

THESIS ABSTRACT

NAME: Mohammad Tamim Alkhodary

TITLE OF STUDY: On the Practical Implementation of Compressive Sensing to Ultra Wideband Channels

MAJOR FIELD: Telecommunication Engineering

Date of Degree: December 2011

Compressive sensing (CS) was proposed by many researchers as a solution to the formidable sampling requirements of the promising Ultra wideband Technology (UWB). Previous research was evaluated by simulating the IEEE UWB channel model. This research studies the behavior of compressive sensing for practical UWB channels and proposes approaches to enhance its performance. Both measured data and directional models are used for evaluation.

Four practically-based dictionaries are proposed to enhance the sparsity of the UWB signals. Those dictionaries accounts for the practical effects of the channel like pulse dispersion and the unavoidable effects of antenna. It is shown that CS is able to reconstruct the UWB signals more efficiently with reasonable complexity.

In addition to waveform reconstruction, the proposed dictionaries are used for channel estimation. Two receivers are evaluated; single shot full profile-correlator and a Rake receiver. The Rake receiver employs CS in adjusting its parameters to take advantage of the energy available in the strongest propagation paths. The bit error rate performance of the CS based channel estimation for the different proposed dictionaries was evaluated as a function of signal to noise ratio. It is shown that CS based on the strongest atoms has an excellent performance at relatively low complexity.

مُلَخص الرسالة

الاسم: محمد تميم الخضري

عنوان الرسالة: التطبيق العملي لتقنية الاستشعار عن الضغط على القنوات فائقة عرض النطاق

التخصص: هندسة الاتصالات

تاريخ التخرج ديسيمبر ٢٠١١

تقنية الاستشعار عن الضغط (CS) أُقترحت من قبل العديد من الباحثين كحل مثالي لتردد التقطيع هائل السرعة في تكنولوجيا النطاق فائق العرض (UWB). تشير الأبحاث السابقة إلى فعالية هذا المقترح من خلال محاكاة معيار الهيئة العالمية لمهندسي الكهرباء والالكترونيات (IEEE).

يختص هذا البحث بدراسة سلوك تقنية الاستشعار عن الضغط لقنوات النطاق الفائق العرض (UWB) المستنتجة من الحياة العملية. وتقترح نهجا لرفع أدائها. وقد تم استخدام معيار اتجاهي للقناة، وبيانات مقاسة في البيئة العملية. يقترح هذا البحث أربعة مجالات عملية لزيادة تبعثر الإشارات الفائقة العرض. تلك المجالات تأخذ بعين الاعتبار الآثار الفيزيائية للقناة مثل تشتت الإشعاع والآثار التي لا يمكن تجنبها من الهوائي. وتبين أن تقنية استشعار الضغط قادرة على إعادة بناء الإشارات الفائقة العرض بأكثر كفاءة مع تعقيد مقبول.

بالإضافة إلى إعادة بناء الإشارة، تم استخدام المجالات المقترحة لتقدير القناة. وتم تقييم اثنين من المستقبلات؛ المستقبل ذو ربط العلاقة بين الإشارة المستقبلة وقالب معرّف مسبقا، ومستقبل ريك. مستقبل ريك يوظف تقنية استشعار الضغط في تعديل معاملاته للاستفادة من الطاقة المتاحة في أقوى مسارات الانتشار. تم تقييم تقدير القناة المبنية على تقنية استشعار الضغط بحساب نسبة الأخطاء في البيانات المرسلة لكل نسبة تشويش إلى طاقة الإشارة. كما أن المجالات المقترحة أُستخدمت في هذا التقييم. تبين أن المجال المبني من أقوى المراجع يتميز بأدائه الجيد مع تعقيد بسيط.

CHAPTER 1

1 INTRODUCTION

Ultra-wideband (UWB) radios are promised to be the next generation of the transmission system that can support high data rate and power-constrained applications such as wireless sensor and body area networks. Its unprecedented features will create a new era of communication systems to change the way people and intelligent machines communicate and interact with each other.

UWB radios operate over a wide range of frequencies, and with different signal characteristics. For example, automotive UWB radars are licensed to operate in the 24 GHz band; and the band for data communication application ranges from 3.1-10.6 GHz under power restrictions. The wide bandwidth is associated with low power transmission. Consequently, UWB appears below ambient noise level for other narrowband system [Woo08].

However, despite inherent advantages of UWB transmission, UWB receiver is hampered by relatively complex structures. Many challenges have been encountered in receiver design. Compressive sensing (CS) proposes a pleasing solution for many of these challenges.

Compressive sensing (CS), or Compressed sensing, in signal processing is the process of acquiring and reconstructing a signal that is supposed to be sparse or compressible. The reconstruction is done by a small number of samples in contrast to conventional way of sampling.

CS has been reliably implemented to the IEEE 802.15.4a model that has not considered the impact of pulse dispersion and pulse variation due to the physical effects of the practical UWB channels [Mol04]. Hence, any change in the pulse shape leads to degradation in the performance of CS within the practical environment. This thesis examines the performance of CS dealing with real practical measurements of UWB. Solutions to boost the performance in the practical environments are proposed.

1.1 Organization of the Thesis

Chapter 1 briefly describes UWB communication and the challenges associated with the receiver design, followed by an overview of the concept of CS and how CS addresses these challenges in an efficient way. A literature review and relevant research is provided.

Chapter 2, represents one application of CS to UWB signals, where we validate the ability of CS to reconstruct the UWB received signals based on IEEE 802.15.4a channel model proposed in [Mol04].

In Chapter 3, we look at this application from practical perspective and see how far the practical channel characteristics will affect the capability of CS to reconstruct UWB realistic signals. By designing a suitable dictionary, the performance of CS in practical channels will be improved; witch has been done in the same chapter.

The evaluation of the proposed methods will be addressed in Chapter 4 by employing CS to estimate the practical UWB channels and consequently to be used in the detection stage of CS-full profile-Correlator (CS-FP-Correlator) as well as in Rake receiver. Bit-Error-Rate (BER) versus Signal to Noise Ratio (SNR) will be the criterion of our evaluation.

Chapter 5 will be dedicated to the conclusion. The advantages, disadvantages and the drawbacks of this research will be addressed. Future work will be mentioned in the same chapter as well.

The appendix represents the table of abbreviation demonstrating all abbreviations mentioned in the thesis. Table of variable is also represented.

1.2 Technical Background

At the beginning of this section we are going to give a brief introduction about UWB that might help in understanding the terminologies in the rest of this work. Section 1.2.3 is about CS which is the second area of research involved to develop a novel of UWB receiver.

1.2.1 Ultra wideband Communications

UWB technology has emerged to be the vivid future of wireless communication, where it copes with many significant disadvantages of conventional wireless communication systems. UWB radio has unique attractive features, such as the extremely large signal bandwidth, which is in order of hundreds of Megahertz or even several Gigahertzes, besides this it has low power consumption and shared spectrum resources. UWB

applicability ranges from low-data-rate applications like sensor networks and high precision localization and navigation systems [Hir03], [Yan04].

UWB is a generic term that characterizes any transmission system which employs spectral bandwidth exceeding 500 MHz [Ree05], or a fractional bandwidth (B_f) greater than 0.20, where the fractional bandwidth is given by

$$B_f = 2\left(\frac{f_H - f_L}{f_H + f_L}\right), \tag{1-1}$$

As depicted in Figure 1-1, f_H and f_L are the upper and the lower cut-off frequencies of the $-10\ dB$ bandwidth. The center frequency is defined as $f_C := \frac{f_H + f_L}{2}$.

According to [Yan04], UWB systems with $f_c > 2.5\ GHz$ need to have a bandwidth of at least $500MHz$ at $-10\ dB$ power spectrum density, while, the systems having $f_C < 2.5\ GHz$ should have a fractional bandwidth of at least 20 %.

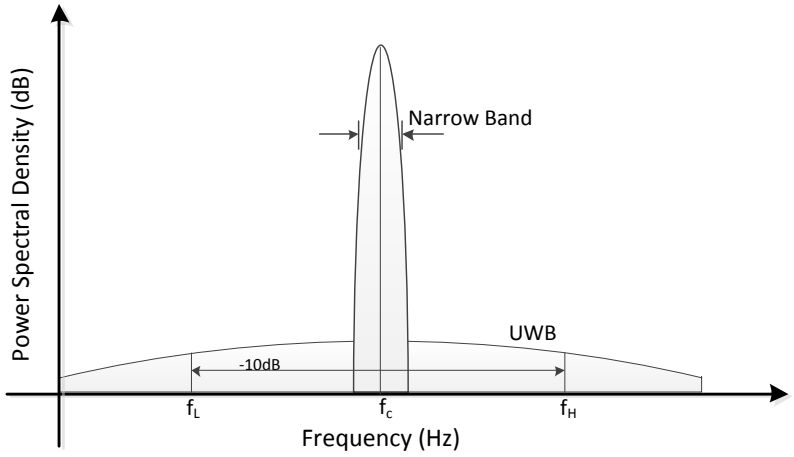

Figure 1-1 UWB spectrum vs. narrowband spectrum.

There are two prominent types of UWB signals: "Impulse Radio Ultra-Wideband" (IR-UWB) and "Multicarrier Ultra wideband" (MC-UWB) [Ree05]. The former is based on sending very short duration pulses, in order of Nanoseconds, to convey information. The

latter uses multiple simultaneous carriers to carry information. Each type has its relative technical pros and cons. The spectrum occupancy of IR-UWB is shown in Figure 1-2(a), while the spectrum occupancy of MC-UWB is shown in Figure 1-2 (b). This thesis is based on IR-UWB.

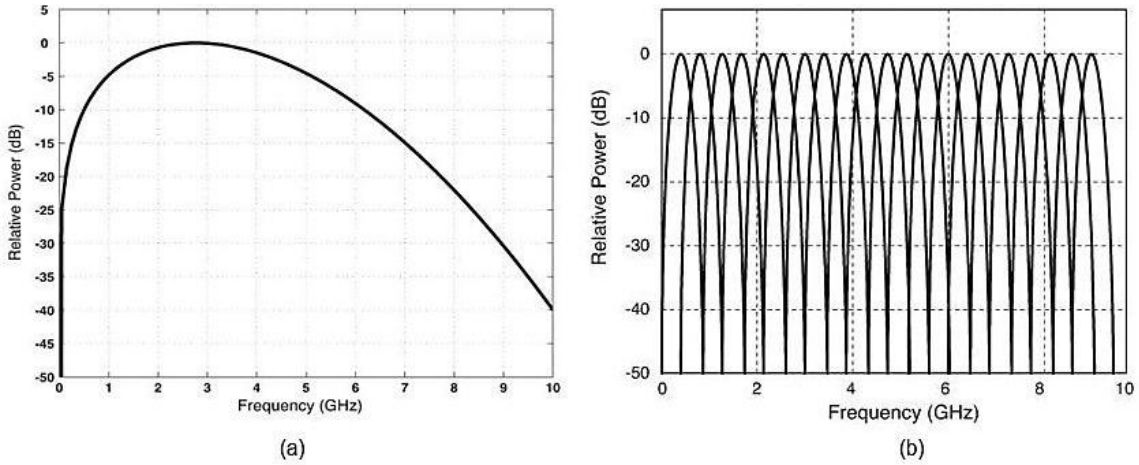

Figure 1-2 Spectrum occupancy of (a) IR-UWB and (b) MC-UWB [Ree05].

1.2.2 IR-UWB

IR-UWB with its huge advantages has been recognized as a great solution for future wireless personal networks. IR-UWB technique has the possibility of achieving Giga bits/s data rates, hundreds of meter operation range, Pico joule energy per bit, centimeter accuracy of positioning, and low cost implementation [Yan04]. It also offers great flexibility of spectrum usage and allows unlicensed usage of several gigahertz of spectrum.

Because of ultra-short pulses used in UWB, it is very robust against multipath, and more multipath components can be resolved at the receiver, resulting in higher performance. Due to the ultra-short duration pulses sub-centimeter ranging is possible, and it is very hard to spy on the UWB signal.

Unlike classical communications, in IR-UWB, no up and down radio frequency conversion is required; which reduces the implementation cost, and allows low power transmitter implementation.

The basic model for an unmodulated IR-UWB pulse train can be expressed as

$$s(t) = \sum_{i=-\infty}^{\infty} A_i(t)p(t - iT_f), \qquad (1\text{-}2)$$

where $A_i(t) = \pm\sqrt{E_p}$ is the amplitude of the pulse with energy of E_p, $p(t)$ is the normalized pulse waveform, and T_f is the frame time that is defined as the time interval in which one pulse is transmitted. In the remaining parts of thesis, UWB implies IR-UWB

1.2.2.1 Transmitted Pulse

The UWB pulse waveform can be any pulse that satisfies the spectral mask[1] regulatory requirements. The common pulse shapes discussed in IR-UWB literature are the Gaussian pulse and its derivatives [Ree05]. The reason for this name is referred to the similarity with Gaussian function that can be represented as

$$p(t) = \frac{1}{\sqrt{2\pi\sigma^2}} e^{\frac{(t-\mu)^2}{2\sigma^2}}, \qquad (1\text{-}3)$$

where, σ is the standard deviation of the Gaussian pulse in seconds, and μ is the delay in time for the midpoint of the Gaussian pulse in seconds. The pulse width is denoted by τ_p which is a function of the standard deviation given as $\tau_p = 2\pi\sigma$. The nominal center

[1] On February 14, 2002, the FCC issued a report, which classified UWB operation into three separate categories, and gave each category a particular frequency mask shape to restrict its frequency range [Ree05].

frequency and the spectrum bandwidth depend on the pulse width. The $-3dB$ bandwidth is approximately equal to 116 % of $\frac{1}{\tau_p}$ [Ree05], [Ben06]. Figure 1-3 depicts the first derivative of Gaussian pulse with duration of approximately 0.3 nsec, and -10 dB bandwidth of 9 GHz.

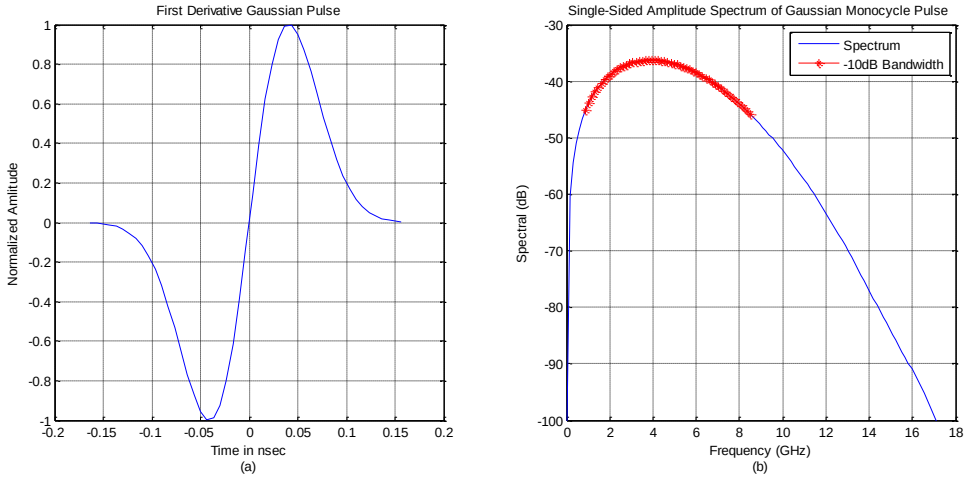

Figure 1-3 (a) First derivative of Gaussian pulse (b) frequency band representation of the pulse in (a).

1.2.2.2 IR-UWB Receiver Challenges

UWB receivers face several challenges including narrowband interference cancellation, antenna design, timing synchronization, and channel estimation, among others [Yan04]. The extremely high bandwidth of the received IR-UWB signal (up to 7.5GHz) requires high-speed analog-to-digital converters (ADC) [Par07]. For such speed the usage of ADC increases and likewise demands an accurate timing control system.

The conventional approach of sampling, however, consumes a lot of power, gives relatively low resolution, and can be expensive. Because it requires precise timing control system, the complexity of the circuitry increases. Moreover, oversampling of the received UWB signal maybe required, to improve the timing synchronization and channel estimation. For example, in [Lot02], the required sampling rate is in excess of 25GHz for

an accurate UWB channel estimation. Such huge sampling rates are not easily supported by the current ADC technology. Consequently, alternative approaches for UWB receivers are needed to attain the required sampling rates and the time resolution. Many of these challenges can be reduced or mitigated by means of compressive sensing and its features. Next, we will introduce CS, and summarize its application to UWB.

1.2.3 Compressive Sensing

Compressive sensing (CS), also known as compressive sampling, compressed sensing, and sparse sampling, is a theory targeting to find the sparsest solution for underdetermined linear system [Don06], [Can06], [Can08]. The concept of CS and its principle will be discussed briefly in this section.

Consider a discrete signal X of one dimensional, real-values, and finite-length which can be represented as a column vector of dimensions $N \times 1$ in $\mathbb{R}^N$. In addition, consider an $N \times N$ matrix Ψ consists of a basis vectors of dimensions $N \times 1$ as $\{\psi_n\}_{n=1}^{N}$, i.e. $\psi_n = [\psi'_1, \psi'_2, \dots, \psi'_N]$. Where any signal in $\mathbb{R}^N$ can be represented in terms of these vectors. Therefore, the signal X can be expressed as

$$X = \sum_{n=1}^{N} \theta_n \psi_n = \Psi\Theta \qquad (1\text{-}4)$$

the vector $\Theta = [\theta_1, \theta_2, \dots, \theta_N]^T$ is $N \times 1$ column vector consisting of the weighting coefficients of the signal X in the basis matrix Ψ. Accordingly, X is the representation of the signal in the time domain, while θ is the representation of the signal in Ψ domain.

Assume the signal X is a linear combination of only S basis vectors in Ψ; this means that only S elements of the coefficients vector Θ are non-zero, and the rest $N - S$ elements are zeros, therefore the signal is called S-sparse.

CS senses "measures" the signal by projecting what is called measurements matrix on the received signal, mathematically: taking the inner products between X and a collection of vectors $\{\varphi_m\}_{m=1}^{M}$ as in $y_m =< X, \varphi_m >$ to have measurements vector y of length $M \times 1$. To be more specific, the $M \times N$ measurements matrix Φ contains the measurement vectors φ_m^T as rows, and y can be expressed by projecting X on the matrix Φ as

$$y = \Phi X = \Phi\Psi\Theta = X\Theta \tag{1-5}$$

Note that $X = \Phi\Psi$ which is an $M \times N$ matrix.

In order to have reliable results out of CS algorithms, the basis matrix Ψ and the matrix Φ have to be incoherent, as proved by CS theories [Can06].

The original sparse coefficients can be exactly recovered from the measurement vector y by minimizing the ℓ_1-norm given in the following optimization problem

$$\hat{\theta} = \text{argmin}\|\theta'\|_1 \quad \text{such that} \quad X\theta' = y \tag{1-6}$$

where θ' is the $N \times 1$ vector that satisfies $X\theta' = y$, while, $\hat{\theta}$ is the recovered vector of S-sparse coefficients. In other words, among all consistent solutions of $\theta' = y$, we pick the solution whose coefficient has the minimal ℓ_1-norm.

1.2.3.1 Compressive Sensing Algorithms

The convex optimization problem in (1-6), based on minimizing ℓ_1 subject to linear equality constraints, can easily be reformed as a linear program with more efficient solution algorithms. The underlying result of CS asserts that when θ is sufficiently sparse; the recovery via ℓ_1-minimization is provably exact [Can08]. In fact, the use of the ℓ_1-norm as a sparsity-promoting function traces back several decades. However, ℓ_1-minimization is not the only way to recover sparse solutions; other methods, such as greedy algorithms, have also been proposed [Bar07].

Solving the optimization problem in (1-6) by means of ℓ_1-minimization which can be done by Basis Pursuit (BP) is computationally expensive [Che99] and is not suitable for the state-of-the-art of CS technology [Par07]. Faster and more efficient reconstruction algorithms are available, those use iterative greedy-based algorithms at the expense of slightly more measurements, the most popular of these algorithm are matching pursuit [Zha93], orthogonal matching pursuit (OMP) [Tro07] and tree-based matching pursuit (MP) [La05], among others.

BP employs linear programming and offers good performance but suffers from high computational complexity. MP provides a low-complexity alternative to BP but requires an unbounded number of iterations for convergence. OMP converges in a fixed number of iterations but requires the added complexity of the dictionary orthogonalization at each step. These algorithms for reconstruction are generic, in the sense that they do not exploit any structure (aside from sparsity) that may exist in the sensed signals [Che99], [Dua05].

In particular, MP algorithm is a computationally simple iterative greedy algorithm that tries to recover the signal by finding, in the measurement vector (y), the strongest component (ψ_n) which is defined as atom[1] in the sparsity dictionary [Che99]. This strongest component will be removed from the measurement vector, and the corresponding atom is copied to a new clean dictionary. Then, search again in the dictionary for the strongest atom that is left in the residual of the measurement vector. This procedure is iteratively repeated until the residual of y contains just insignificant information. Signal reconstruction is then accomplished by linearly combine the set of atoms of the clean dictionary (the atoms found in the sparsity dictionary) [Zha93], [Par07]. The flowchart in Figure 1-4 shows in detail the steps of MP algorithm, where the conditional diamond controls the iterations of the algorithm by two parameters, T_0 which determines the maximum number of iterations, and ϵ sets the minimum energy that is left in the residual signal.

[1] An atom can be considered as a basis element that composes signal.

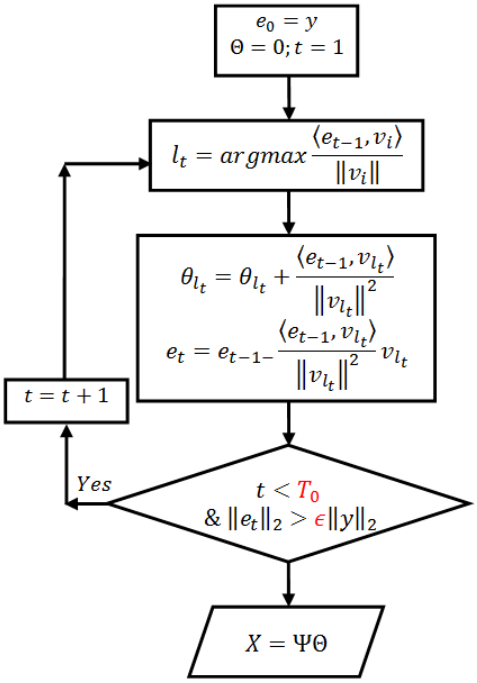

Figure 1-4 Matching Pursuit algorithm flowchart.

1.3 Literature Review for Application of CS to UWB

This section provides a literature review of the recent research in the area where CS has addressed the challenges of IR-UWB receiver. The published research has two main objectives. First objective is reducing the sampling rate which in turn reduces the use of ADCs resources. To achieve this objective, CS was applied to UWB signal reconstruction and channel estimation. The second objective is to mitigate the narrowband interference (NBI). Figure 1-5 classifies the research work related to implementation of CS to UWB. The main references are listed under each branch. The following subsections summarize the main contributions in each of the three main fields: signal reconstruction, channel estimation, and NBI mitigation.

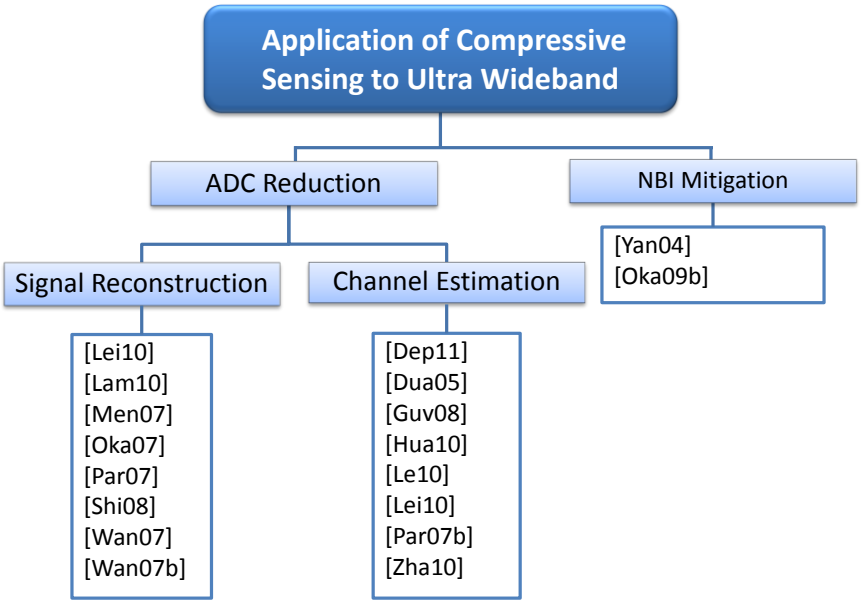

Figure 1-5 Summary of research activities in the area of CS application to UWB.

1.3.1 Signal Reconstruction

Recently, additional attention has been paid to reduce the complexity of UWB receiver design by means of CS. The modern developed framework of CS [Don06], [Can06] provides a computational efficient way to exploit the sparsity of the signal detection. Based on the phenomena that transmitting an ultra-short pulse through a multipath UWB channels results in a sparse received signal, CS is indeed applicable to detect and recover the received UWB signal [Par07], [Oka09] . This section shed some light on the literature that has been published on this subject.

Paredes et al. is one of the first researchers who investigated the ability of CS to reconstruct an IR-UWB signal. [Par07], [Wan07], [Wan07b], and [Men09] have shown that the received UWB signals can be reconstructed from a set of random projections, leading to a reduced sampling rate. In particular [Men09] implemented a low-speed ADC for 60 GHz UWB received signal. As a result the sampling rate has been reduced to 2.2%

with 0.3dB loss of BER performance with prior condition that the sparsity of UWB is less than 1%. Similarly, [Par07] proposed an approach which outperforms the traditional detector using just 30% of the ADC resources.

The prior assumption that the IR-UWB signal is sparse in time domain is not the only hypothesis. Paredes et al., in [Par07], proposes a novel dictionary (Ψ), as in (1-5), where the IR-UWB signal can be represented as a linear summation of its atoms. The resultant representation is sparser than in time domain. Since the received UWB signal is formed by scaled and delayed versions of the transmitted pulse, as shown in Figure 1-6, and since the dictionary of sparsity should contain elements (atoms) that can fully represent the underlying signal, the elementary function to generate the atoms of the dictionary should be closely related to the pulse waveform in IR-UWB system i.e. the Gaussian pulse or its derivatives, Figure 1-3 (a).

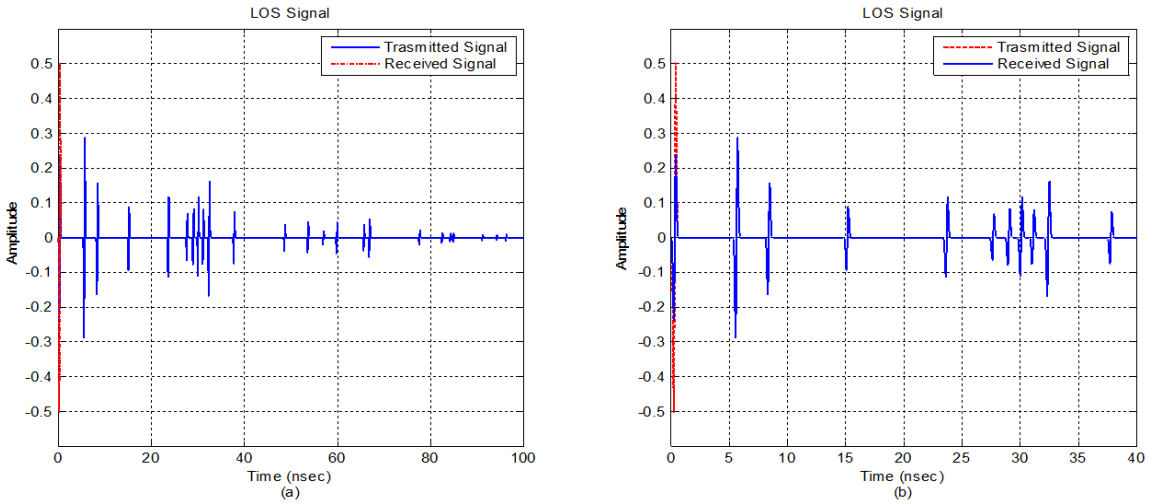

Figure 1-6 Transmitted and received of indoor LOS UWB signal (b) zoomed version of (a)

.

This approach increases the sparsity representation of the received IR-UWB signal, which in turn, boosts the recovery ability of CS, as well as reduces the number of iterations of MP algorithm, or the number of required measurements [Wan07b], [Par07b].

Guangming, in [Shi08], sampled and detected UWB echo signals which assumed to be sparse in a pre-construction matched dictionary. This study indicated that the low-dimensional random measurement method based on the CS theory can be used to sample UWB signal and the sampling rate can be greatly reduced. The linear frequency-modulated echo signals in radar system were processed using the UWB echo signal detection system. The study showed that the noise-free UWB echo signal can be exactly reconstructed and detected even it is sampled at about 10% of the Nyquist rate. For noisy signal, increasing the amount of samples still can guarantee overwhelming detection probability.

The Bayesian Compressive sensing was used in [Lei10] to reconstruct the IR-UWB signals generated by the IEEE 802.15.3a model. The signal assumed to be sparse in time domain. The reconstruction error was normalized by the signal energy.

Several recent publications have proposed a CS-based receiver structure to IR-UWB. The basic structure of CS-based IR-UWB systems receivers is illustrated in Figure 1-7. It consists of an analog front-end followed by a noise-limiting band-pass filter (BPF), then M-mixers and integrators and a digital signal processing (DSP) back-end. The set of basis waveforms $\{\psi_n\}_{n=1}^{N}$ represents the measurement ensemble. The main difference to the conventional receivers is the analog-filtering and DSP back-end, where the received signal is under-sampled, i.e. the ADC is performed at symbol rate f_{symbol} rather than

Nyquist rate $f_{Nyquist}$. The structure in Figure 1-7 has a modest number of ADC's in contrast with the conventional receiver. This feature makes CS highly attractive for detection part in IR-UWB receivers.

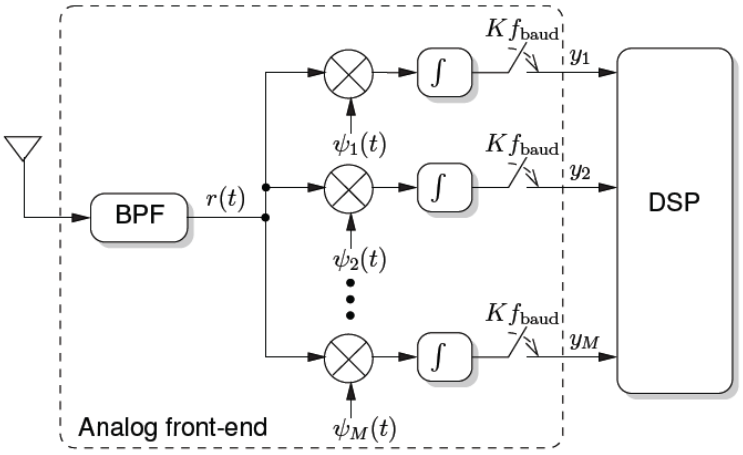

Figure 1-7 Illustration of CS-based receiver for IR-UWB [Lam10].

1.3.2 Channel Estimation and Receiver Design

The emerging theory of CS is not limited to the reconstruction of sparse signals from a small set of random measurements, but also provides a powerful way to estimate the UWB channels.

Two approaches have been developed by [Par07] for UWB channel estimation. In the first approach, CS capabilities are exploited to recover the full channel profile from a reduced set of random projections. This recovered profile is subsequently used as a template in a correlator-based detector [Par07b]. In the second approach, the pilot training signal is projected randomly and then the MP algorithm is used to identify the strongest atoms in the projected signal that, in turn, are related to the strongest propagation paths of UWB channel. Those strongest paths can be used as the fingers in the detection stage of Rake

receivers. The bit error rate performances of these two proposed approaches were analyzed and compared to that of full sampling rate correlator-based detector. The simulation results showed that for the LOS and NLOS propagation scenario of UWB indoor residential channels, the detectors based on CS channel estimation performs well compared with traditional correlator with the advantage of reducing the usage of ADC resources in the channel estimation stage.

Since IR-UWB has very narrow pulse, UWB channels will be rich of multipath diversity [Mol04]; subsequently the first arrival component is not necessarily corresponded to the strongest path. This leads to difficulty in estimating the time of arrival [Le10]. A precise detection is required to estimate the time of arrival, thus making the maximal likelihood techniques in [Guv08] impractical for coherent receivers, since they essentially need a prior information and extremely high sampling rate ADC. On the other hand, non-coherent UWB-systems reduce the complexity of the receiver by detecting the first arrival path via energy block and processing the signal with square-law device. Nevertheless, the performance still has low accuracy [Le10]. The proposed CS-based receiver in [Le10] increase the accuracy of time of arrival as well as reduces the number of ADC. This receiver is consisting of three main parts, as it is depicted in Figure 1-8.

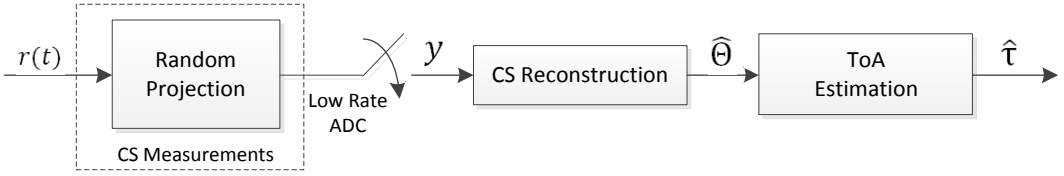

Figure 1-8 CS-based UWB receiver for time of arrival estimation.

At first block of the receiver, the projection is done in analogous domain, i.e. the received signal is projected on an analog signal. Followed by low rate ADCs and sample the resulted signal at sub-Nyquist rate.

The reconstruction part is implemented by orthogonal matching pursuit algorithm, which is a fast greedy algorithm used to reconstruct a sparse signal form the given random projected signal. The outcome of OMP is a vector contains the original path gain, combines with the delay factor which is determined by the indices of the vector.

The signal prior to the projection stage does not have to be sampled or a discrete-time signal, since the random projections can be easily performed in the analog domain by a bank of synchronized high speed analog mixers with pulse amplitude modulation (PAM) waveform random generators followed by low-rate ADC [Par07] besides plenty of ways of analog random projection [Dua05].

A similar approach of IR-UWB channel estimation is proposed in [Lei10], which employs Bayesian compressive sensing (BCS). The CS theory has been used to exploit the sparse of the impulse response of the channel. The method takes account of the prior knowledge that the impulse response is sparse in the time domain and provides estimation for the posterior density function of additive noise encounter when implementing the compressive measurement

Though it was aimed for positioning, the study in [Dep11] estimated the time different of arrival in which we can considered as a part of channel estimation. A Fast Orthogonal Matching Pursuit (FOMP) algorithm was proposed and embedded in the Time Difference of Arrival algorithm (TDOA) for fast object positioning. The FOMP was improved to

work with the TDOA algorithm can yield the peak location while the signal reconstruction procedure is ongoing.

In [Hua10] An FIR filter was adopted at the transmitter to get a measurement matrix to improve the reconstruction accuracy of CS. There was no need to add a measurement matrix element in the receiver, which magnifies the noise in the UWB channel. IEEE 802.15.4a was considered as UWB channel model, and then the first derivative of the Gaussian pulse was selected as the transmitted pulse waveform. The correlation detection was used to and channel estimation method we proposed is used in the of UWB signals. The estimation of the impulse response has been reconstructed via orthogonal matching pursuit algorithm.

Another UWB channel estimation approach is proposed in [Zha10] based on CS using the channel's sparsity in time domain. A random filter which is "all pass" in frequency domain and both real in time and frequency domain was utilized. Subsampling and basis pursuit reconstruction algorithm were used to estimate the channel. The research showed that the mean square error is near to the Carmer-Rao Bound at high signal to noise ratio.

1.3.3 Narrowband Interference Mitigation

IR-UWB shares the spectrum with coexisting legacy systems, thus, the interference is unavoidable. A strict power limitation is imposed by the desire to minimize the interference with these coexisting systems and among UWB communicators as well [Yan04]. Fortunately, the interference bandwidth is usually narrow in contrast with the IR-UWB bandwidth; therefore, CS has a great opportunity to suppress this interference.

Wang et al. in [Wan08] extend the CS-based receiver from [Wan07b] by an NBI subspace estimator. This estimator is based on the representation of the NBI signal in the discrete cosine transform domain. The random measurement ensemble $\{\psi_i(t)\}$ is then adjusted such that it projects the received signal into the null-space of NBI. Hence, adaptive analog is achieved to mitigate the NBI.

The receiver proposed by [Oka09] avoids tuning of analog notches by using a deterministic ensemble $\{\psi_i(t)\}$. It exploited the fact that the IR-UWB signal is sparse in time domain, and hence a frequency-domain measurement ensemble, $\{\psi_i(t)\}$, are sinusoids with frequencies uniformly spaced. The notable observation is that the NBI signal can be captured by small number of measurement functions $\{\psi_i(t)\}$, and thus NBI mitigation causes only modest performance degradation.

Out of the three reviewed topics that combine CS with UWB, this thesis concentrates on signal reconstruction and channel estimation. NBI is beyond the scope of our work.

1.4 Thesis Contribution

The advent of CS techniques opened new windows that promise new effective ways of sampling and signal reconstruction. This field of research has attracted researchers from diverse areas of communications and signal processing. UWB is one of those areas that have taken advantage of CS to reduce the complexity of receiver design, especially in the sphere of analog to digital converters.

Although there are few researches who have employed CS to reconstruct UWB signals, none of them have considered real-life practical UWB signals. Our work is concentrated

mainly on the behavior of CS in practical UWB channels under the effects of pulse dispersion and shape corruption.

The accuracy of reconstruction, by means of MP algorithm, is proportion with computation efforts depending on a couple of parameters of the MP algorithm. Based on the IEEE 802.15.4a model of the UWB channel we have examined and optimized the values of these parameters to keep the balance between the quality of reconstruction and the computation complexity.

Unlike the IEEE 802.15.4a model, which is made of delayed and scaled pulses, the realistic received UWB signals have various pulse shapes due to the physical effects of the realistic channel and the antennas radiation pattern. Since CS performance relies on the fact that the desirable signal has to be sparse in a certain domain "dictionary", we have implemented and evaluated the performance of Matching Pursuit algorithm in reconstructing practical profiles. The degradation in the performance is further mitigated using the following proposals:

- Design a dictionary based on the practical received signal at boresight (zero degree to transmitted antenna).
- Design a dictionary out of atoms of variable pulse width in order to compensate the pulse dispersion for the later arrivals.
- Design a directional dictionary from practical templates taken at different angles.
- Design a directional dictionary based on the atoms of the strongest contribution taken from the previous directional dictionary.

For evaluation of the above signal reconstruction in channel estimation and in a full estimation system, we have implemented the above CS based on directional dictionary in a full profile correlator receiver and in a Rake receiver (multi-correlator).

The flowchart in Figure 1-9 depicts the hierarchy of this work and show the area of our contribution.

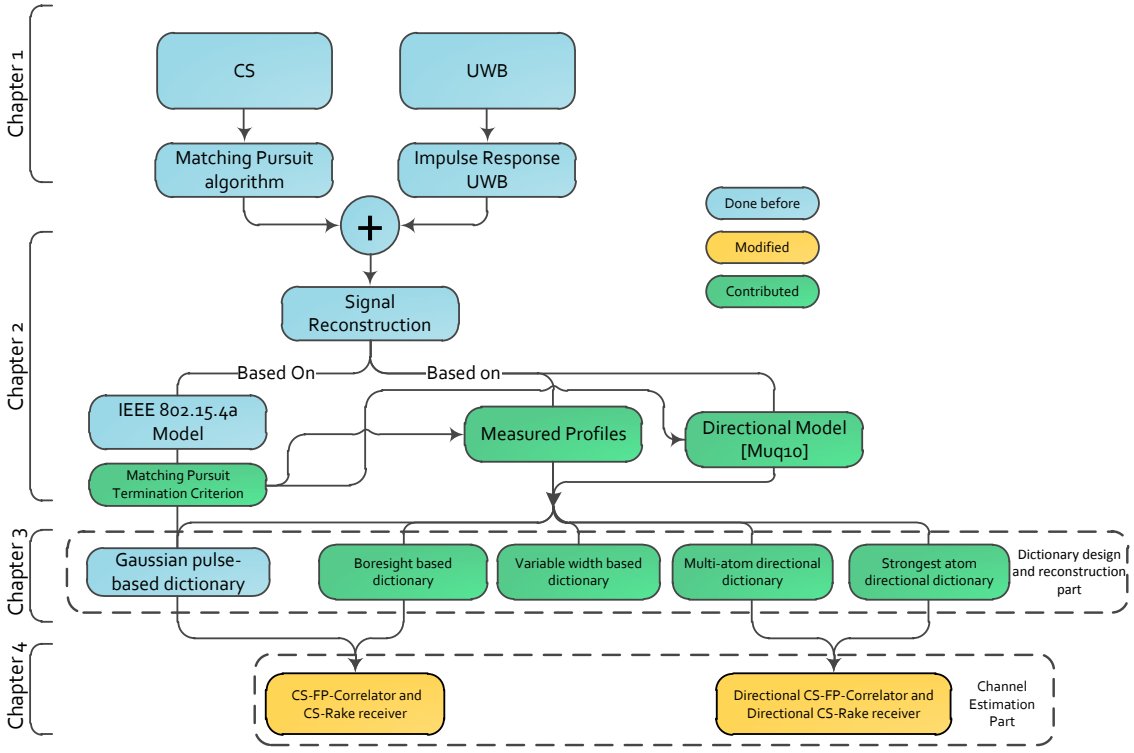

Figure 1-9 Thesis Contribution hierarchy

The contribution can be summarized as follows:

1) We have evaluated the performance of the Matching Pursuit algorithm in reconstruction of practical measured UWB signals and signals based on directional model (more practical model).

2) We have evaluated the impact of the increment of MP iteration on the reconstruction accuracy, and based on this evaluation we have selected the proper parameters for our case.
3) We have redesigned the sparse dictionary to account for the pulse dispersion and pulse shape change due to antenna dependence. The performance of the proposed dictionaries was evaluated.
4) The shape of the (reference template) is considered in the channel estimation stage of Rake-receiver and CS-FP-Correlator.
5) The performance of the proposed modified CS over a full UWB communications with channel estimation.

To the best of our knowledge all the published work on application of CS to UWB systems are based on the IEEE802.15.4a model which does not account for pulse dispersion or variation of pulse shape due to antenna dependency, or the thermal noise and narrowband interference that are always available in practical systems.

CHAPTER 2

2 CS SIGNAL RECONSTRUCTION FOR UWB IEEE 802.15.4A CHANNEL MODEL

Sampling rate is the bottleneck of IR-UWB receiver design; this chapter casts this problem into the emerging framework of CS. The chapter starts by describing the structure of IR-UWB signal that is based on IEEE 802.15.4a model. Then, we move to demonstrating the ability of CS to reconstruct the IR-UWB signal, by investigating sparsity in time domain.

A sparse dictionary is then built based on the transmitted pulse that helps CS techniques to reconstruct IR-UWB signal more accurately. Last part in this chapter adapts MP algorithm's parameters in order to be used in the rest of this thesis.

2.1 UWB Signal Structure and Channel Model

The IEEE 802.15.4a IR-UWB model proposed by the working group in [Mol04] is based on the Saleh-Valenzuela model where multipath components arrive in Poisson-distributed clusters [Sal87], [Mol04]. Furthermore, within each cluster, the path arrivals are also described by a Poisson process. Both cluster inter-arrival times and path inter-arrival

times, are exponentially distributed with model parameters that are experimentally determined.

Consider a simple baseband communication model, transmitting a pulse $p(t)$ through a noise-free UWB communication channel. The received UWB signal, $r_x(t)$ can be modeled as

$$r_x(t) = p(t) * h(t) = \sum_{k=0}^{K-1} \sum_{l=0}^{L-1} \alpha_{k,l} p\big(t - T_l - \tau_{k,l}\big), \tag{2-1}$$

where, $p(t)$ is the ultra-short pulse expressed in (1-3). $h(t)$ is the impulse response of the UWB, modeled as

$$h(t) = \sum_{k=0}^{K-1} \sum_{l=0}^{L-1} \alpha_{k,l} \delta\big(t - T_l - \tau_{k,l}\big), \tag{2-2}$$

where δ is the Dirac delta function, $\tau_{k,l}$ is the delay, and $\alpha_{k,l}$ is the gain associated with the l^{th} path within the k^{th} cluster of the IR-UWB channel. L is the number of propagation paths and K is the number of clusters. Extensive efforts have been devoted to the characterization of UWB channel [Par07], [Muq03].

Different communication environments are proposed by the Working Group: indoor residential, indoor office, industrial, outdoor, and farm environments; for different propagation scenarios: line-of-sight (LOS) and non-line-of-sight (NLOS). For outdoor environments, the operating range is greater than 10 m and up to few hundred meters.

For the reason of fair comparison, in the coming chapter, with the available practical UWB profiles, we restrict our simulation to indoor residential environment for both LOS and NLOS propagation scenarios.

2.2 Signal Reconstruction and the Impact of Sparsity Dictionary

The sparse dictionary plays a decisive influence on the accuracy of reconstruction; many natural signals have concise representations when expressed in a convenient basis. UWB signal can be consider as sparse in time domain, where the pulse duration is shorter than the propagation path, hence the reflections will arrive as completes pulse until the energy decays. As IEEE model suggested, one can take advantage of multipath diversity, and builds a dictionary based on shifted and scaled version of the transmitted signal.

In this section we examine the performance of CS in two domains; Time domain where no need to design any dictionary. The second domain is the multipath diversity domain.

2.2.1 Signal Reconstruction Based on Sparsity in time Domain

The time duration between pulses is specified by the statistics of the paths arrival given by the channel model. If the average inter-arrival time is greater than the pulse duration, the received UWB signal will have less overlapping between arrivals of different paths, thus more sparsity is anticipated. The sparsity of IR-UWB signal is a function of pulse duration and arrival time between different paths. For instance, in indoor LOS propagation scenario, inter-cluster arrival rate is estimated to be 0.047 path/nsec. [Mol04]. On the other hand, UWB channel is richer of multipath in case of NLOS propagation scenario, leading to more pulse overlapping and consequently less sparsity. This observation is clearly shown in Figure 2-1 where the Gaussian monocycle pulse $p(t)$

defined in (1-3) and plotted in Figure 1-3 (a) is transmitted through two different propagation scenarios within indoor environment

Figure 2-1(a) shows a received waveform for an indoor residential environment with LOS propagation, while Figure 2-1 (b) shows a waveform in the same communication environment but with NLOS propagation (CM2). We can clearly see that NOLS channel is denser, less sparse, and has more pulse-overlapping than LOS scenario.

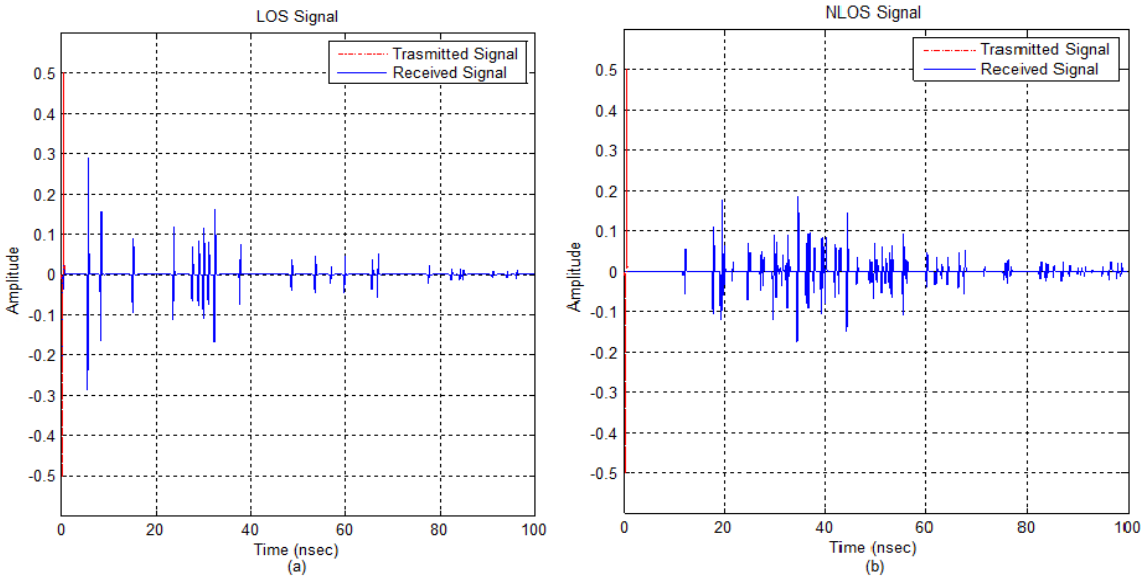

Figure 2-1 Noise free indoor signal with (a) LOS and (b) NLOS propagatoion scenarios.

In both LOS and NLOS cases, though to a different degree, transmitting an ultra-short pulse through a UWB communications channel leads to a received signal that has a relatively few nonzero values in comparison with the number of zero values. This phenomenon gives CS techniques the ability to exactly reconstruct the UWB signal.

If we consider r_x being a discrete time representation of UWB received signal expressed by

$$r_x = \left[r_x(0), r_x(t_s), \dots, r_x\left((N-1)t_s\right)\right]^T, \tag{2-3}$$

where t_s is the sampling period, N is the number of samples.

CS consists mainly of two stages: acquisition and reconstruction stage where CS algorithm is executed as depicted in Figure 2-2. The measurements (samples) are taken from the targeted signal during the acquisition stage[3], the resultant signal y has much less rate and can be processed and stored more conveniently. Whenever needed the CS algorithm in the second stage can reconstruct the full rate signal. To be able to take the measurements we have to define the measurement matrix Φ that has dimensions of $M \times N$. The elements of Φ have to be random and incoherent with the dictionary Ψ . The measurement matrix has i.i.d items generated by Gaussian distributed random variable with zero mean and unit variance i.e.$\Phi \sim N(0,1)$. [Don06], [Bar07].

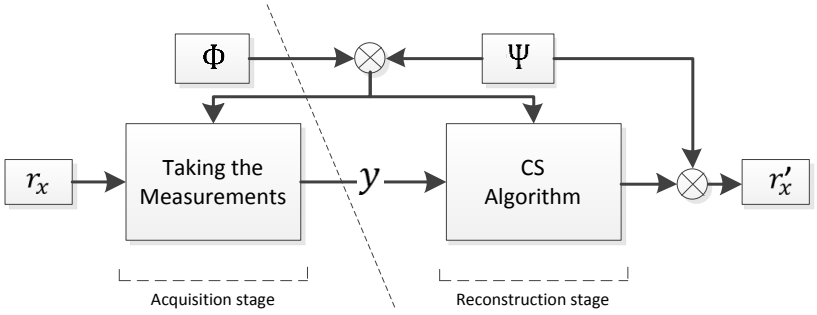

Figure 2-2 CS Stages.

In this section, we are trying to reconstruct the IR-UWB signal, r_x, by assuming that it is sparse in the temporal domain as we have mentioned earlier, thus the sparsity dictionary Ψ will be the identity matrix. The measurement vector $\boldsymbol{y}$ can be represented as $y = \Phi r_x$. Figure 2-3 illustrates the process of taking measurements. The randomness of the measurement matrix is demonstrated by the choice of the colors of the matrix entries.

[3] In some references called projection stage, where the required signal is projected on random basis.

The sparsity of the targeted signal is demonstrated by the fact that many entries equal to zero which is reflected by the white color squares.

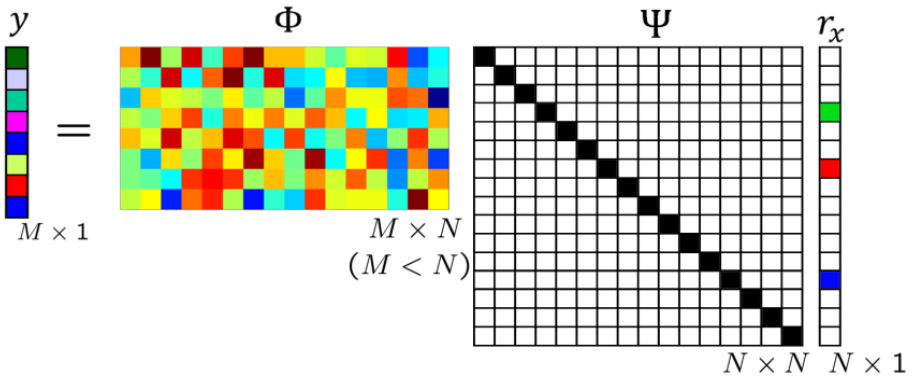

Figure 2-3 Illustration of the random projection process in time domain.

After taking the random projection, MP algorithm is now ready to take place. Let us call $V = \Phi\Psi$ the "holographic dictionary" to be passed with the measurement vector y to MP algorithm, illustrated in Figure 1-4. Executing the algorithm yields the results shown in Figure 2-4.

To illustrate the similarity between the original signal r_x and the reconstructed one r_x', two criteria of error measurement are represented. The mean square error (MSE) given by $E[|r_x - r_x'|^2]$ where E indicates the expected value. The second criterion is the normalized error given by $\frac{\|r_x - r_x'\|_2}{\|r_x\|_2}$ to demonstrate the variation of error from the energy of the original signal.

Figure 2-4 (a) depicts the received IR-UWB signal, r_x, for an indoor residential channel realization with LOS propagation scenario based on the model in (2-2). This signal consists of 5000 points within 100 ns, i.e. the sampling rate is 50 GHz, targeted for reconstruction from a reduced set of random projections. To illustrate how the number of random measurements affects the precision of reconstruction, Figure 2-4 (a) is the original

signal to be reconstructed, while Figure 2-4 (b) depicts the reconstructed signal acquired from 1000 random measurements, i.e. the sampling frequency has been reduced 80 percent to be 10 GHz. A notable observation is that CS recovered the most significant values of the IR-UWB signal, but it failed to recover many of weak arrival paths. In additional, there are several spurious components introduced in the reconstructed signal leading to a an error normalized by signal energy equals to 0.2906 and mean square error (MSE) of 2.5×10^{-4}. The error increases as the number of measurement decreases. Figure 2-4 (c) depicts a reconstructed signal observed by sampling rate of 5 GHz. In this case the normalized error is 0.719 and the MSE is 15×10^{-4}. The worst case appeared in Figure 2-4 (d) when the signal is reconstructed using 2.5 GHz corresponding to 250 random measurements. At this sampling frequency the MSE becomes 34×10^{-4} and the normalized error increases to 1.07, meaning that the error exceeds the signal energy.

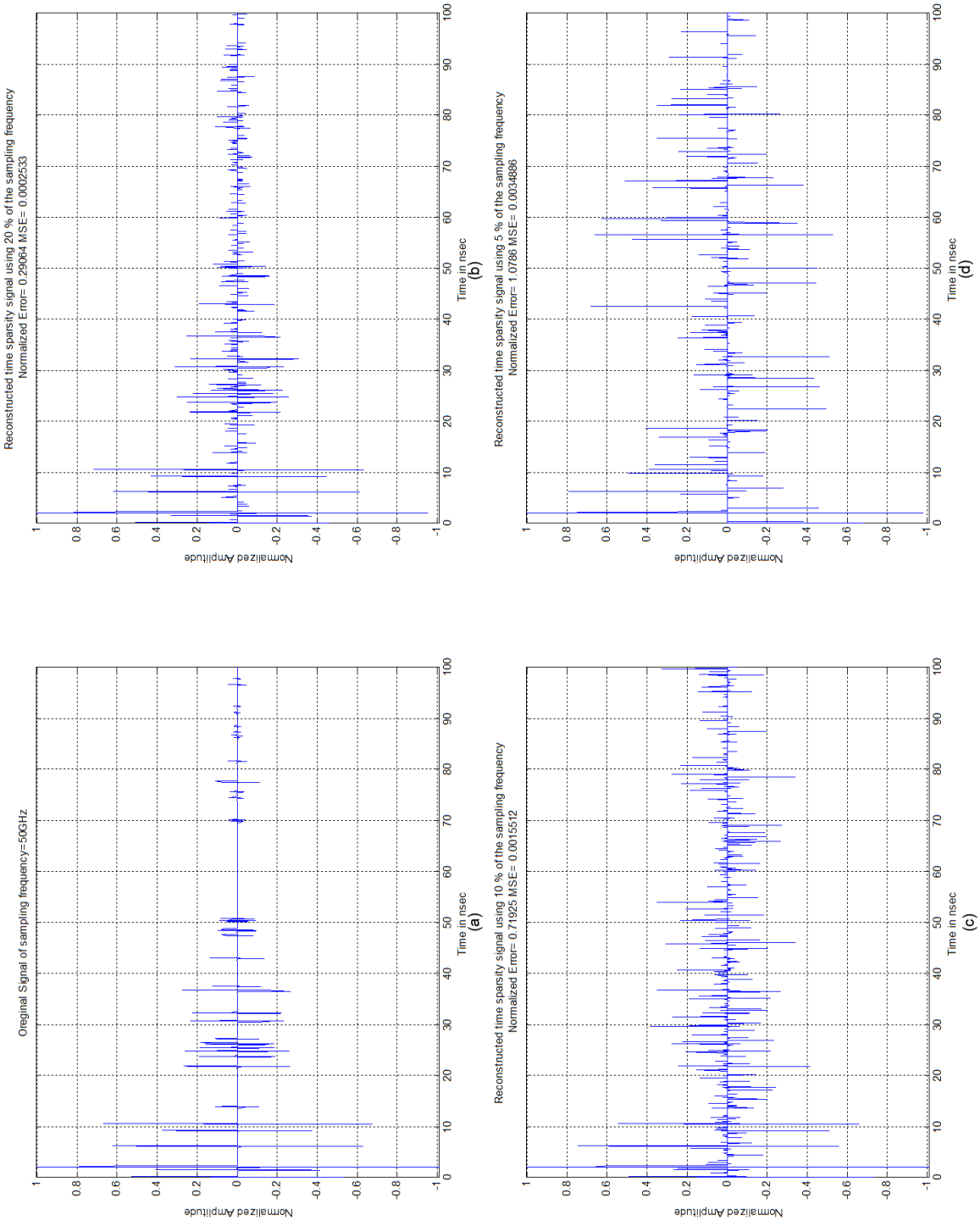

Figure 2-4 Reconstructed IR-UWB LOS signals via MP with assumption of sparsity in time at different sampling frequencies (a) original signal of f_s=50 GHz (b) f_s=10 GHz (c) f_s=5 GHz (d) f_s=2.5 GHz.

Therefore for the reconstruction of the UWB signals based on time sparisty, to improve the ability of CS reconstruction, one has to increase the number of random measurements. Similar conclusions hold true in general for any kind of signals [Don06], [Can06], [Tro07], [Mdu05]. This, however, requires more sampling rate, and subsequently demand for additional ADC resources. An alternative solution is needed.

The sparsity in time domain assumption becomes worse or invalid for the case of NLOS propagation scenario. For instance, Figure 2-5 (a) shows NLOS IR-UWB signal that is clearly less sparse than the LOS signal in Figure 2-4 (a). Beside, when we try to reconstruct a NLOS signal that has a time resolution of 20 psec (same resolution of the signal in Figure 2-4 (a) and similar indoor environment) by 10 GHz, we end up with a normalized error of 0.578, and MSE of 15×10^{-4} which is more than what we get for the LOS case.

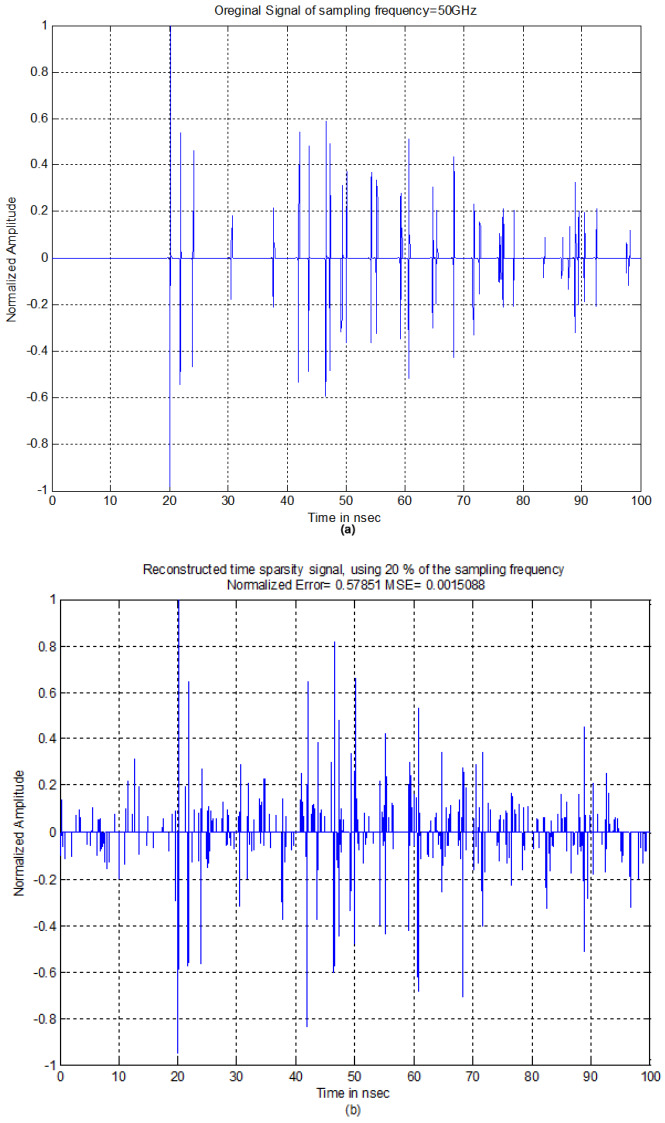

Figure 2-5 Reconstructed UWB NLOS signals via MP with assumption of sparsity in time.(a) Original signal (b) The reconstructed version of (a) via MP and 10GHz of sampling frequency.

Since the objective is reducing the sampling rate, we have to find another way to increases the performance of CS algorithms. A common and powerful approach is to increase the sparsity of the underlying signal in some domain [Can06], [Can08], [Don06]. In other words, design a dictionary where the received UWB signal can be completely represented in a sparser way.

Based on the fact that the received IR-UWB signal in (2-1) is a linear combination of the signal contribution of the various propagation paths, a more appealing approach to design the dictionary is explained next.

2.2.2 Signal Reconstruction Based on Multipath Diversity

Transmitting ultra-short pulse results less overlapping between the pulses. This is because the duration of the pulse is usually shorter than the inter-travel time between the paths. In other words, UWB channels, in general, are rich in multipath diversity, offering, in turn, higher energy compaction, sparseness and thus higher probability of exact reconstruction via CS [Par07].

This section relies on the fact that received IR-UWB signals given by (2-1) can be thought of as a linear combination of the signal contributions of the various propagation paths that compose the UWB multipath channel. These paths reflect different versions of the transmitted signal. Since CS theory has more reliable outcomes as the underlying signal has more sparsity in some domain [Can06], [Don06]. Thus, defining a suitable dictionary to represent the underlying IR-UWB signal is essentially important.

By examining the characteristics of the IR-UWB received signal, we can figure out a simple way to generate a dictionary, where the transmitted pulse is used as a basis atom that provides a better sparse representation of the received IR-UWB signals.

The received IR-UWB signal is formed by scaled and shifted versions of the transmitted pulse, as shown in Figure 1-6, and since the dictionary has to contain all basis (atoms) that could provide the best representation of the received IR-UWB signal, it is logical to think

that the basic function to generate the atoms of the dictionary should be replicas of the pulse waveform used to carry information, which in our case the first derivative of Gaussian pulse shown in Figure 1-3 [Par07].

Going into details, the dictionary is generated by shifting the transmitted pulse, $p(t)$, with a minimum step of Δ, in (1-3), leading to a set of parameterized waveforms specified by

$$\psi_j = p(t - j\Delta) = p(t - j\Delta)e^{-\frac{(t-j\Delta)^2}{2\sigma^2}} \quad j = 0,1,2, \ldots \tag{2-4}$$

This, in turn, defines the dictionary of sparsity, Ψ in (1-5), as

$$\Psi = \{\psi_0(t), \psi_1(t), \ldots\}. \tag{2-5}$$

The atoms in the dictionary are delayed versions of the UWB transmitted pulse. The minimum step Δ is dedicated to resolve or alleviate the overlapping between the arrived pulses especially within clusters. By setting Δ greater than the width of the basic pulse, atoms in (2-4) become orthogonal to each other. Despite the fact that the orthogonal property is a desirable characteristic of a basis to guarantee unique representation of the signal, the rich multipath diversity introduced by the UWB channel produces pulse spread that is better captured by a redundant dictionary. Thus, Δ is set such that overlapping between atoms occurs [Par07].

Though (2-4) is expressed in term of continuous time, t and Δ, in practice both are discretized. By setting Δ to be multiple of the sampling frequency, the dictionary becomes a complete and redundant dictionary.

At this point we are ready to use the designed dictionary in our reconstruction problem. If we re-express the received UWB signal, given by (2-1), by a discrete time vector as

$$r_x = \left[r_x(0), r_x(t_s), \dots, r_x\left((N-1)t_s\right)\right]^T, \tag{2-6}$$

Thus, we can write the measurement vector in a discrete representation as

$$y = \Phi r_x, \tag{2-7}$$

where Φ is the $M \times N$ measurement matrix of elements taken from normal distribution i.e. $\phi_{i,j} \sim N(0,1)$. Finally, the resultant vector out of random projected signal, y, and the new sparse dictionary, Ψ, which is the uniformly sampled version of the dictionary, are passed as parameters to MP algorithm. The outcome is a vector, Θ, as in (1-4), of sparse coefficients that represents the contribution of the atoms in the dictionary. The reconstructed signal is eventually obtained by

$$r_x = \Psi\Theta = \sum_{n=1}^{N} \theta_n \psi_n \,, \tag{2-8}$$

where θ_n is the contribution amount of the atom ψ_n in the dictionary Ψ.

The reconstructed signals are shown in Figure 2-6. To have a fair comparison between the reconstruction with time sparsity assumption and the sparsity in the designed dictionary, we used the same sampling frequencies which were used in Figure 2-4. In Figure 2-6 (b) we sampled the projected signal by 10 GHz to obtain 1000 random measurements in order to reconstruct the signal of Figure 2-6 (a) which results in a normalized error of 0.014, and MSE of 6.52×10^{-7}. Figure 2-6 (c) and (d) have slightly more error as a consequence of fewer measurements (lower sampling rate). Where, the recovered signal in Figure 2-6 (c) is obtained by sampling the projected signal using a sampling frequency of 5 GHz. This results in MSE of 26.6×10^{-7} and normalized error of 0.029. Specious recovered elements clearly appeared in Figure 2-6 (d) when the sampling frequency reduced to be

2.5 GHz, consequently increasing the MSE to be 403×10^{-7} and the normalized error to be 0.116.

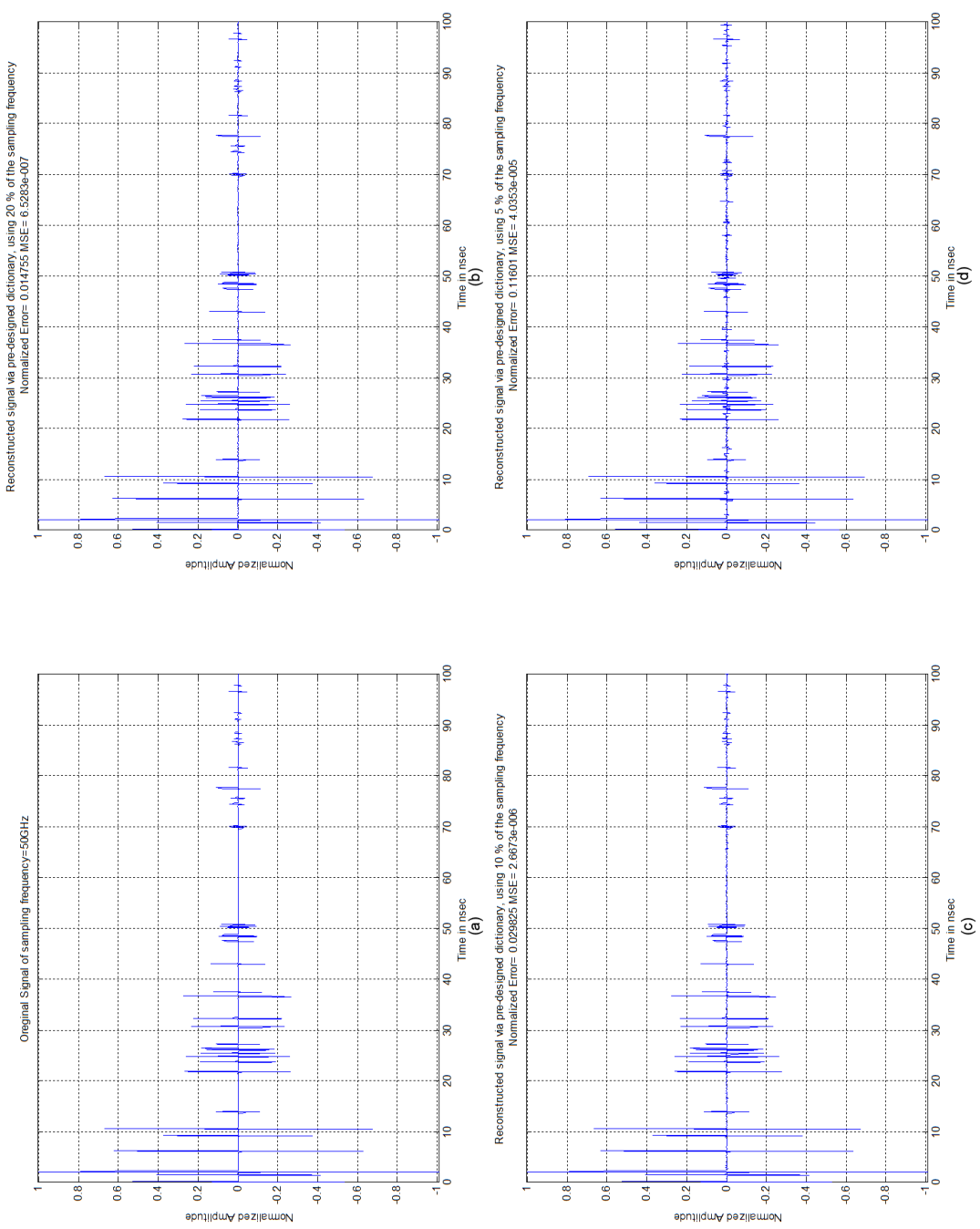

Figure 2-6 Reconstructed IR-UWB LOS signals via MP with assumption of sparsity Gaussian pulse-based dictionary at different sampling frequencies (a) original signal of f_s=50 GHz (b) f_s=10 GHz (c) f_s= 5 GHz (d) f_s=2.5 GHz.

With the aim of comparing the performance of CS in time sparsity assumption and the multipath diversity dictionary, it can be deduced from Figure 2-4 and Figure 2-6 that the UWB signal reconstruction using multipath diversity outperforms the reconstruction using time sparsity assumption. Yielding a reconstruction error that more than 20-fold smaller. Similar work has been done in [Lei10],

Since the NLOS signals have less sparse due to distraction and scattering, it is important to examine the performance of MP to reconstruct the NLOS propagation signal with assumption of sparsity in the pre-designed dictionary.

Figure 2-7 proves that MP is efficiently able to reconstruct not only the LOS UWB signals, but it goes beyond that to much less sparse signals as in NLOS signal in Figure 2-7 (a), and the same holds true for other scenarios. By using the dictionary defined in (2-6), and sample the projected signal by 10GHz, Figure 2-7 (b) shows the reconstructed signal with normalized error of 0.046 and MSE of 9.477×10^{-6}.

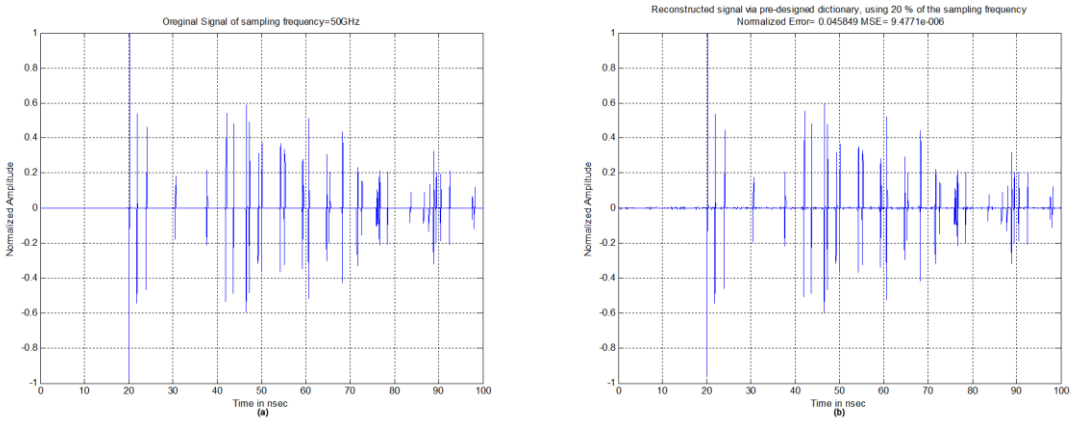

Figure 2-7 Reconstructed UWB NLOS signals via MP using predesign dictionary (a) Original NLOS Signal (b) Reconstructed signal using sampling frequency of 10 GHz.

Therefore, by building a dictionary that contains the basis functions of the desirable signal; a remarkable improvement in performance can be achieved. In addition, by having

only two percent of the original samples, CS can reconstruct all signal components carrying significant amount of energy in the received UWB signal.

In the previous part, we have demonstrated that if we sample the IR-UWB received signal at notably reduced sampling rate, by means of CS, it is possible to recover the signal with a very small error. This, in turn, leads to a reduced usage of ADCs resources and improved subsequently the signal detection as it will be describe in chapter 4.

2.3 Termination Criteria for Matching Pursuit Algorithm

Before getting further into the performance of CS on UWB signals, it is important to take the complexity of the MP algorithm into the consideration, and try to reduce it as much as possible. MP algorithm has been proven to achieve an accurate outcome of the signal reconstruction as a linear combination of the dictionary atoms. For general dictionary, the complexity is approximately calculated by $\mathcal{O}(N\mathrm{M})$ for each iteration [Krs06], [Zha93]. Where M is the number of measurements and N is the number of the signal samples. Since the required number of iterations is unbounded, [Dua05], thus, the complexity of MP is also unbounded. As a matter of fact, the complexity of the MP algorithm is dominated by three factors: the number of measurements, M, the number of samples in the signal N, and the termination parameters (T and ϵ), those termination parameters would break the algorithm loop as shown in Figure 1-4.

Many factors play a role when deciding the suitable values for T and ϵ, such as the dictionary of sparsity, the number of measurements, and incoherency [Zha93]. Experimental investigation was curried out to determine the suitable values for the

maximum number of iterations T, to achieve a small and acceptable amount of the residual error. The result shows the relationship between the residual ratio, ϵ, and number of iteration which depicted in Figure 2-8.

The relationship obtained by modifying MP algorithm, shown in Figure 1-4, via eliminating the termination condition ($\|e_t\|_2 > \epsilon\|y\|_2$), thus the algorithm keeps running until the maximum number of iterations is reached. This determines the minimum residual error that could be achieved by certain number of iterations. The modified MP algorithm is used to recover 100 UWB signals by 100 trails, where in each trail a different random measurement matrix Φ is generated. The residual ratio, $\epsilon = \frac{\|e_t\|_2}{\|y\|_2}$, is averaged over all signals and trails. The number of the signal samples, N, and the number of measurements were kept fixed.

Figure 2-8 depicts that the residual ratio, ϵ, lessen exponentially as the number of iterations increases.

We can deduce that after certain amount of residual, increasing the number of iteration is essentially useless; actually it is harmful in term of processing time and wasting of power resources. Since, the amount of residual will not change significantly in excess of 400 iterations, we will restrict the residual ratio, ϵ, to 0.013.

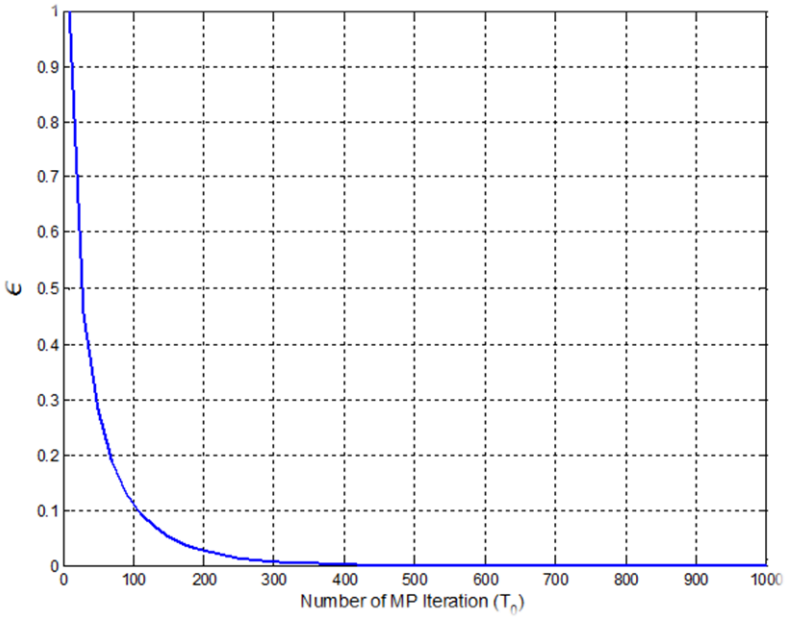

Figure 2-8 Effects of number of iteration on the residual ratio of the NLOS signal.

2.4 Sampling Frequency vs. Reconstruction Accuracy

The number of measurements or sampling frequency is key factor when it comes to reconstruction accuracy. Even when sample at sub-Nyquist frequency, with CS reconstruction we are able to recover all frequencies involved in the signal, not only the band below half the sampling frequency as in the conventional approach of sampling.

In Section 2.3 the appropriate values of MP algorithm parameters have been adjusted, T is set to 400 iterations and residual ratio $\epsilon = 0.013$. In this section, we are examining how the number of measurements that affect the reconstruction capability of MP algorithm with the pre-defined dictionary. We examine two different levels of sparsity by considering LOS and NLOS scenarios.

Since we are concentrating on the indoor environments, it is useful to examine how much the variety in sparsity between LOS and NLOS will affect the performance of CS.

The dependence of the accuracy of reconstruction on the sampling rate is illustrated in Figure 2-9. As expected, NLOS reconstruction requires more sampling rate than the required for LOS scenario, as a consequence of more sparsity. Furthermore, there is still a small amount of error even in high sampling rate due to the randomness in measurements and other issue like orthogonality of atoms in the sparsity dictionary. Nevertheless, these errors are negligible [Par07].

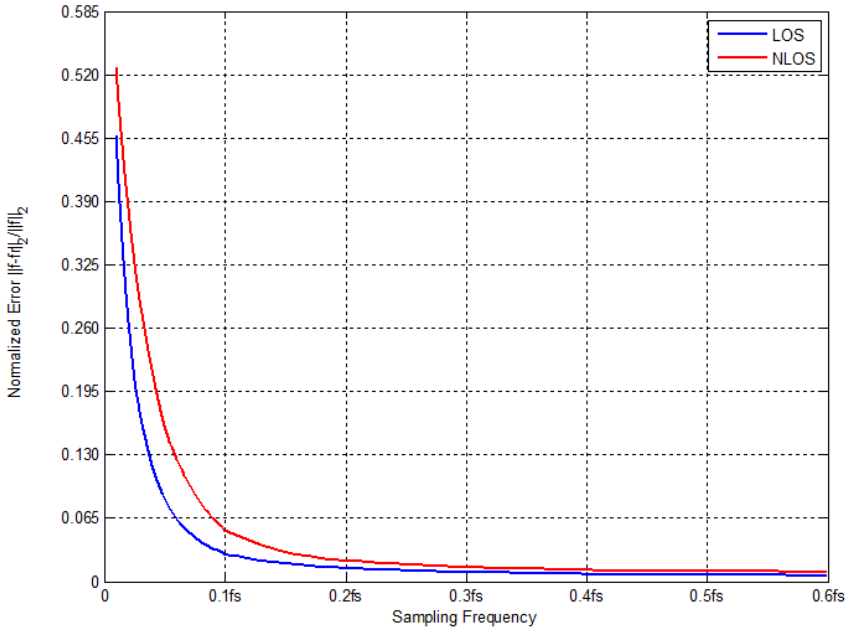

Figure 2-9 The impact of Sampling frequency on the reconstruction accuracy, f_s is the original sampling frequency.

2.1 Chapter Summary

In this chapter we have presented the technical background for the UWB channel model. We also have demonstrated the ability of CS to reconstruct IR-UWB signal, generated by IEEE 802.15.4a model, using time domain sparsity and a pre-designed dictionary. The predefined dictionary based on the assumption that multipath components are delayed and

scaled version of the transmitted pulse. This assumption was proved to be more efficient than the time sparsity assumption.

In the next chapter we well cast this approach onto practical profiles and study the behavior of CS in practical channels.

CHAPTER 3

3 CS SIGNAL RECONSTRUCTION IN PRACTICAL UWB CHANNELS

3.1 Introduction

Analysis of wireless channels often means examining a huge bank of measured impulse responses and finding an appropriate statistical model. The UWB channel has a lot of characteristics associated with different impacts on the propagating signal. Attempting to apply narrowband models or a model with a limited number of parameters like the IEEE 802.15.4a channel model to design or evaluate UWB receivers can be misleading. To simulate a realistic UWB channel, one has to include the alteration of the transmitted pulse due to physical phenomena such as reflections or diffractions as well as the antenna frequency dependent response. For wideband systems, pulse distortion caused by RF components, pulse dispersion produced by the antenna, and time jitter generated by non-ideal oscillators cannot be ignored . These phenomena affect directly the performance of the overall communication system. In case of narrowband communication systems, these transient temporal effects are only a small fraction of the symbol duration and may often be ignored [Ree05].

In UWB signal reconstruction, transient effects like pulse dispersion will reduce the validity of the assumption that UWB signal is sparse in the multipath-based dictionary as will be discussed in this chapter.

The analysis of indoor UWB channels based on simulation of the entire transmission link using statistical methods is useful in assessing the system performance [Has93]. This approach, however, requires extensive propagation measurements and all factors have to be taken into consideration to be able to accurately evaluate the performance of the system in that practical environment. Some research of CS and UWB worked on the IEEE statistical model as in [Oka09] and other build their assumption on Saleh and Valenzuela model in [Sal87] while other considered the channel model of IEEE802.15.3a standard [Spe00]. The work of the previous researcher was validated in Chapter 2.

The previous chapter evaluated CS reconstruction and ran simulation based on the IEEE 804.15.4a channel model assuming no frequency dependence. In this chapter we extend the work to examine the performance of CS in the presence of physical effects like the ones cause by the channel and the antenna. To the best of our knowledge this extension was not done before.

This chapter first explains the impact of the antenna on the transmitted pulse. Based on realistic UWB profiles, we then validate the sparsity in time assumption. The transmitted pulse based dictionary (designed in previous chapter) is then used in MP algorithm to recover the practical profiles. The performance has some degradation due to the physical realistic effects that have not been considered. Alternative practical dictionaries are designed to increase the sparsity and hence improve the performance of MP algorithm.

The same approaches are applied to the directional UWB channel model proposed in [Muq10].

Since the reconstruction quality depends on the sampling frequency (among others), last part of this chapter evaluates the signal reconstruction using the proposed dictionaries versus sampling frequency, for both measured and directional model profiles.

3.2 Impact of Antenna on the Pulse Shape

To transmit an extremely short pulse as in UWB systems, the antenna has to be uniquely designed and able to deal with the wide bandwidth. One of the challenges in the implementation of UWB systems is the development of a suitable antenna that would enhance the transmission performance. Since the usual data demodulation in UWB is based on the pulse shape [Qiu05], the clean impulse response (that has minimal pulse distortion) is a primary requirement for an efficient UWB antenna.

Though, the antenna characteristics in frequency domain are important, the response of UWB antenna can be better described in terms of its temporal characteristics [Ree05]. The ideal UWB antenna (that has minimal pulse distortion) has to generate a radiation fields with constant magnitude and phase shift that varies linearly with the frequency. Moreover, the radiation pattern should be spherical and has similar response at all directions. When these dual requirements are met, the radiated signal will be only a time derivative of the input signal [Ahm04].

Plenty of antennas design are proposed in [Lic04] to have UWB bandwidths, some of them are depicted in Table 1 with their impulse and frequency responses. The impact of

the choice of the antenna on the transmitted signal cannot be overlooked. Since our practical measurements are obtained by TEM horn antenna, we briefly explain its characteristics in the next subsection.

Table 1 Typical UWB antennas

Antenna Name	Impulse Response	Frequency Response
TEM horn	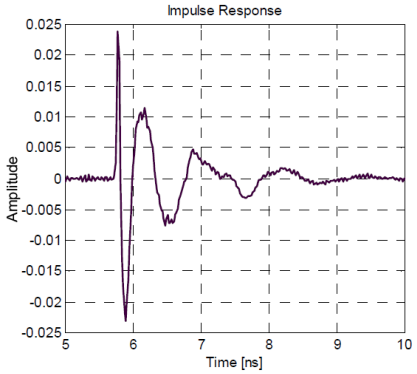	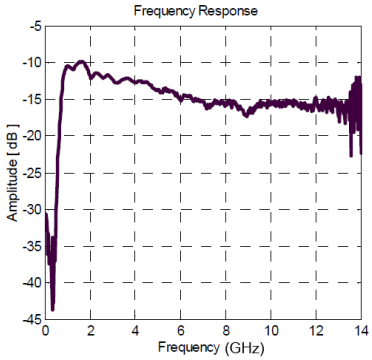
Bi-conical	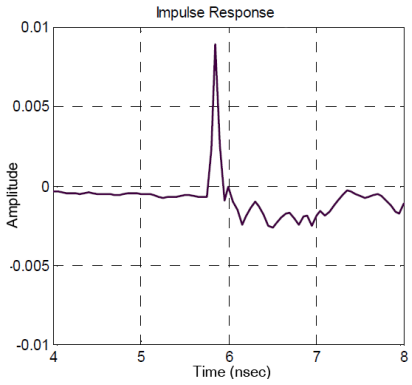	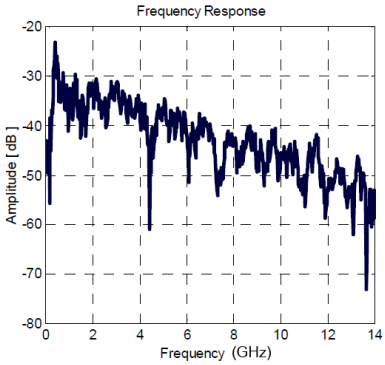
Vivaldi	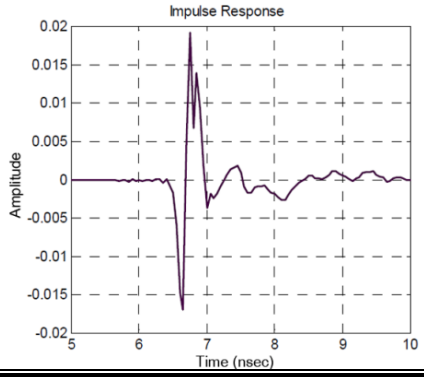	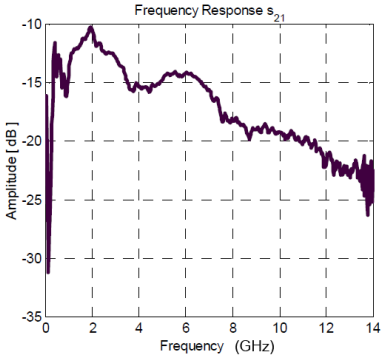

3.2.1 TEM Horn UWB Antenna

The TEM (transverse electric and magnetic) horn is a traveling-wave antenna. Because it is quite broadband in receiving mode, both in magnitude and phase, TEM horn is a perfect choice for impulsive free-space measurements. TEM horns have been traditionally used for low-dispersion launching and receiving of UWB pulses. Research conducted since the late 1970s has led to a further reduction of dispersion caused by the TEM horn abrupt edges, the antenna is commonly loaded with chip resistors or a conductive film as one solution to suppress the reflection from the TEM horn edges, Figure 3-1 shows a TEM horn having an operating frequency range of approximately 1 to 18 GHz. The frequency and the impulse responses of a TEM horn antenna is shown in Table 1.

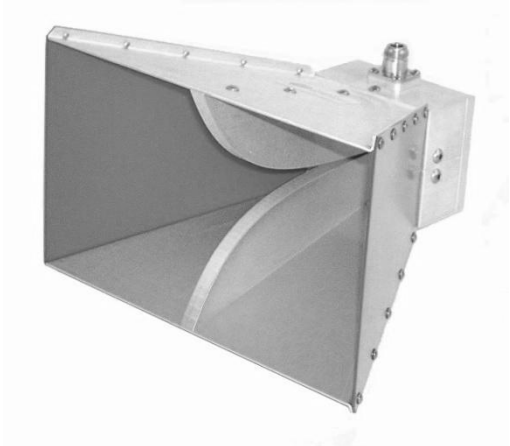

Figure 3-1 TEM horn antenna of 18GHz bandwidth [May11].

In [Muq03] radiated measurements were used to characterize the TEM antennas. The relation between the multipath angle and the pulse shape was also presented in the same source. Since the antenna pattern plays an important role for both the receiver and the transmitter, we briefly illustrate the effects of the angle of arrival on the pulse shape using the TEM antenna. According to [Muq03], [Muq10], [Lic04] and others, TEM antenna investigations exhibit that multipath components have different waveforms regardless of

the medium. In this regard, experiments are done in [Muq03] where the transmitter and the receiver antennas are positioned in boresight direction. The transmit antenna is then kept fixed; the receive antenna is rotated along the elevation angle at different angles, specifically, $0^0, \pm 15^0, \pm 30^0, \pm 45^0, \pm 60^0$ to obtain the vertical measurement. Similarly, the horizontal measurements are taken but by rotating the receiver antenna along the azimuth angle with the same previous angle angles. Figure 3-2 illustrate the procedure and the results of this experiment. The figure shows both the direct path and the reflection from the floor. Similar experimental results obtained in [Lic04] for Vivaldi antenna.

Accordingly, the realistic received UWB signals are composed of different pulse shapes corresponding to the different propagation paths. Thus it is useful to design a dictionary based on the received pulse shapes as will be done in Section 3.4.2.3.

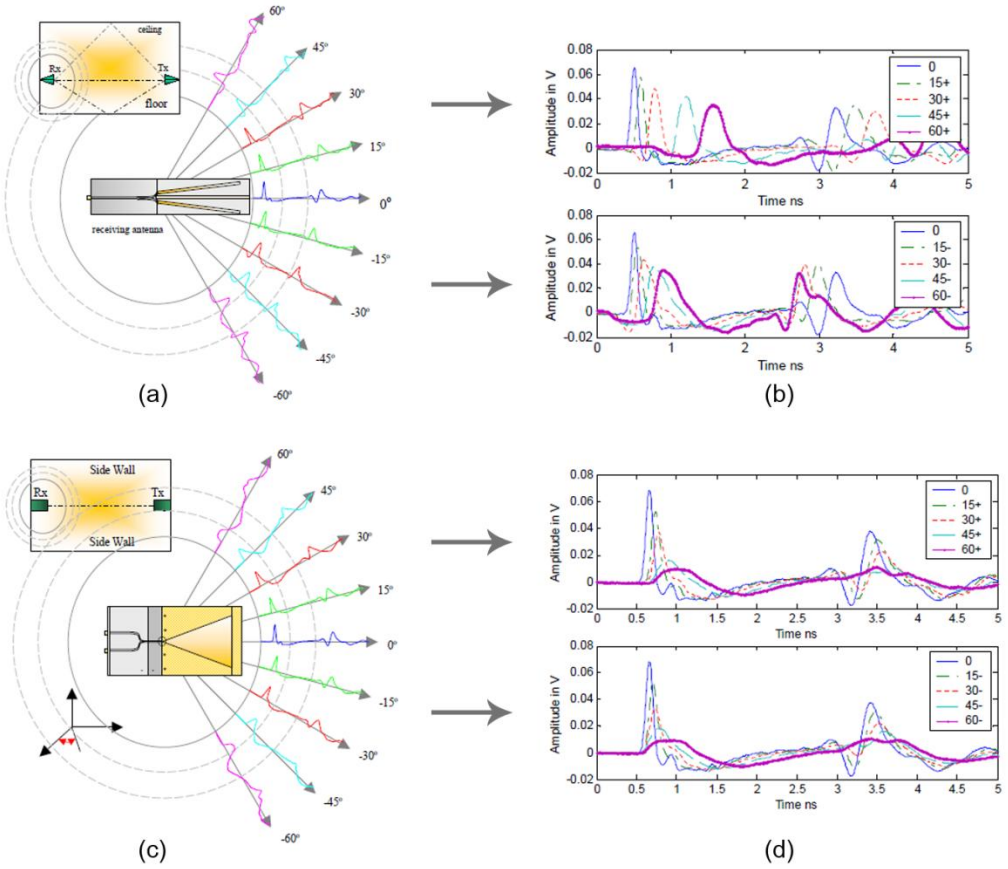

Figure 3-2 Received waveforms at different receiver angles (a) experimental view for the horizontal measurements (b) horizontal negative and positive elevation angles (c) experimental view for the vertical measurements (d) vertical negative and positive elevation angles [Muq03].

3.3 Sources of Practical Profiles

The evaluation of the proposed modifications to reconstruct UWB signals using MP algorithm will be validated against practical profiles. The sources of these practical profiles are either measured UWB signals or/and profiles generated using the directional model [Muq10] which accounts for the antenna effects. This section presents the details of the measurements and the directional model.

3.3.1 Measured Profiles

Time-domain measurement profiles are provided by [Muq03] and obtained using a sampling oscilloscope as receiver and Gaussian pulse generator as transmitter. Two low noise wideband amplifiers were used at the receiver side. The width of the transmitted pulse is 0.34 ns. The received signals were sampled at a rate of 1 sample per 20 ps. An acquisition time window of 100 ns was selected to ensure that all observable multipath components are accounted for. The sampling rate leads to 5000 points correspond to the 100 ns time window. In indoor environments, the time-varying part of the impulse response is typically due to human movements. By conducting the measurements during low activity periods and by keeping both the transmitter and the receiver stationary, the channel can be treated as being semi-stationary. This allowed to average 32 measurements, thus effectively canceling out the noise [Muq06]. The measurements were performed using directional TEM horn antennas. As can be deduced for the Figure 3-3, sparsity is a concern in measured profiles. For the measurements in hand, 63 profiles of LOS propagation scenario are used.

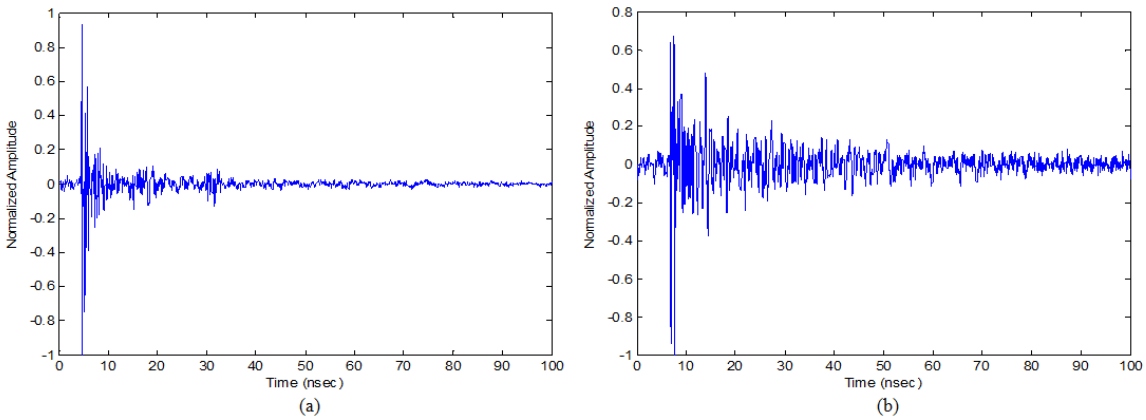

Figure 3-3 (a) Measured LOS signal (b) Measured NLOS signal.

3.3.2 Directional UWB Channel Model

Unlike IEEE 802.15.4a model where the received waveform is a summation of scaled and shifted versions of the transmitted pulse; Muqaibel in [Muq10] proposed a directional model where the received waveform is a summation of scaled, delayed, and modified pulse shapes. The difference in pulse shape is due to the antenna directional response. Hence, the relative angles between the transmitter and the receiver antennas have been included in the directional model.

The directional model assumes that the channel is composed of ideal specular reflectors. The relative vertical angle, θ, and horizontal angles, φ, between the transmitter and the receiver, are considered. The directional impulse response is given by

$$b(t,\theta,\,\varphi) = \sum_{l=0}^{L-1}\sum_{k=0}^{K-1} \alpha_{k,l}\delta\big(t - T_l - \tau_{k,l}\big)\delta\big(\theta - \Theta_l - \omega_{k,l}\big)\delta(\varphi - \Phi_l - v_{k,l}), \quad (3\text{-}1)$$

where Θ is the cluster vertical (elevation) angle with uniform distribution on $[0,\pi)$; ω is the ray vertical angle with zero mean of Laplacian distribution; Φ is the cluster horizontal (azimuth) angle with uniform distribution on $[0,2\pi)$; v is the ray horizontal angle with zero-mean Laplacian distribution.

Using an antenna simulator with the above model directional profiles can be generated. A directional simulator of the TEM antenna is developed in [Muq07]. The antenna simulator can be used to generate waveforms transmitted and received at different angles. Figure 3-4 shows the TEM simulated received waveforms where the receiver elevation angle is rotated in 15^0steps. Due to the symmetry assumption of the simulated antenna,

positive and negative angles result in the same pulse shape, wherefore the simulation is done at $0^0, 15^0, 30^0, 45^0, 60^0$.

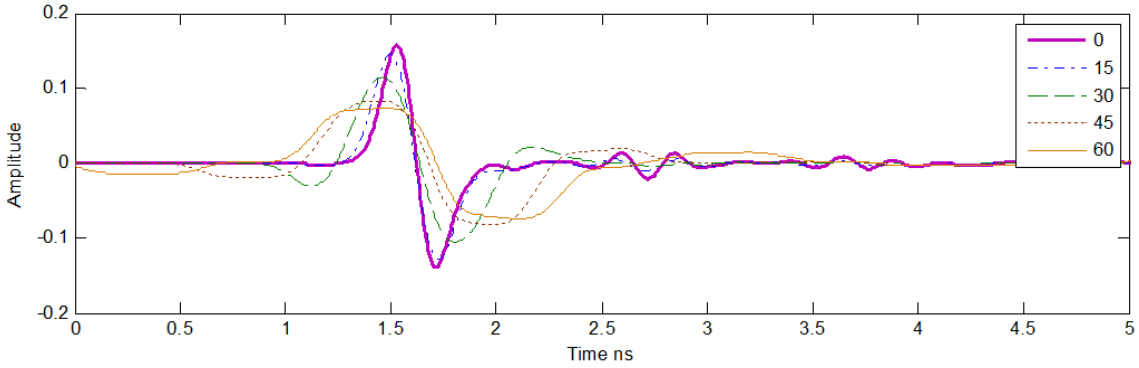

Figure 3-4 Simulated TEM waveforms received at different angles [Muq10].

An example of a full directional profile generated by the above method is depicted in Figure 3-5. Notice that this profile is noiseless. AWGN can be added if needed.

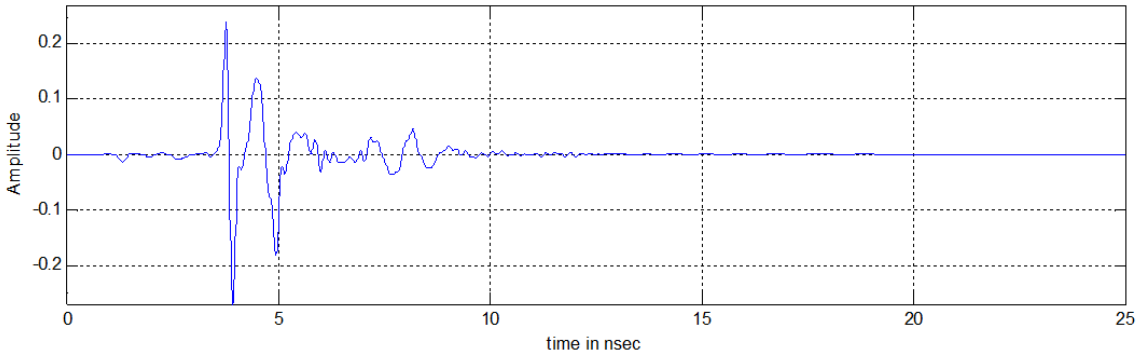

Figure 3-5 Directional UWB profile.

3.4 Methodology for Practical Signal Reconstruction

The results discussed in this section are based on measured profiles. Whenever he directional channel model is used it will be mentioned explicitly.

3.4.1 Reconstruction Based on Sparsity in Time Domain

Sparsity in time domain works unquestionably in case of spikes sparsity, i.e. the signal is nothing but few impulses scattered among the signal (bins) or samples, meaning that the algorithm will recover the signal as spikes rather than a complete pulse shape. The fact that the UWB profile is made of scaled and shifted version of a reference pulse is ignored. Losing the details of the pulse shape is harming in many modulation schemes. Any change or mismatch in pulse shape will affect directly the detection process.

The resultant signal out of MP algorithm assuming sparsity in time assumption is presented in Figure 3-6. The reconstruction is based on 25 GHz sampling frequency (half of the signal samples). The sub-figure (a) represents the measured LOS signal and, (b) shows the recover signal via MP with an assumption that the signal is sparse in time domain. Remember, in this case we do not define any sparse dictionary in this section; instead the dictionary Ψ in (1-4) will be a unity matrix.

The normalized error[1] of the recovered signal is 0.48. Figure 3-7 has more clear shot of the reconstruction error. Spikes are recovered instead of full pulse shape.

[1] Normalized error has been introduced in section 2.2.1 which is given by $\frac{\|r_x - r_x'\|_2}{\|r_x\|_2}$

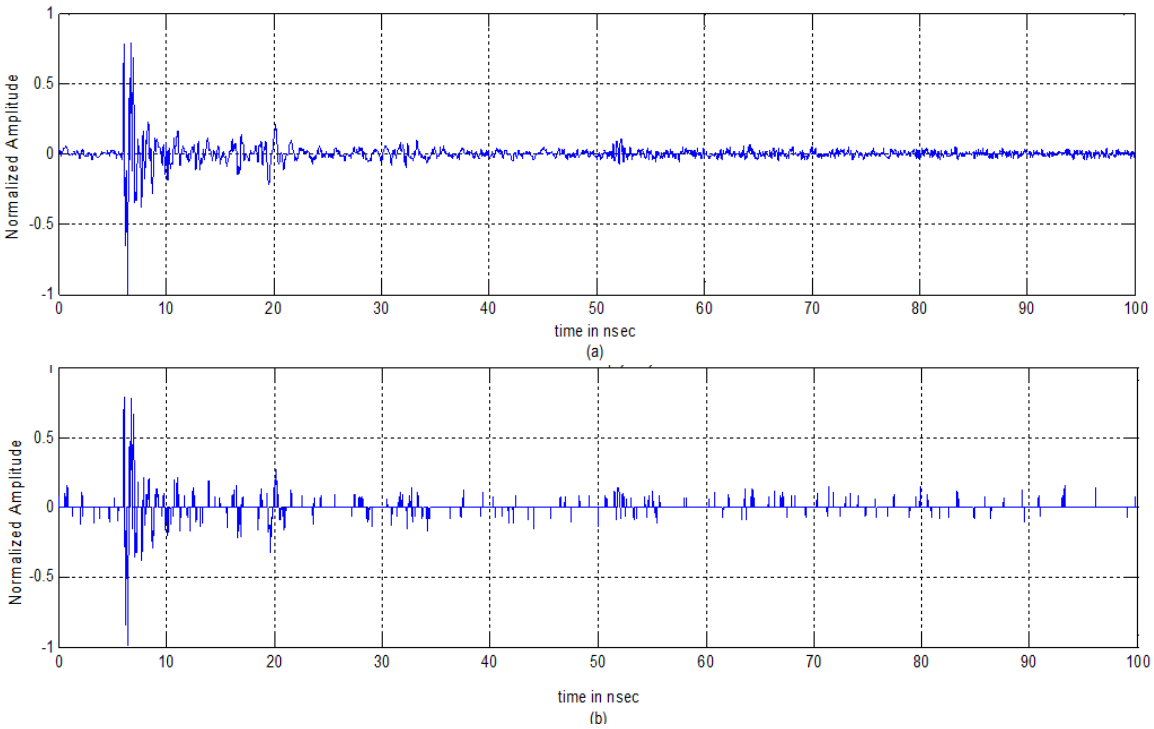

Figure 3-6 (a) Practical LOS UWB signal. (b) Recovered version of (a) via MP and time sparsity domain.

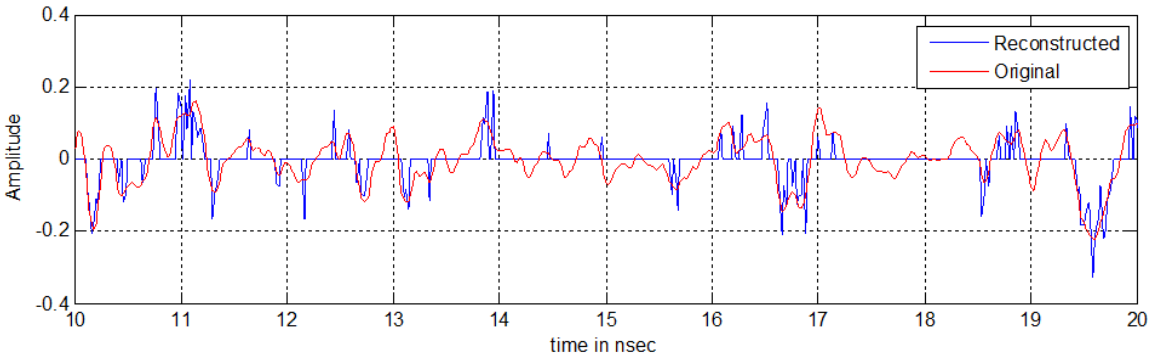

Figure 3-7 Comparative zoomed in version of Figure 3-6.

Reconstruction assuming time domain sparsity requires high sampling frequency, leading to a conclusion that CS is unreliable to reconstruct the practical UWB signals.

3.4.2 Reconstruction Based on Pre-Design Dictionary

The ultimate goal of practical signal reconstruction algorithm is to be effective and reliable in real-life channels, in Section 2.2.2 CS has reliably reconstructed the noiseless

UWB signals based on the IEEE 802.15.4a model. For real channels, accurate and precise channel characterizations cannot be under estimated [Muq02].

In this section we will start by applying the predesigned dictionary based on the transmitted pulse, assuming that the received pulse shape does not change due to different propagation paths, and see how this assumption will vary from the theoretical results that we have got in Section 2.2.2. The atom of the dictionary in this case is based on the practical received pulse. Afterword, variable width dictionary (shifted pulses and gradually increasing in width) is built to address the effects of dispersion for the later arrivals. Finally, we will go beyond that to consider different pulse shapes received at different angels and how these shapes will enhance the reconstruction outcomes.

3.4.2.1 Gaussian Pulse-Based Dictionary

Building a dictionary out of only shifted versions of the transmitted signal, as in Section 2.2.2, results in a reconstructed profile composed of only shifted and scaled version of the transmitted signal with some interfere with each other. Although, this technique works fine in the hypothesis of the IEEE 802.15.4a model, we would like to examine its performance when dealing with practical profiles that are contaminated with AWG noise and impacted by physical effects.

As depicted in Section 3.3.1, the transmitted pulse used in the practical profiles is Gaussian monocycle of width 0.34 ns, defined in (1-3). Denote the transmitted pulse by $p(t)$, therefore the dictionary atom is defined as

$$\psi_j = p(t - j\Delta) = p_n(t - j\Delta)e^{-\frac{(t-j\Delta)^2}{2\sigma^2}} \quad j = 0,1,2,\ldots \tag{3-2}$$

Where Δ is the amount of the shift in each atoms as shown in the figure below

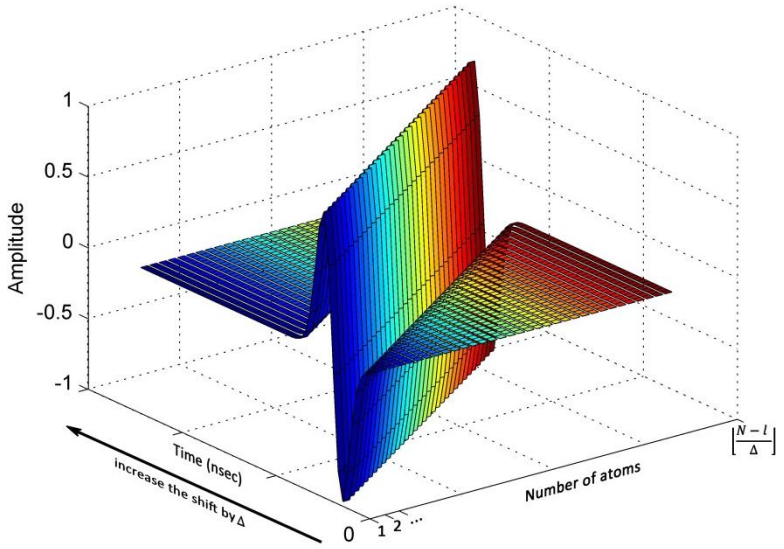

Figure 3-8 Pre-defined dictionary based on Transmitted signal

By implementing this dictionary, we ignore the variation of the pulse shape due to the channel or the antenna response. Since the dictionary's atoms are noiseless, the reconstructed signal should be noise-free signal. However, errors will appear as a result of wrongly detected atoms. Those atoms have relatively small energy and are negligible.

Implementing MP algorithm using this dictionary results in the signal in Figure 3-9 (b) with a normalized error of 0.324 and MSE of 3.1×10^{-4}. The zoomed version in Figure 3-10 shows the improvement in the reconstruction and similarity between the original signal and the reconstructed one. The normalized error is reduced by about 68 percent compared with the previous case where sparsity in time domain is assumed. Hence, the practical UWB signal is sparser in a pre-defined dictionary "Multipath Diversity" than in the time domain.

None of the effects of channel or antenna has been included in this scenario. Next, we are going to include more practical aspects in designing the dictionary.

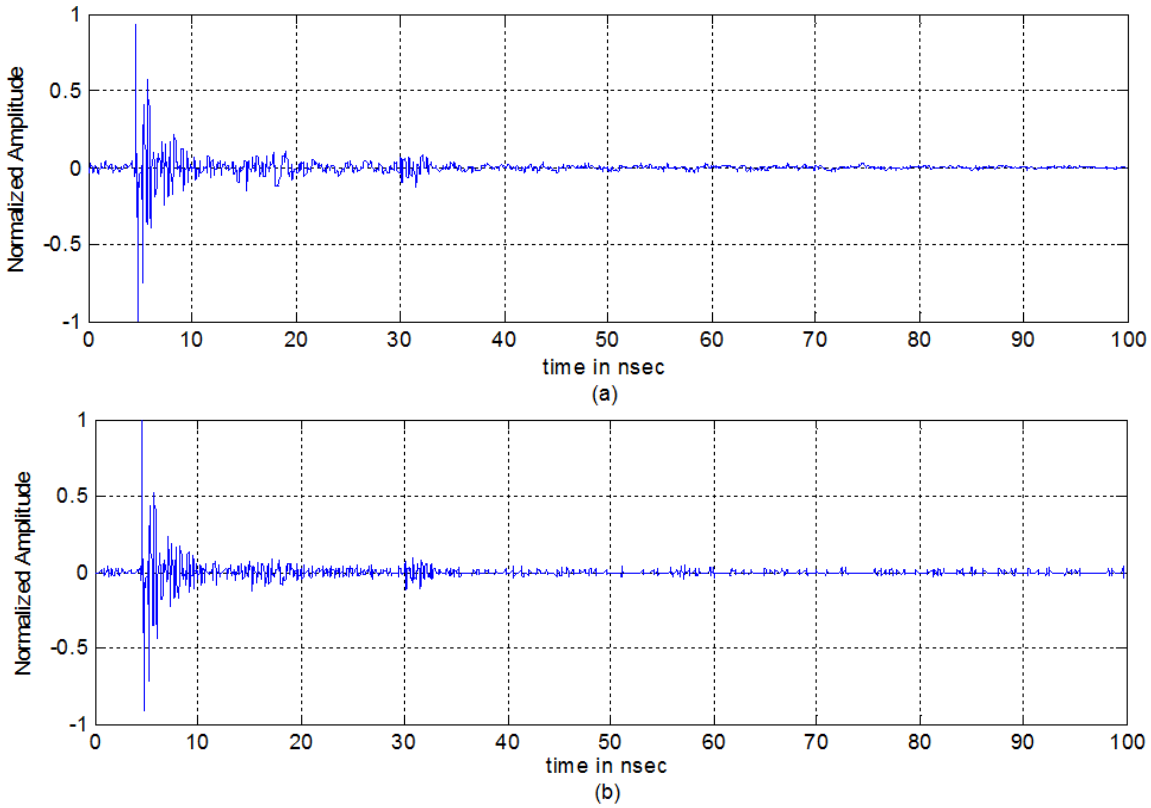

Figure 3-9 (a) Original signal (b) Recovered version of (a) via MP and transmitted pulse based dictionary.

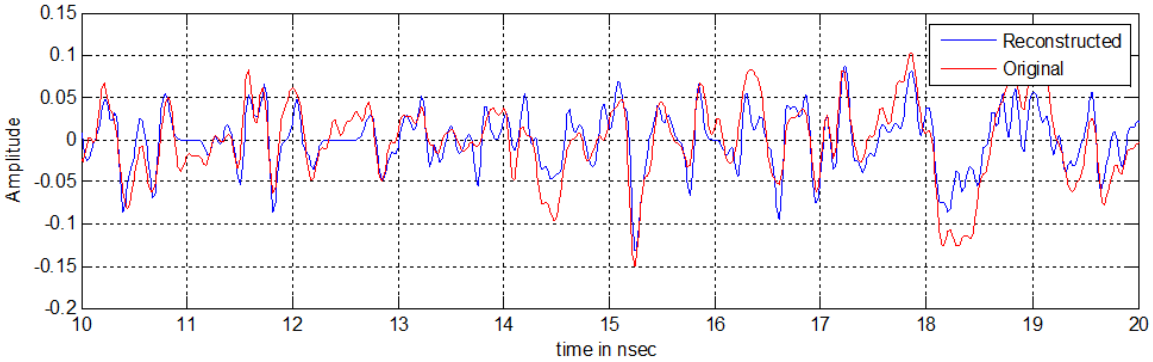

Figure 3-10 zoomed version of Figure 3-9.

3.4.2.2 Boresight Signal-Based Dictionary

The real life transmitter does not generate perfect Gaussian signals as was assumed earlier. In the following, we examine the impact of utilizing a measured atom rather than

the theoretical one. Figure 3-11 contrasts the theoretical (Transmitted) Gaussian pulse and the practical pulse received at zero degree angles of the transmitter and the receiver antennas (bore sight); it depicts the dispersion and corruptions caused by physical channel which did not consider previously.

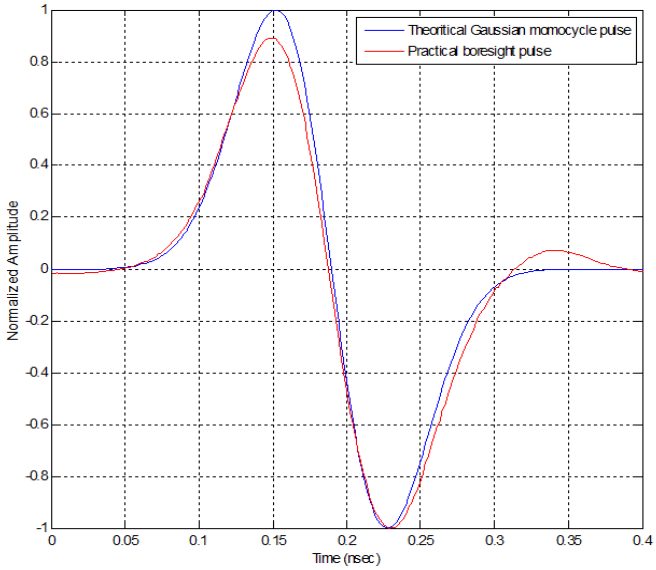

Figure 3-11 Contrast between Practical and theoretical Gaussian Pulse.

In order to include the physical effects of UWB channels, we well build a practical dictionary based of the practical pulse in Figure 3-11. Each atom of the practical dictionary will be a shifted version of the practical pulse as

$$\psi_j = p_0(t - j\Delta) \quad j = 0,1,2, \dots \left\lfloor \frac{N - l_0}{\Delta} \right\rfloor, \tag{3-3}$$

Where, $p_0$is the practical pulse received at zero degree, l_0 is the length of the practical pulse received at zero degree.

Unlike the theoretical based dictionary; applying MP using practical dictionary results in more improvements in signal reconstruction. This is shown in Figure 3-12 where the

amount of normalized error has been reduced to be 0.285. More visual inspection is depicted in Figure 3-13 as a zoomed in version of Figure 3-12.

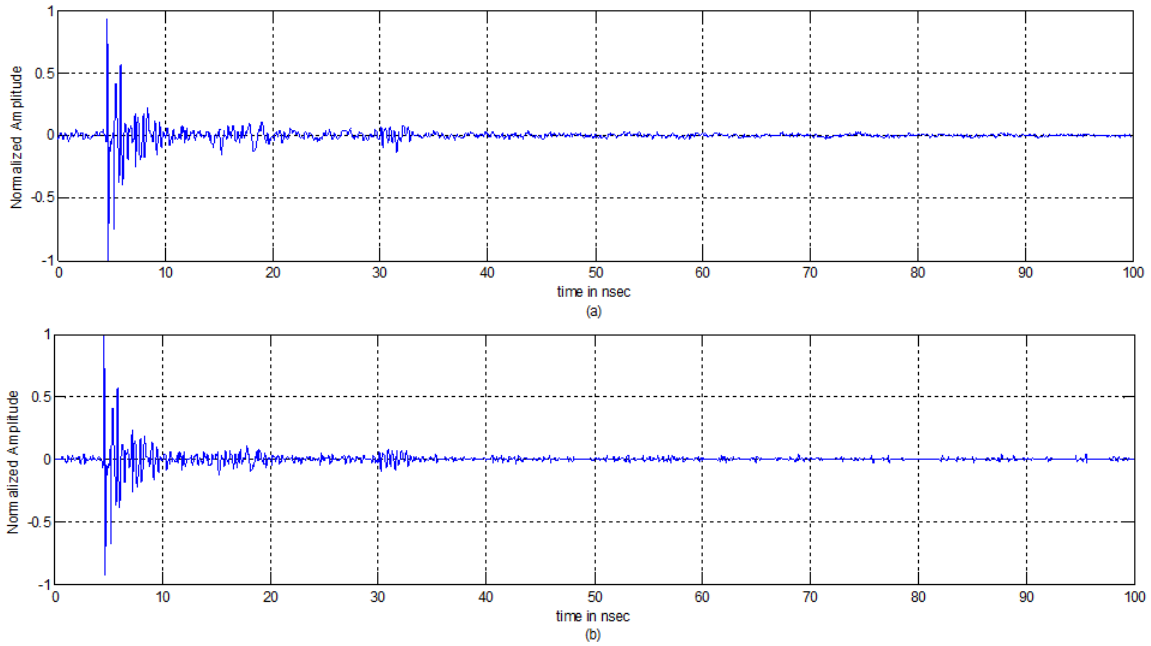

Figure 3-12 Reconstructed signal using the practical dictionary.

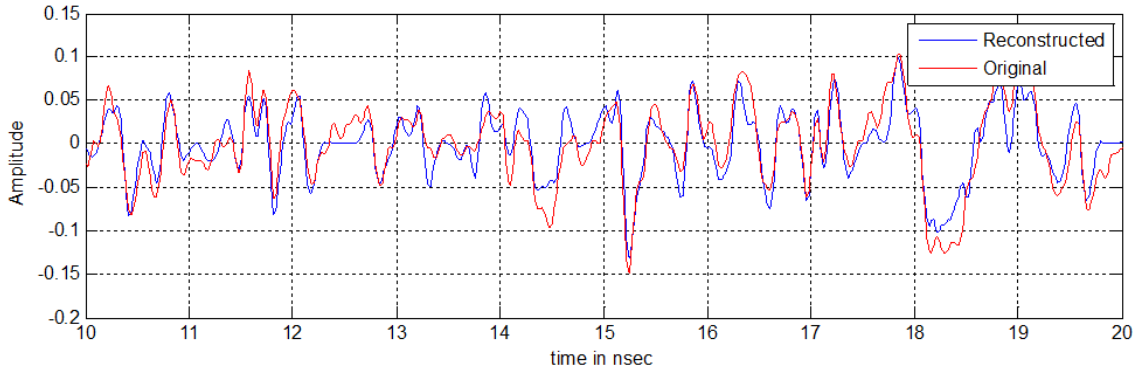

Figure 3-13 Zoomed in version of Figure 3-12.

3.4.2.3 Variable Width Atoms Dictionary

The UWB received profile may be viewed as a series of pulses with specific inter-pulse spacing. Each path of the multipath channel has its own impulse response or frequency transfer characteristics. The frequency independence assumption is widely adopted in tapped delay line models. This assumption is not convincing for UWB systems as in the

case for radar target identification. Therefore, we should consider individual path distortion and dispersion in the design of a dictionary that is associated to the UWB channel propagations and antenna response.

Pulse dispersion is an inevitable adverse effect induced by the physical characteristics of the UWB channels that have to be carefully addressed. Although the realistic channel has many effects on the transmitted pulse, dispersion is one of the most significant effects. Pulse dispersion decreases the correlation between the transmitted and the received pulses more than other effects do [Qiu02], which in turn causes degradation to MP reconstruction.

The temporal dispersion varies with the antenna angles, as in Figure 3-14. The pulse width increases as the relative antenna angle increases. It is observed statistically that late arrivals are correlated with larger angles and hence will suffer from more dispersion. Building a new dictionary that assign wider pulses to later arrivals is a rational idea.

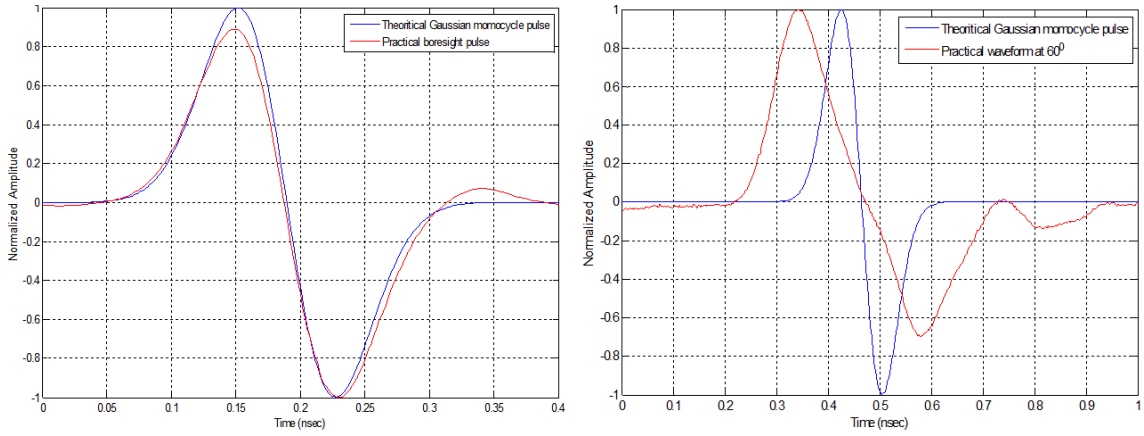

Figure 3-14 Received signals at angles of 0 and 60 degree.

Variable width dictionary is a dictionary composed of shifted and widened versions of the theoretical pulse. The pulse duration of the first atom is set to be equal to the practical

boresight duration and zero shift. The next atoms have a gradual increase in duration and delay. The last atom will have a duration the match the duration of the practical waveform received at the maximum reception angle for the used antenna which is 60^0 in the case of the used TEM horn. Let the j^{th} atom in the variable width dictionary be indicated by ψ_j given by

$$\psi_j = p(\sigma_j, t - j\Delta) \qquad j = 0,1,2, \dots , \tag{3-4}$$

where σ_j is the parameter to control the increment of the pulse duration in each atom, thus, the maximum value of j is controlled by the length of the received signal; i.e. atom generator will be stopped if the shifting exceeds the signal length.

Using the variable width dictionary to reconstruct an UWB signal results in the signal depicted in Figure 3-15 (b) which has a normalized error of 0.257. The reconstruction quality is better than the two cases of the Gaussian pulse-based dictionary where no dispersion is assumed. A comparative and zoomed version of the original and the reconstructed profiles are shown in Figure 3-16 .

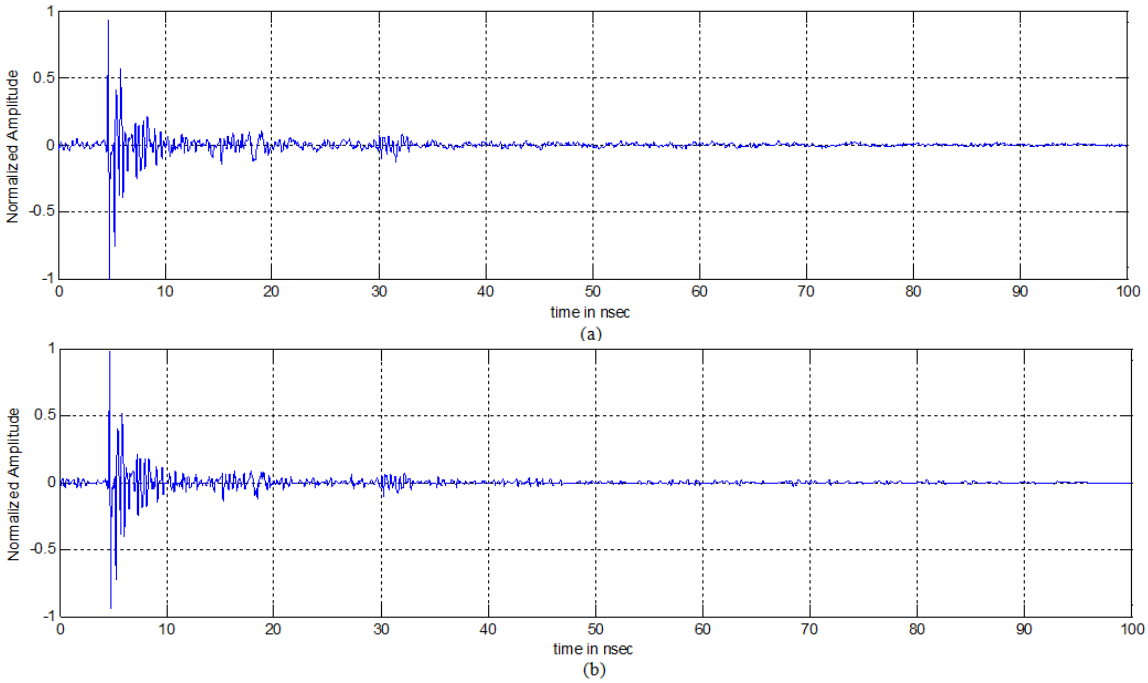

Figure 3-15 (a) Original (b) Reconstructed signal using variable width dictionary.

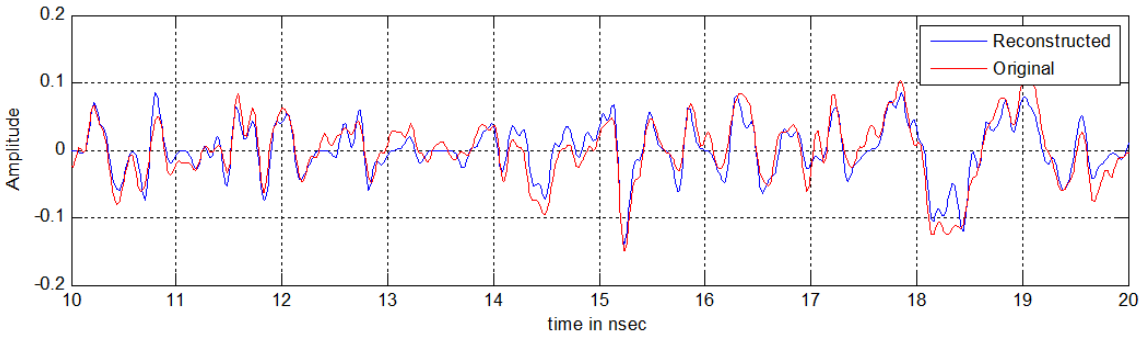

Figure 3-16 zoomed version of Figure 3-15.

3.4.2.4 Multi Atom Directional Dictionary

The hypothesis that the received pulses through different paths have the same waveform requires that both the transmitter and the receiver antennas to have spherical patterns shape at all frequencies. Recall that if the antenna is electrically large compared to the wavelength of the center frequency of the received signal, the waveforms radiated in different directions from the transmitter antenna look considerably different in the far field region [Muq10]. This fact can be used to improve the reconstruction.

Figure 3-17 demonstrates the variation and the dispersion of pulse shapes at different received angles. Therefore the practical profile will be made up of shifted, scaled, dispersed and slightly modified pulses of the transmitted signal. The measurements in the figure were carried out in an open environment to avoid any reflections by any obstacle, leading thus, to pure measurements impacted by the antenna effects only. Furthermore, the antenna effects vary from one antenna to another according to its characteristics and radiation pattern [Muq02].

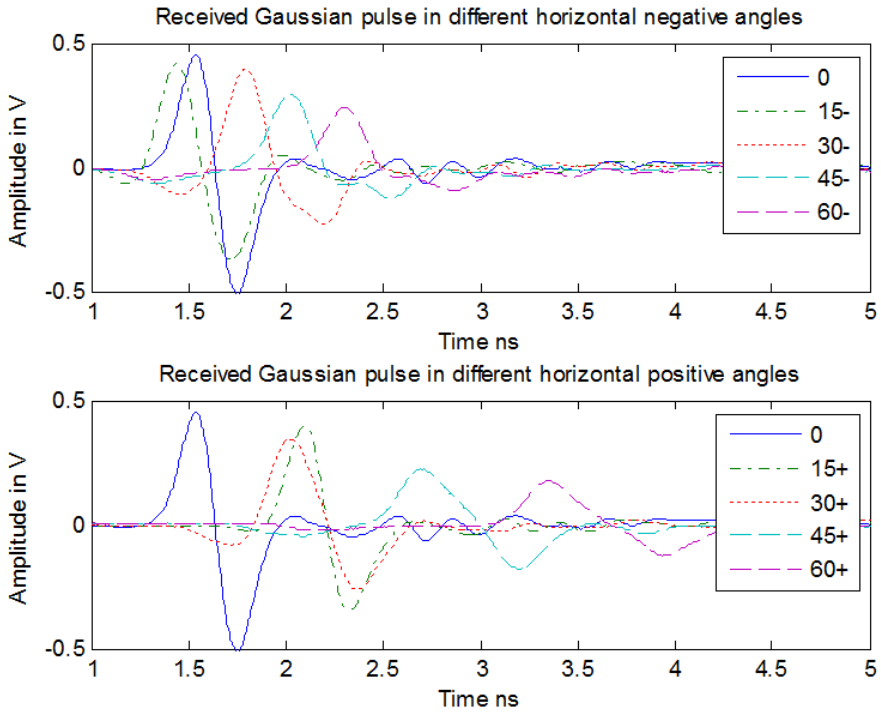

Figure 3-17 Received Gaussian pulse in different angles [Muq10].

Accordingly, the multi-atom directional dictionary is made up of different pulse shapes corresponding to the different received angles. Let the received pulse at any angle be called directional reference. For the measurements in hand, we have nine directional references where the transmitter and the receiver antenna are kept at a fixed height and

fixed position. The received antenna is, then, rotated along the elevation angle by 15^0 step, thus the measurements are performed at the angles of $0^0, \pm 15^0 \pm 30^0 \pm 45^0 \pm 60^0$.

In a similar way to Section 2.2.2, each directional reference will be shifted along the signal length to compose the directional dictionary. Denote the atom of the directional dictionary by ψ given by following

$$\psi_{i_j} = p_i(t - j\Delta) \quad i = 1,2, \dots ,9 \; ; \; j = 0,1,2, \dots \left\lfloor \frac{N - l_i}{\Delta} \right\rfloor. \tag{3-5}$$

The first subscript, i, indicates the directional reference number, and the second subscript. j, indicates the amount of shift. $p_i(.)$ is the i^{th} directional reference, Δ is the minimum step shift, and l_i is the length of the i^{th} directional reference. Since we have nine directional references, the first subscript is varying from 1 to 9. Subsequently the directional dictionary can be represented as

$$\Psi = \left[\psi_{1_0}(t), \dots , \psi_{1_{N-l_1}}(t), \psi_{2_0}(t) \dots , \psi_{9_{N-l_9}}(t)\right]. \tag{3-6}$$

An illustrative diagram of the resultant dictionary is shown in Figure 3-18. The multi-atom directional dictionary can also be viewed as multi-dimensional dictionary or as being built up of sub-dictionaries of all references.

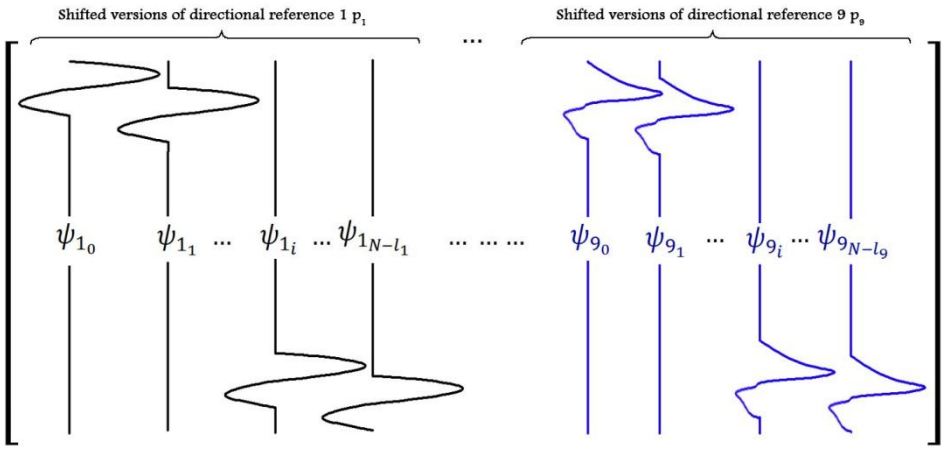

Figure 3-18 Illustration of the directional dictionary.

Using the directional dictionary gives MP higher chance to find atoms that have large correlation to the received signal, as well as increases the sparsity of the UWB signals.

Having defined the directional dictionary, it is the time to use it as a sparsity domain to reconstruct a realistic UWB signal. Figure 3-19 show the reconstructed signal using the multi-atom directional dictionary. The reconstruction indeed has improved, and the normalized error is now less by more than 51 percent compared with the reconstruction error in the case of boresight dictionary in Section 3.4.2.2. The normalized error is now 0.24 and the MSE= 1.27×10^{-4}. In Figure 3-20 the similarity between the reconstructed signal and the original is notable.

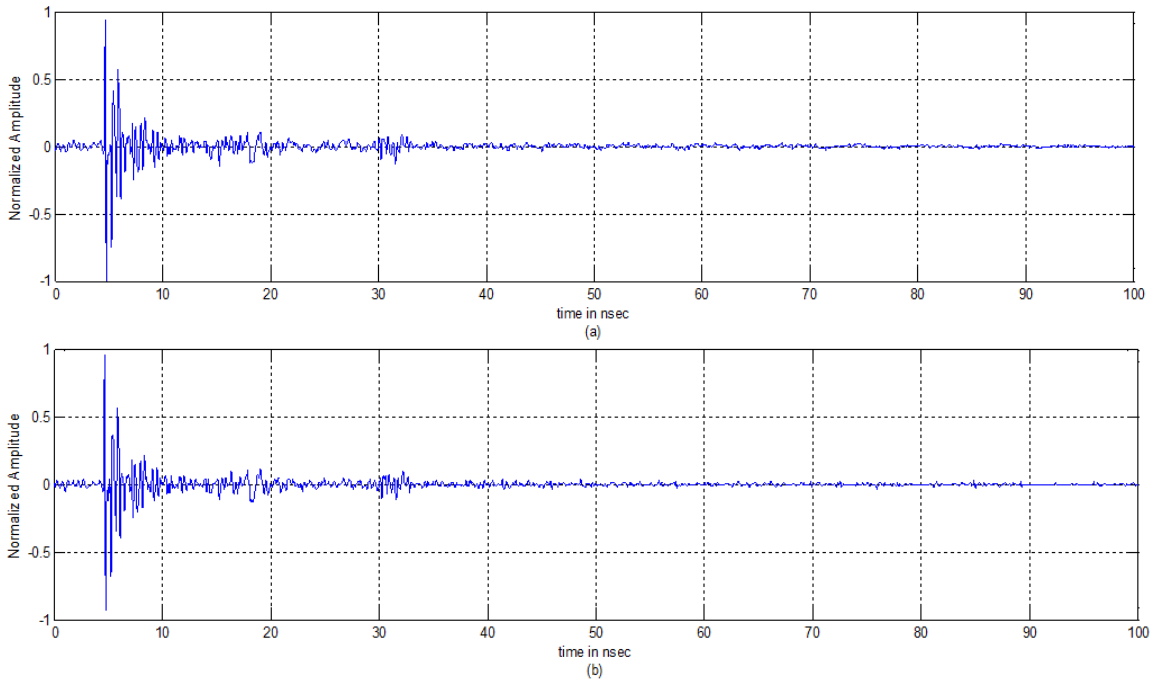

Figure 3-19 (a) Original (b) Reconstructed signal using directional dictionary.

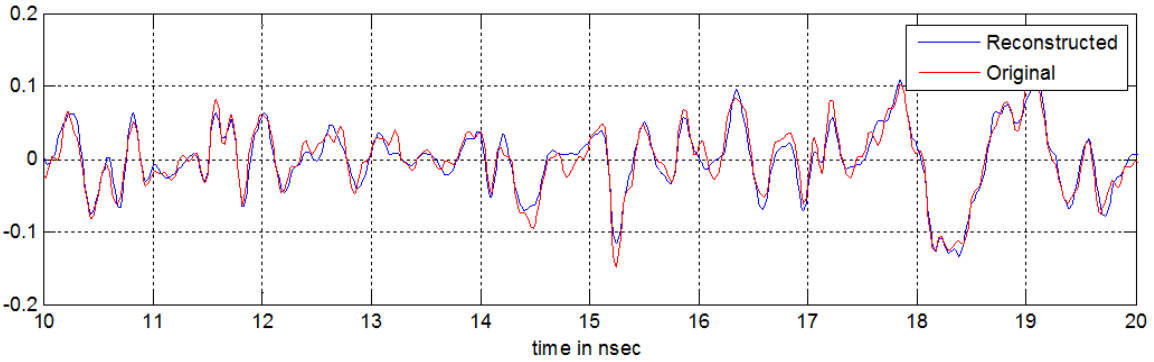

Figure 3-20 Zoomed version of Figure 3-19.

The same results were verified by simulation using the directional model. We made use of the simulated waveform in Figure 3-4 to be atoms in the simulated multi-atom dictionary. This dictionary is then used for reconstruction. The original and the reconstructed signals are shown in Figure 3-21. The normalized error is 0.0487 and the MSE is 2.19×10^{-8}. As a result of the noise free profiles, the reconstruction error of the directional model is much less than the measure directional dictionary. Figure 3-22 shows visually the quality of the reconstruction.

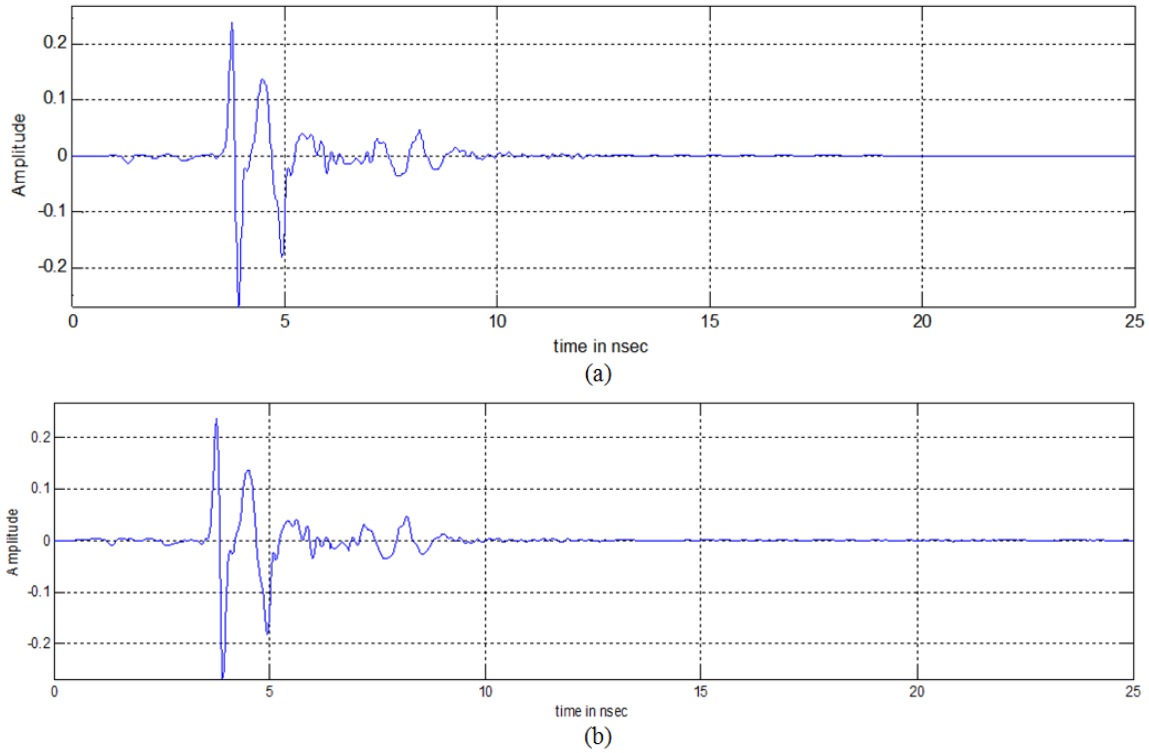

Figure 3-21 (a) Original signal (b) Reconstructed Muqaibel Model signal using (simulatied directional dictionary).

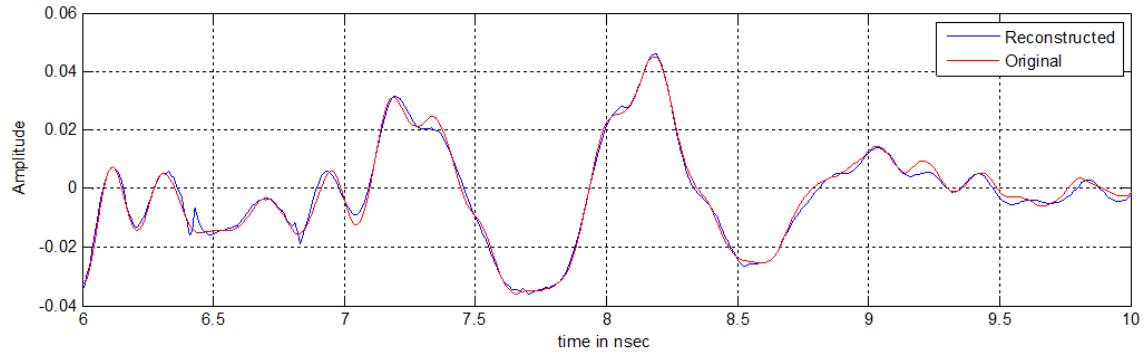

Figure 3-22 Zoomed version of Figure 3-21.

An intuitive question might be raised; do all the directional references contribute by the same amount of energy? Muqaibel in [Muq10] showed that many components from the measurement profiles are identified as having a large elevation angle of arrival. This fact can be proven in our approach of multi-atom directional dictionary by analyzing the output vector "Θ" of the MP algorithm. Since the mission of the MP algorithm is to allocate the strongest atoms in the dictionary and then provides the contribution amount of

all atoms as vector "Θ". Consequently, we can analyze the vector Θ to get the number of occurrence of each directional reference, as well as the amount of that contribution.

Figure 3-23 depicts the number of occurrence and the amount of contribution of each directional reference, where the positive and negative references of the same angel have been combined.

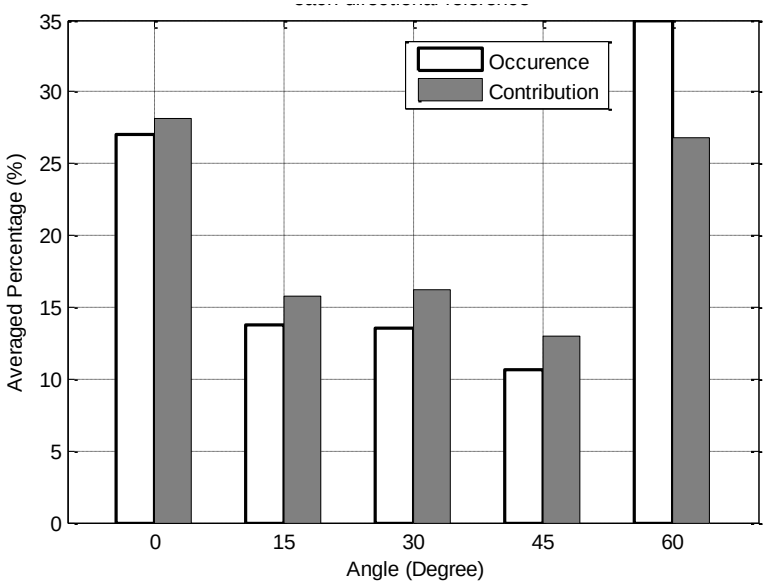

Figure 3-23 Number of occurrence and the amount of contribution of each directional reference.

It is inferential that the directional reference of 60 degree has the largest number of occurrence; on the other hand, the directional reference of zero degree contributes more than the any other reference, even though it has fewer occurrences than the one of 60 degree. This is an intriguing result, because the first and the strongest paths have to be in the shortest path. The late arrivals which have weaker energy and more temporal dispersion match the dispersion of 60 degree reference.

3.4.2.5 Strongest Atoms Directional Dictionary

Although the complexity due to the demand of high sampling rate has been reduced, the computational requirement in MP algorithm has been increased as a consequence of the large size of multi atom dictionary. The complexity of MP can be approximated to $\mathcal{O}(CMNT_0)$ [Mdu05], where M is the number of measurement, T_0 is the maximum iterations, N is the number of samples in the UWB signal, and C is a constant depends on the dictionary (Ψ) size. In case of multi atoms the size of the dictionary, and hence C, grows linearly with the number of atoms. The complexity of MP increases linearly as the size of the used dictionary. If we assume that the durations of all atoms in a nine atoms dictionary are equal, the complexity in this case is nine-fold of the boresight dictionary.

Since the multi atom directional dictionary is composed of sub-dictionary of each directional reference, hence we can reduce the complexity of MP by rebuilding a new dictionary out of the strongest contributed references, i.e. the references of zero and sixty degree in our case.

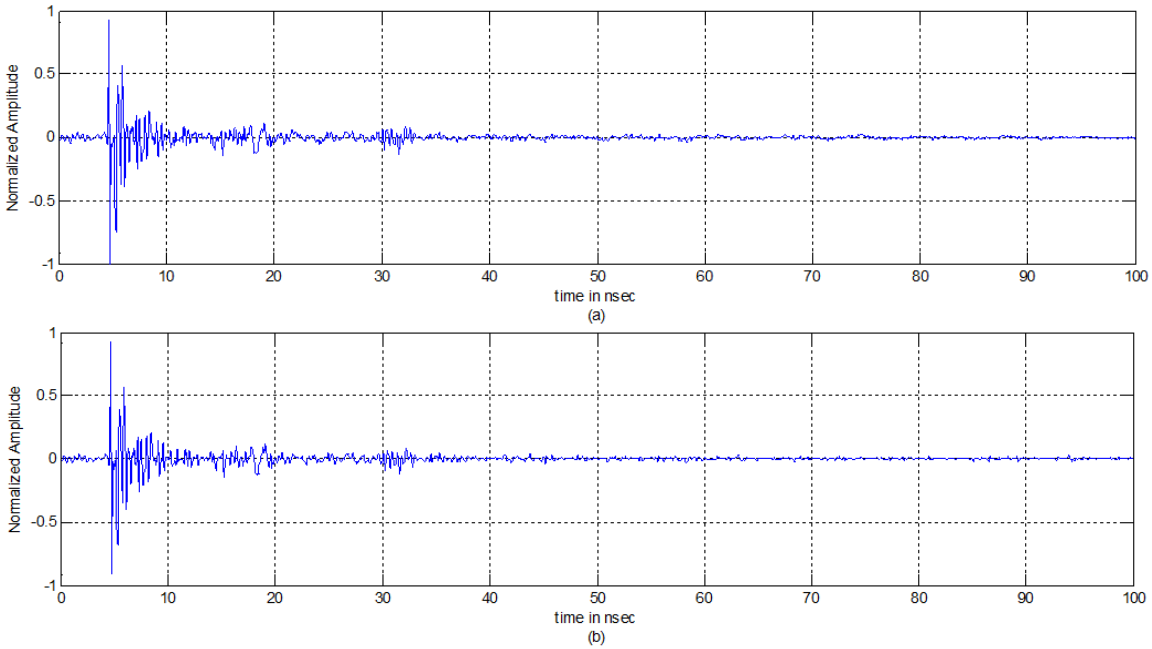

Figure 3-24 (a) Original signal (b) Reconstructed signal using the strongest atoms

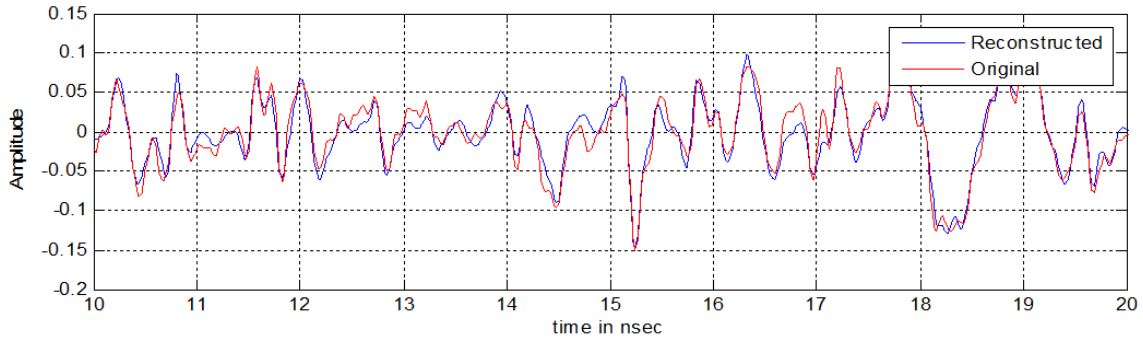

Figure 3-25 zoomed version of Figure 3-24

The reconstructed signal using the strongest atoms dictionary is shown in Figure 3-24. Notably, the normalized error is 0.209 which is very close to the error when using the full multi-atom directional dictionary.

Although we have neglected the weak references and removed their dictionaries, the reconstruction error did not increase dramatically from the error in Figure 3-19. Speaking in numbers, the amount of contribution of the neglected directional references is 45 percent of the reconstructed signal; however this does not mean that we are not able to capture this amount of the signal energy. Instead, MP will find the best match in the

existing references, leading to a small error due to the difference in shape. Accordingly, using the strongest directional references does not adversely affect the reconstruction capability and it definitely reduces the complexity of MP algorithm. Using more than one dictionary with atoms having different expected shapes improves the reconstruction dramatically.

3.5 Results and Analysis: Reconstruction Quality

In this section, we present the reconstruction results for all available practical profiles in a statistical sense. All the proposed methods are evaluated in reconstructing measured profiles. The directional model profiles are used for the case of the boresight-signal dictionary, the multi-atom directional dictionary, and the strongest path directional dictionary. The reconstruction ability of CS is a function of the number of random projections i.e. the sampling rate [Can06], [Can08], [Don06], hence, the normalized error of the reconstruction is plotted versus sampling frequency. For the purpose of fair comparison, all signals have the same length. MP termination criteria have been selected according to Section 2.3. The practical results are compared against the theoretical (optimum) result obtained in 2.4 for the case of IEEE 802.15.4a model.

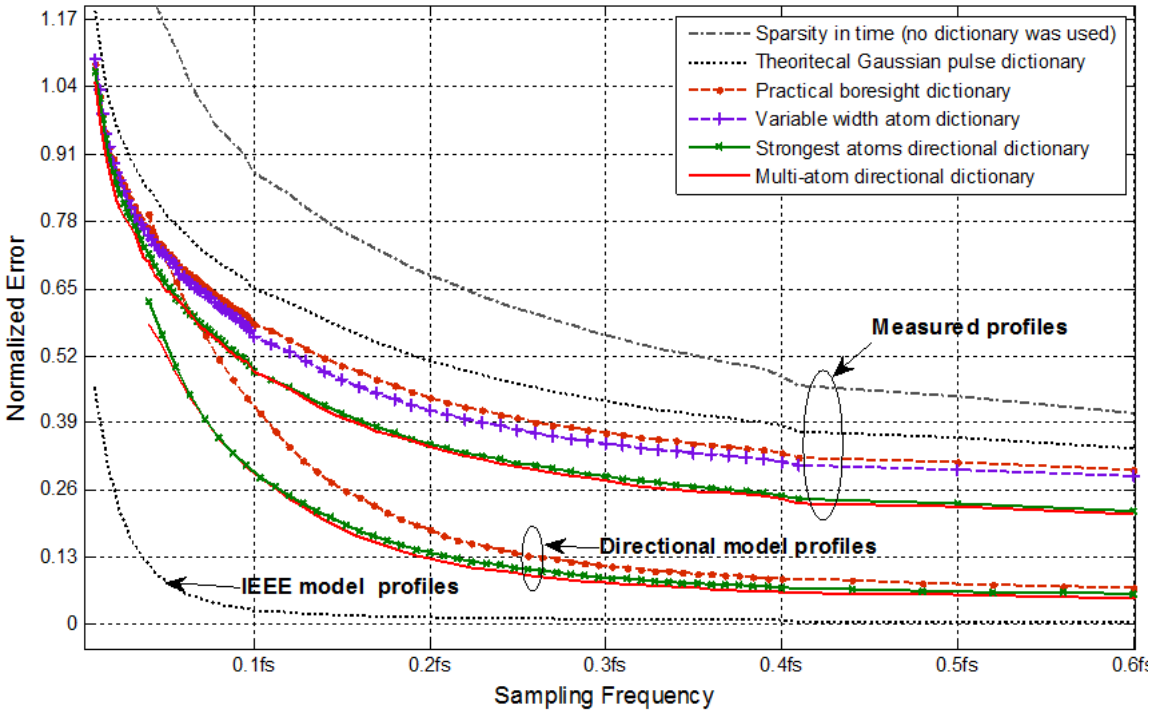

Figure 3-26 Reconstruction error of practical LOS profiles versus sampling frequency incensement.

It is observable from Figure 3-26 that the increment in sampling frequency enhances the reconstruction quality in all approaches. The largest reconstruction error occurs in the case of time sparsity assumption, where no dictionary was used. The error is reduced by useing Gaussian pulse-based dictionary, but it is still relatively high. Since they are more practical, the boresight-based dictionary and the variable width atom dictionary enhanced the reconstruction from the case of Gaussian pulse-based dictionary.

Significant reconstruction improvement is achieved by using the directional dictionaries, where the error in the case of multi-atom dictionary and the strongest atom dictionary is the least one in contrast to the error using the other dictionaries. The dictionary of the strongest atoms performs very closely to the multi-atom dictionary. The variable width dictionary does not consider the change in pulse width, hence its performance worse than the directional dictionaries, but it is still better than boresight based dictionary.

Due to the large similarity between the dictionary atoms and the profiles components, the error in IEEE curve declines faster in low sampling frequency. Since the directional dictionaries do not include the arrivals from all angles, the decline in practical profiles is less.

Since the profiles of the directional model are noiseless, (unlike the practical profiles), the behavior of the directional model is better than the measured profiles, and they almost emulate the measured profiles when noise is added

In order to examine the behavior of the practical dictionaries to reconstruct the IEEE profiles, we reconstruct the IEEE profiles using the strongest atoms directional dictionary that has the boresight and 60^0received waveforms. Then merge to the strongest atom dictionary to the Theoretical Gaussian dictionary. Figure 3-27 shows both cases compared with the case of the theoretical Gaussian dictionary behavior.

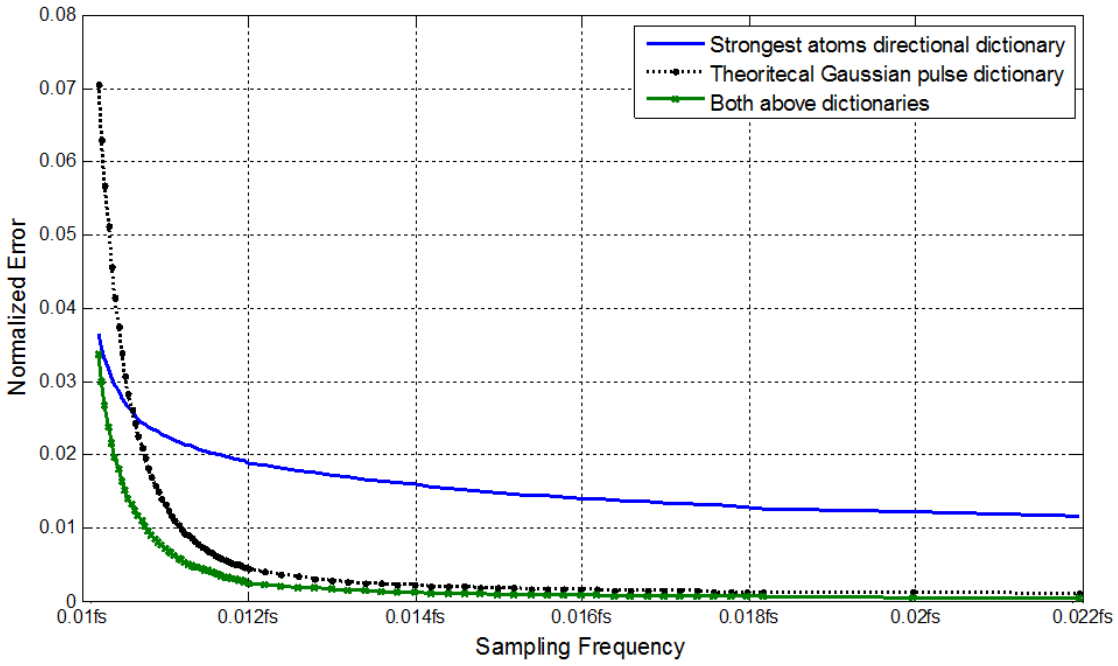

Figure 3-27 Behavior of the practical dictionaries to reconstruct IEEE profiles.

.

Using the strongest atom dictionary to reconstruct the IEEE profiles is better than the using the Gaussian pulse dictionary, especially in the range of low sampling frequency. This can be interpreted as; the interfering waves might results in a change in pulse shape that matches a practical atom. Consequently, the sparsity of IEEE has increased in strongest atom dictionary.

3.6 Chapter Summary

Firstly, we followed the hypothesis that the UWB signals are shifted and scaled version of the theoretical Gaussian signal. Building a dictionary based on this hypothesis works acceptably and ideally for the case of by IEEE 802.15.4a model. Where, we can reconstruct the signal by only 0.2 of the original sampling frequency, but this does not work well for the practical profiles. Changing the dictionary to be based on the received signal at zero degree improves the accuracy of the reconstruction. Since, the practical profiles are made up of different pulse shapes unlike the theoretical one; we first introduced dispersion then we built dictionaries based on the received waveforms at different angles.

In order to reduce the computational efforts in the directional reconstruction, we can restrict the dictionary atoms to the strongest contribution atoms which perform very closely to the multi-atom dictionary, and hence, reduce the complexity. The multi-atom dictionaries are used to improve the detection in the next chapter.

Figure 3-28 serves as a roadmap for the work in this section. From top to down, the quality of reconstruction improves and the complexity of the dictionary may or may not increase. The used methodology is indicated within rectangles, while, the oval shapes depicts the issues associated with the corresponding dictionary.

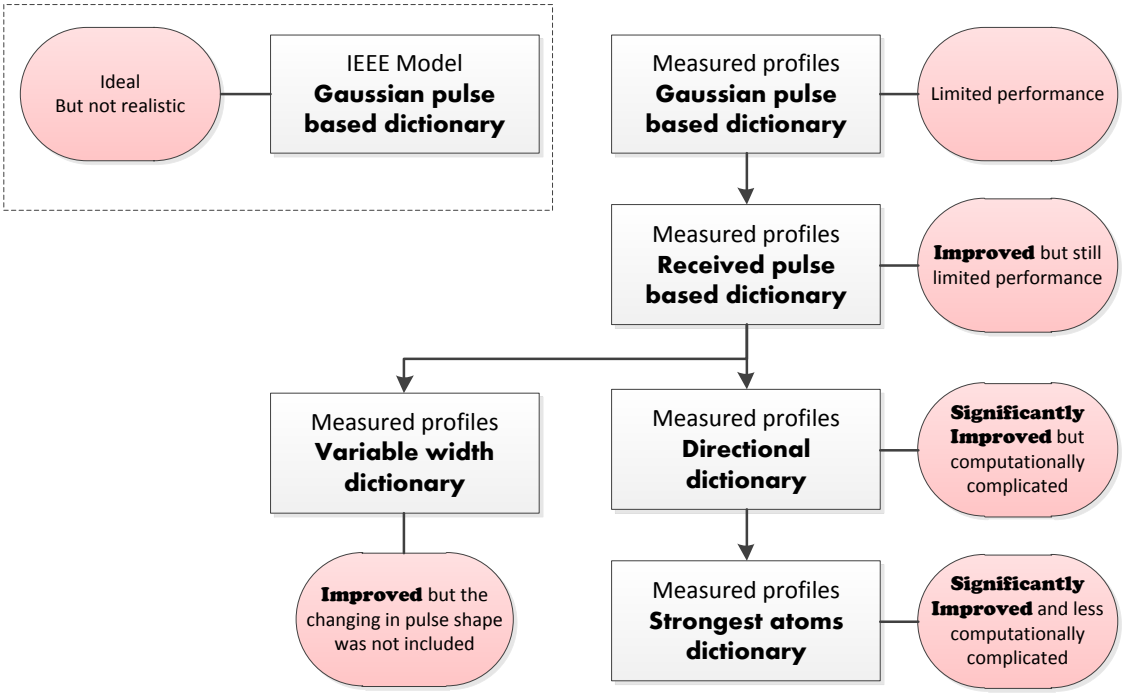

Figure 3-28 Demonstrative flowchart for pre-designed dictionaries.

CHAPTER 4

4 PRACTICAL UWB CHANNEL ESTIMATION BASED ON CS

In previous chapter we have evaluated and improved the ability of CS in reconstructing practical UWB signals. In this chapter we concentrate on channel estimation.

The required sampling rate for accurate UWB channel estimation is very high, in some cases it exceeds 60 GHz [Lot02]. CS implementation can be extended to a broader range of signal processing and statistical inference tasks. CS is well suited for UWB channel estimation.

In Chapter 2 CS has been applied to the IEEE model of UWB signal. Chapter 3 proposed practical-based dictionaries to enhance the reconstruction performance for practical UWB profiles. In this Chapter, we take advantage of CS and the proposed dictionaries to estimate the UWB channel in practical environments. This takes us to the next part of the thesis.

4.1 Introduction to UWB-CS Channel Estimation

By looking at the UWB channel, given by (2-2), we realize that this channel model consists of a set of parameters as $\{\alpha_i, \tau_i\}_{i=1}^{L}$ which represent various propagation paths that have to be well estimated. The number of multipath components L could be quite large, leading to large time dispersion in the transmitted pulse [Ree05]. The average number of multipath for LOS propagation is approximately 1160 paths in an indoor environment and within 300 Nano second, while the average number of paths capturing 85% of the energy is just 70 paths. Hence, many of those paths are negligible. Thus, determining the most significant paths, indicated by L_c, and eliminating the weak paths leads to a reduction in the channel complexity [Lot02].

The MP signal reconstruction approach, discussed in Section 2.2.2, is a searching process in the dictionary Ψ for the strongest paths (atoms) embedded in the "the residual signal". The path contribution is dropped from the residual signal. If the targeted residual error is not reached, the search and drop process is repeated T_0 iterations as shown in Figure 1-4. When MP is used for channel estimation, the outcome is a vector that is composed of the contribution of atoms corresponding to various propagation paths. This vector is expressed as

$$\Theta = [\theta_1, \theta_2, \dots, \theta_z]^T, \tag{4-1}$$

The received signal is the weighted sum of the atoms in the dictionary, mathematically written as

$$r_x = \sum_{i=1}^{Z} \theta_i \psi_i(t)\,, \tag{4-2}$$

where $\theta_i$is an approximation of the path gain related to the i^{th} propagation path, and the atom ψ_i in the dictionary Ψ is a shifted version of the transmitted pulse. Furthermore, the path delay is determined by observing the delay location of the i^{th} component in the received UWB signal. Accordingly, we can derive a technique to estimate the channel parameters out of vector Θ [Par07], i.e. the path gain and the corresponding delay of the most significant paths via MP algorithm. Figure 4-1 (a) shows a sample impulse response based on the IEEE 802.15.4a for 100 nsec. The estimated channel response, Θ, using transmitted pulse multipath based dictionary at half the sampling rate is shown in Figure 4-1 (b).

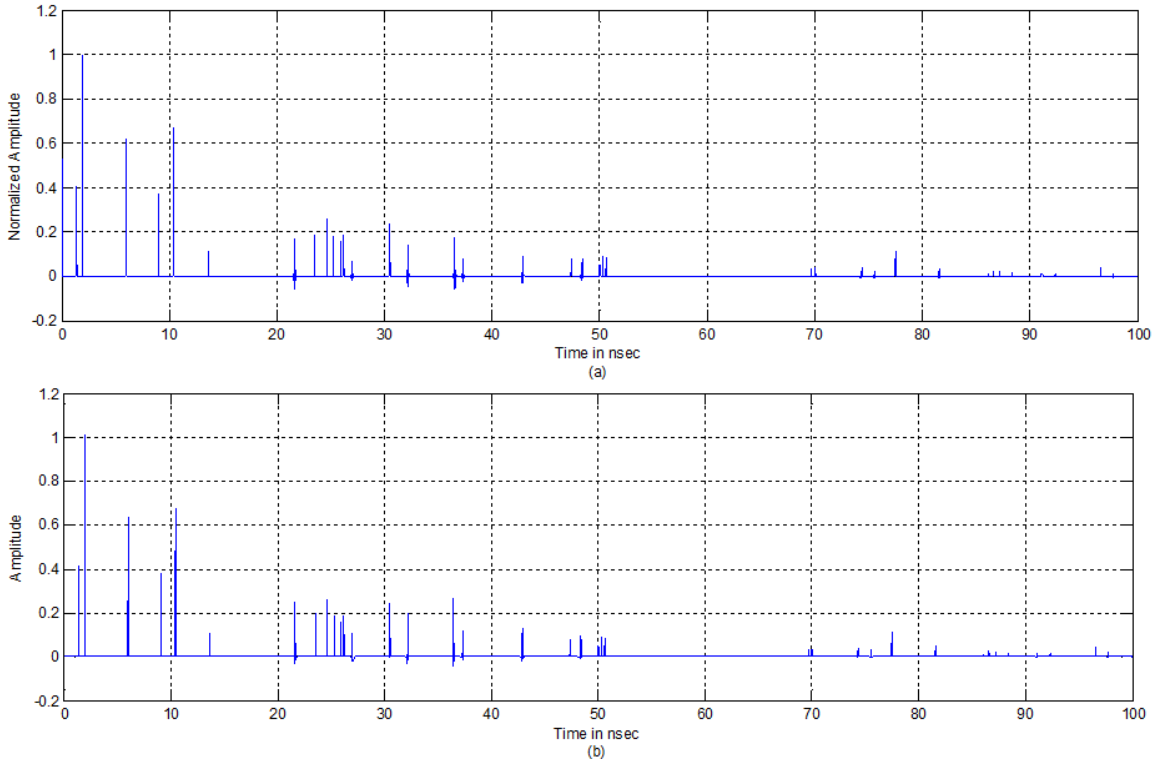

Figure 4-1 Reconstructed IEEE 802.15.4a channel impulse response (a) Original, (b) Reconstructed.

Consider the sparse vector Θ given in (4-1) obtained by MP algorithm. To start with the strongest paths, we sort θ_k in descending order as for $k = 1, \dots, Z$ to be the set $\{|\theta_1|, |\theta_2|, \dots, |\theta_Z|\}$. Accordingly,$\theta_1 = \max\{|\theta_1|, |\theta_2|, \dots, |\theta_Z|\}$ and $\theta_Z = \min\{|\theta_1|, |\theta_2|, \dots, |\theta_Z|\}$. Let $\ell_k$be the index in the sparse vector of the k^{th} sorted element. Therefore, the estimated channel parameters for the i^{th} propagation path are

$$\begin{aligned} \hat{\tau}_i &= \ell_i \Delta \\ \hat{\alpha}_i &= \theta_{\ell_i}, \end{aligned} \tag{4-3}$$

where, $\hat{\tau}_i$ and $\hat{\alpha}_i$ are the path delay and the path gain respectively, for $i = 1,2, \dots, L_c$. Δ is the minimum shifting step used to build the dictionary. The number of MP iteration,T_0, can be set to L_c to recover the strongest paths of UWB channel. The number of iteration in channel estimation is much less than needed signal reconstruction. To illustrate this idea, Figure 4-2 (b) shows only 10 taps of the channel impulse response. These taps are obtained with 10 iterations, i.e. $T_0 = 10$. The energy captured by these 10 paths is 90 percent of the full channel realization.

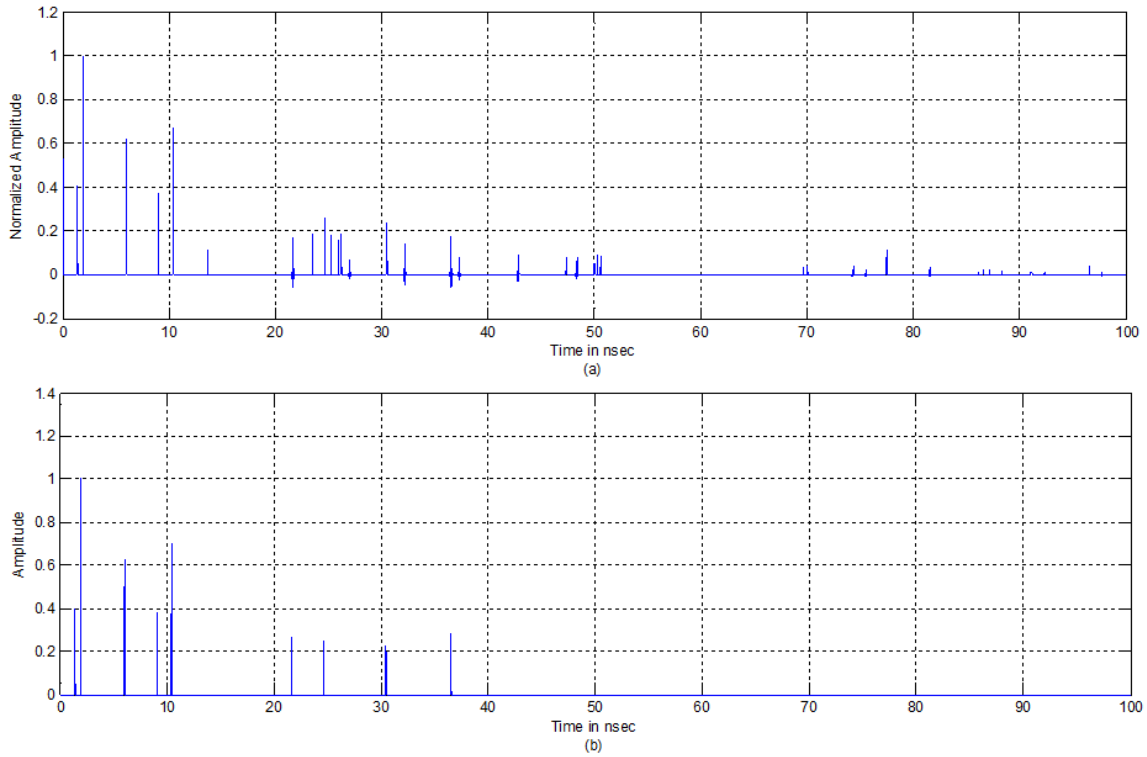

Figure 4-2 CS-Estimated channel impulse response utilizing 10 strongest paths (a) original, (b) CS-estimated.

The same holds true for the case of practical profiles. Consider the boresight dictionary defined in Section 3.4.2.2, the sparse vector, Θ, represents the impulse response of the practical channel. Figure 4-3 shows the reconstructed practical signal using $T_0 = 20$, the normalized error is 0.44. (The large value for the error is due to the fact that we are comparing with a noisy signal even if no arrivals are present. A more meaning full comparison is when the signal is compared with the one reconstructed with large number of profiles)

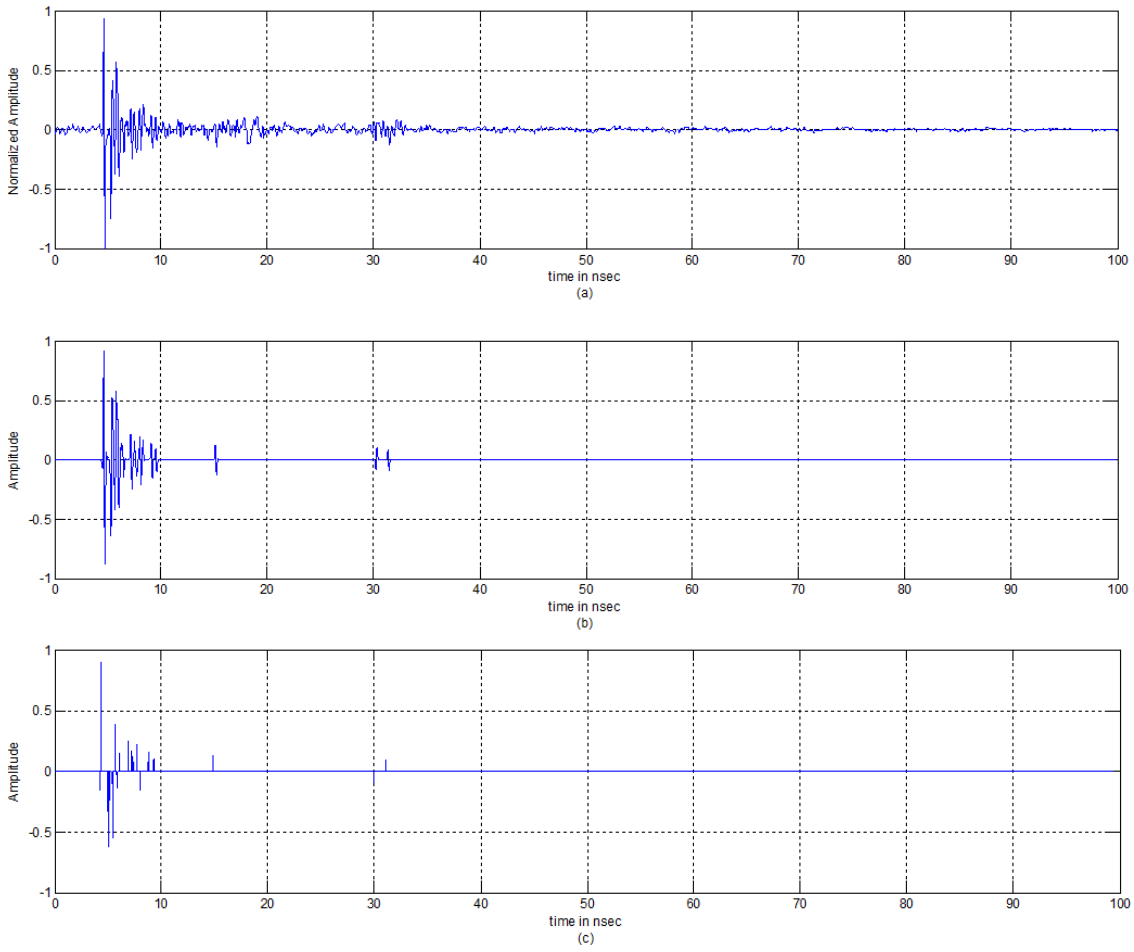

Figure 4-3 CS-Reconstructed practical profile utilizing 20 strongest paths (a) measured profile, (b) CS-Reconstructed profile (c) CS-estimated impulse response.

The CS-estimated impulse response for the practical profile of Figure 4-3 (a) is depicted in Figure 4-3 (c). The amount of energy captured by 20 paths is 80 percent relative to the energy of the impulse response when 400 paths are considered.

Unlike the boresight-based dictionary, the sparse vector of the multi-atom dictionary does not directly represent the impulse response of the channel. Because multi-atom dictionary consists of sub-dictionaries, the sparse vector,Θ, will also consist of many parts. It starts by the contribution of the first dictionary, followed by the contribution of the second dictionary, and so on. For example, if we use nine sub-dictionaries, the length of the vector, Θ, is nine-fold of the case of one dictionary. Figure 4-4 shows the sparse vector, Θ,

of the multi-atoms dictionary, where the number of iteration,T_0, is 400. The strongest path appears in the boresight dictionary. The -60^0dictionary has many small paths as a result of the late arrivals with more pulse dispersion.

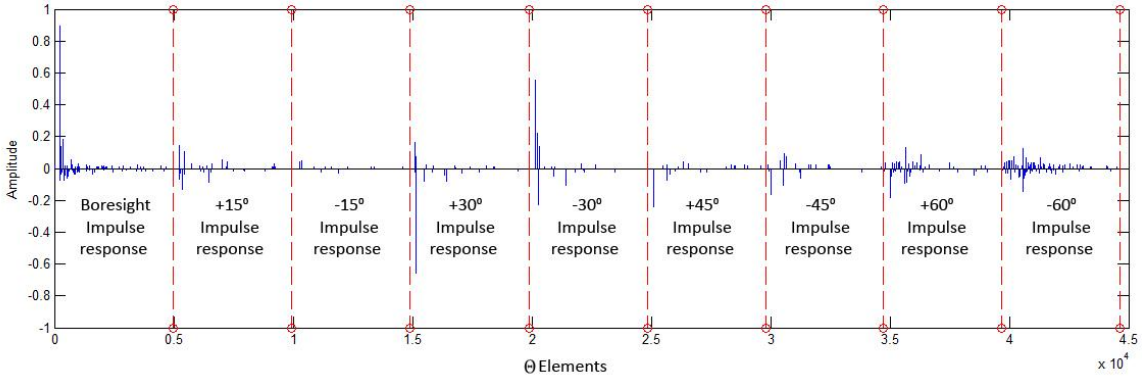

Figure 4-4 The sparse vector of the multi-atom dictionary Θ, resultant by 400 iterations.

Therefore reconstructed signal is the algebraic sum of the corresponding atoms of the multi-atom dictionary scaled by the path gains and properly time aligned.

To select the strongest 20 paths, we can run the MP algorithm for only 20 iterations. The resultant sparse vector, which captures 86 percent of the energy available in Figure 4-4, is depicted in Figure 4-5.

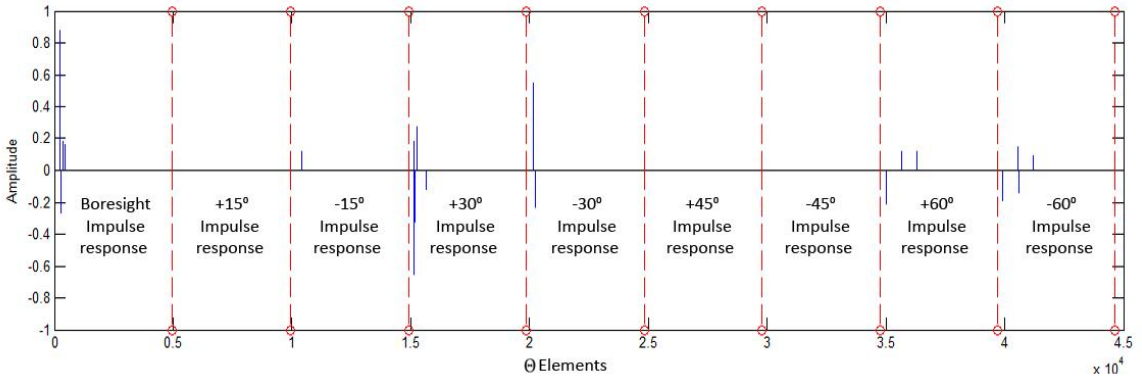

Figure 4-5 Sparse vector of the multi-atom dictionary Θ resultant by 20 iterations.

We have shown that MP algorithm recovers the strongest paths through the first little iterations, thus large amount of complexity can be reduced, and great amount of energy

can be captured. When using a dictionary with multi-atoms, the corresponding atom of each element in the spars vector has to be well considered.

4.2 UWB Signal Model

This section describes the signal model that is used in designing CS based UWB receiver. At first, consider a peer-to-peer UWB communication system transmitting k binary information where each bit is represented by N_f ultra-short pulses with a symbol duration of T_s, thus the transmitted signal can be expressed as

$$s(t) = \sum_{k} b(k) \sum_{j=0}^{N_f-1} p\left(t - jT_f - kT_s\right), \tag{4-4}$$

where $T_f = \frac{T_s}{N_f}$ is the frame time, each symbol time requires N_f frames as shown in Figure 4-6. The amplitude of the pulse stream is modulated by the binary information symbol, $b(k) \in \{-1, +1\}$, hence we are employing binary phase modulation [Ree05]. $p(t)$ is the pulse used to convey information given by (1-3) with a duration of T_p. Since we are assuming there is no overlapping, T_p has to be much less than the frame time i.e. $T_p \ll T_f$ to allow enough time for full decay.

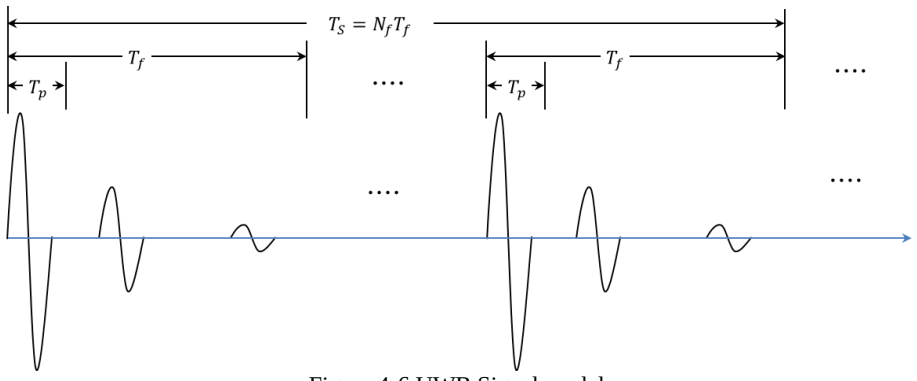

Figure 4-6 UWB Signal model.

Let the UWB channel be time invariant during N_s symbols, and the path gain and the delay in (4-3) remain constant during N_S symbol durations. In addition, let the maximum delay spread of the multipath channel be denoted by τ. To avoid the inter-pulse-interference between consecutive frames, T_f must be greater than $\tau + T_p$.

Therefore, the received UWB frame of the k^{th} transmitted information symbol can be expressed as

$$\begin{aligned} r_f &= b(k) \cdot p(t - kT_s) * h(t) + \eta(t) \\ &= b(k) \cdot \sum_{\ell=0}^{L-1} \alpha_\ell p(t - kT_s - \tau_\ell) + \eta(t)\,, \end{aligned} \tag{4-5}$$

where $*$ denotes the convolution operation, and $\eta(t)$ is the AWG noise with zero mean. As mentioned in Section 2.1, the received signal consists of a liner combination of the transmitted pulse, $p(t)$.

In order to extend the expression of a received frame in (4-5) to represent one symbol or more during the invariable time of the channel, the noiseless part of $r_f(t)$ in (4-5) can be periodically repeated every T_f second. Leading to

$$r(t) = \sum_{j=0}^{N_f-1} r_f\left(t - jT_f\right) + \eta(t). \tag{4-6}$$

4.3 CS Based UWB Receivers

The previous part of this work concentrated on the accuracy of CS to reconstruct UWB signal assuming that it is sparse in a pre-defined dictionary. Beyond signal reconstruction, CS capability can be extended to be an essential part of UWB receivers. For instance, the reconstructed UWB signal via CS can be used as a template in a correlator-based receiver [Wu06] or by means of CS based channel estimation.

Several approaches have been proposed to optimize the signal detection of UWB [Ree05]. In the following we briefly describe two receivers that are commonly used to exploit the multipath diversity of the UWB channel, Full Profile-Correlator and Rake receiver.

The **Full-Profile-Correlator (FP-Correlator)** receiver demodulates the information by correlating the UWB received frame, $r_f(t)$, with a pre-estimated frame, $\hat{r}_f(t)$. Therefore, the FP-correlator receiver is designed to have a frame-rate sampling. Figure 4-7 demonstrates the block diagram of the FP-correlator receiver.

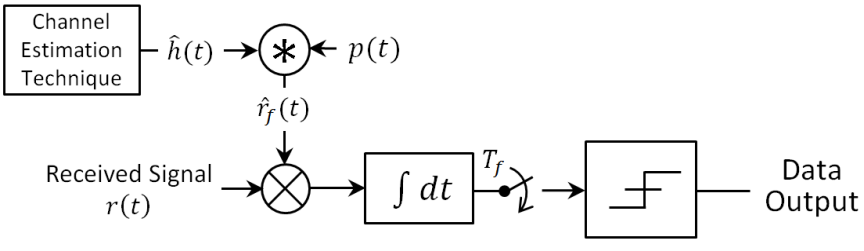

Figure 4-7 FP-Correlator.

Rake receiver, on the other hand, captures the significant amount of the energy found in the multipath components. This process is done by employing a number of fingers, L_r , to benefit from multipath diversity energy. Each finger has an adjustable gain and delay. The finger's outputs are consequently combined by one of the diversity combining techniques like the maximum ratio combining (MRC) [Wu06]. Figure 4-8 shows a Rake receiver with L_r fingers.

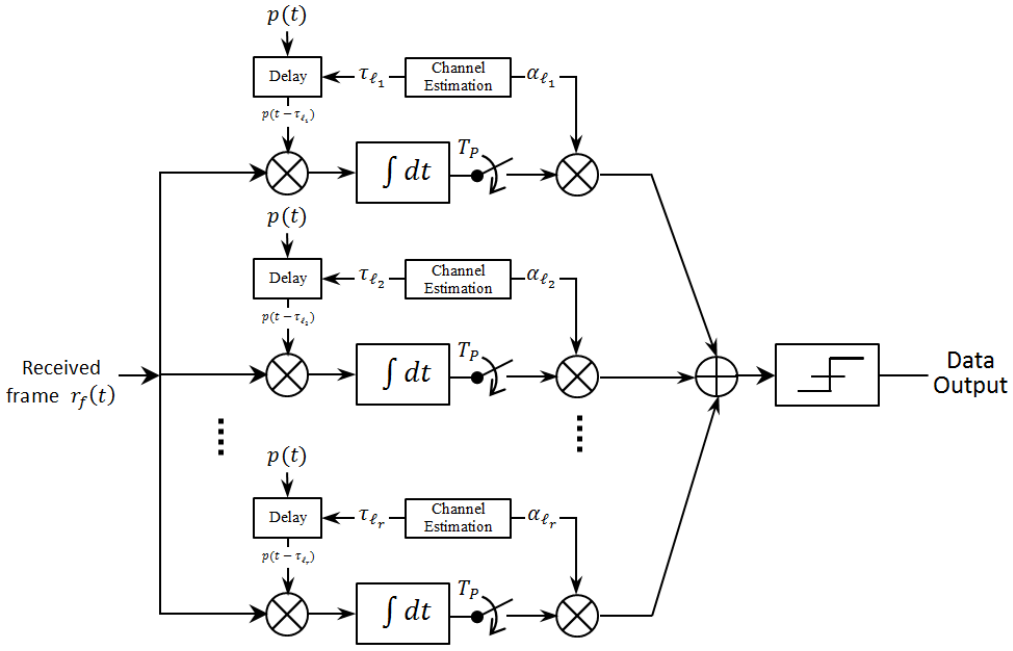

Figure 4-8 Illustrative block diagram of Rake receiver.

Channel estimation is necessary in both receivers, either to obtain the reference profile as in the FP-Correlator receiver, or to find the best values to adjust the finger parameters as in the Rake receiver.

The channel estimation approach in [Wu06] employs several transmitted symbols to estimate the optimal template in the analog domain. Where an analog delay units are used to delay and average a symbol-long received signal, leading to symbol-long channel estimation. This averaged symbol is used as a noisy profile reference in the FP-correlator

based receiver in order to demodulate the information at symbol-rate sampling. Likewise, in [Yan04], and [Liu04b] the channel estimation is done in an analog domain but with a frame-long training waveforms. Although, those approaches do not require high sampling rate, they consume high power in the analog delay part and do not support low data rate at the present time [Par07].

Estimating the path gains and the corresponding delays in the digital domain was done in [Lot02] [Wu06]. To achieve a reliable performance, the estimator requires at least 14-16 samples per pulse width, thus demanding a formidable sampling rate in order of tens of GHz [Qiu05]. Subsequently, it increases the complexity of the receiver design especially for large number of significant path as in NLOS cases. Additionally, this leads to the need for more precision and very accurate timing control, which is not suitable for current ADCs [Ree05].

In the following we present the signal model to be used in the simulations. Similar to the model used by [Par07], a packet consists of training symbols followed by information symbols. Every symbol is made up of frames and the frames are made of pulses. See Figure 4-9 for details.

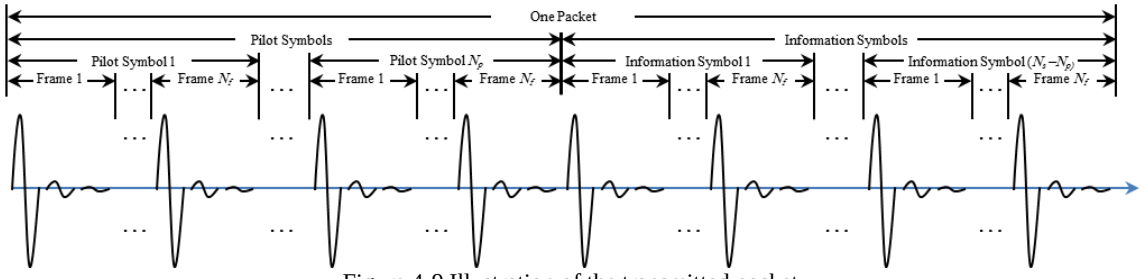

Figure 4-9 Illustration of the transmitted packet.

Let N_p be the number of training symbols (also called pilot symbols), transmitted at the beginning of the packet. This pilot symbols are randomly projected to provide the

measurement vector to the CS algorithm (MP) in order to produce the channel parameters. These parameters are used to generate the impulse response to be employed in both the FP-Correlator and in the Rake receiver as well. The rest of symbols in the packet ($N_s - N_p$) are information symbols.

To distinguish between pilot symbols and the information symbols, we may rewrite the UWB received signal in (4-6) in a detailed form

$$r(t) = \begin{cases} \sum_{k=0}^{N_w-1} b_p\left(\left\lfloor \frac{k}{N_f} \right\rfloor\right) \sum_{l=1}^{L} \alpha_l p\left(t - kT_f - \tau_l\right) + \eta(t) & \text{for } 0 < t \le T_w \\ \sum_{k=N_w}^{(N-N_p)N_f-1} b_i\left(\left\lfloor \frac{k}{N_f} \right\rfloor\right) \sum_{l=1}^{L} \alpha_l p\left(t - kT_f - T_w - \tau_l\right) + \eta(t) & \text{for } T_w < t \le N_s N_f T_f \end{cases}, \quad (4\text{-}7)$$

where b_p and b_i are the pilot and the information symbol respectively. N_w represents the total number of pilot frames, i.e. $N_w = N_p N_f$. T_w is the time duration of the pilot waveforms. Clearly, the upper part of equation (4-7) represents the training symbols, while the lower part represents the information symbols. Thus the number of waveforms used in channel estimation is $N_P N_f$ within T_w seconds.

Though the MP detection does not require perfect coherence [Wan07b], in this research we will build our simulation on the assumption of perfect time synchronization, and there is no overlapping between consecutive frames, i.e. $kT_f \le t \le (k+1)T_f$ for $k = 0,1,\ldots,N_f - 1$. Leading to a representation of a received pilot waveform in a k^{th} frame time as

$$r_k(t) = b_p\left(\left\lfloor \frac{k}{N_f} \right\rfloor\right) \sum_{l=1}^{L} \alpha_l p\left(t - kT_f - \tau_l\right) + \eta(t). \quad (4\text{-}8)$$

Upon this model of UWB signal, next we represent two UWB receivers that employ CS to estimate the channel and in turn demodulate the information.

4.3.1 CS-Full Profile Correlator

According to [Yan04] and [Wu06] the optimum template to be used in the detection stage in UWB receiver is the received signal itself given by (2-1). Recall that the actual received UWB signal consists of shifted and scaled versions of the transmitted pulse. The estimated profile is contaminated by AWG noise. Consequently, if we take random measurements from the received profile and pass them to MP algorithm, the reconstructed profile will be a noisy profile. Since we use N_w waveforms to estimate the reference profile, it is computationally expensive to run MP N_w times. Instead, we can take the random measurements after averaging the N_w pilot waveforms, leading to execute MP algorithm once every channel estimation period, hence less computation efforts and more mitigation of AWG noise.

Briefly, in the CS-FP-Correlator receiver, the reference template is obtained by receiving $N_w$waveforms, averaging them, taking random projected samples, and passing them to MP algorithm to reconstruct the reference template.

Since MP algorithm use the dictionary to reconstruct the UWB signal, illustrated in Section 2.2.2, the denoising operation is performed implicitly; where the dictionary is composed of atoms that are match to the transmitted signal and are noise-free. However, a

new type of errors may appear in the received pilot signal due to the spurious atoms that are wrongly identified as consequences of the AWG noise. The noise component in the projected signal may drive the MP algorithm to introduce redundant atoms in the reconstructed signal that does not exist in the original noiseless signal.

In order to minimize the number of the spurious atoms in the template, we can alleviate the AWG noise by increasing the number of pilot waveforms, N_w. Alternatively, we can threshold (cutoff) the averaged signal under the noise level before taking the random projection. This will cause a reduction in the matching processes in MP algorithm, where the weak arrivals will be clipped.

The channel is estimated by averaging the received pilot signals as following

$$r_p(t) = \frac{1}{N_w} \sum_{k=0}^{N_w-1} r_k(t), \tag{4-9}$$

where $r_p(t)$ is the averaged pilot signal, $r_k(t)$ is the received pilot waveforms defined by (4-8). The averaged pilot signal is randomly projected to produce the estimated channel. The reference profile, $\hat{r}_{CS}(t)$, is used as a template in the detection stage to demodulate the transmitted symbols. The major difference between the normal channel estimation approach in [Wu06] and [Liu04b] and the one with CS, is that the CS-FP-Correlator performs template reconstruction from the random projected signal which has been sampled by a significantly reduced rate.

As soon as the referenced template is estimated, it is used in the detection stage of the receiver, before the decision stage. Since N_f frames represent one symbol, the decision is

statistically taken for the k^{th} symbol by adding up the N_f correlator output related to the information symbol as

$$z(k) = \sum_{j=0}^{N_f-1} \int_{jT_f+kT_f}^{(j+1)T_f+kT_f} r(t)\hat{r}_{CS}\left(t - jT_f - kT_s\right)dt\,, \qquad (4\text{-}10)$$

where $\hat{r}_{CS}(t)$ is the reference frame estimated via MP, and the correlation between the UWB received signal and the template is done inside the integration. An illustrative block diagram of CS-FP-Correlator is shown in Figure 4-10 and depicts the CS-channel estimation stage.

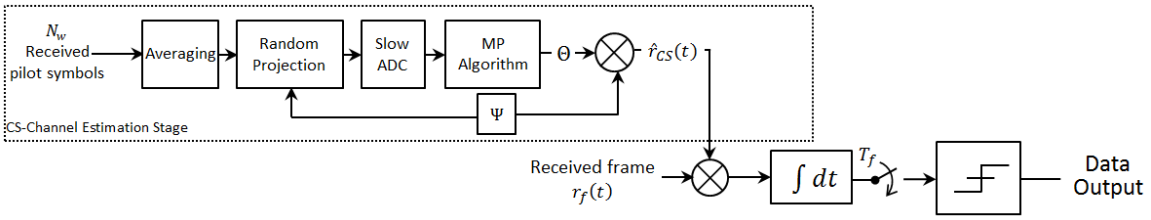

Figure 4-10 CS-FP-Correlator Block diagram.

4.3.2 Rake Receiver Based on CS

Full profile correlation is costly. It is more practical to correlate with individual path arrivals. The idea behind Rake receivers is to exploit the energy available in the multipath. The decision does not depend only on the first or the strongest arrival.

Due to the extremely narrow pulse duration, UWB channels have a lot significant resolvable multipath components. Hence, it is natural to use Rake receiver for UWB channels [Lot02], [Ree05]. Next we evaluate the performance of MP algorithm channel estimation for Rake receiver when practical channels are considered.

Consider the pilot signal model defined in (4-8) , where k indicates the current pilot signal for $k = 1,2, \dots, N_w$, where $\alpha_l$and $\tau_l$are the channel taps to be estimated. Since we employ N_w. As in the FP-Correlator receiver, a wrong estimation might occur due to the noise component in the received pilot signals. It will cause the MP algorithm to add mistaken atoms in the recovered pilot signal, and hence increases the error in the channel estimation.

Similar to what has been done in the Section 4.3.1 to alleviate the effect of AWG noise; we can take the measurements out of the averaged received pilot profiles and use them in MP algorithm to estimate the channel parameters. Hence, by means of CS we can estimate the channel using the random projections of the pilot signals, leading to a reduction in the computational cost and alleviating the noise effect.

Though the advantage of the Rake receiver is to collect the energy distributed in different paths, the complexity of Rake receiver is proportional to the number of its fingers. Usually, the first few paths in UWB channels have the greatest amount of energy. We restrict the significant number of paths to L_c to end up with channel parameters of $\{\hat{\alpha}_\ell, \hat{\tau}_\ell\}|_{\ell=1}^{L_c}$. The resultant vector of MP is the estimated delays and path gains related to the strongest propagation paths. These parameters are then used to adjust the tap delay and the gain in Rake's finger.

The CS Rake based receiver (CS-Rake) feeds the received information signal, given by (4-7), to the L_c fingers, each finger consists of a correlator supplied by a template of the transmitted pulse, scaled by $\hat{\alpha}_\ell$, and delayed by $\hat{\tau}_\ell$, i.e. $\hat{\alpha}_\ell\ p(t - \hat{\tau}_\ell)$. The outputs of these correlators represent the energy available in the selected paths, to be combined by

maximum ration combining (MRC) [Alo99]. The resultant output is used to detect the k^{th} information bit that was transmitted during the j^{th} frame. The output of the MRC can be expressed mathematically as

$$z_r(k,j) = \sum_{\ell}^{L_c} \hat{\alpha}_\ell \int_{kT_s+jT_f+\hat{\tau}_\ell}^{kT_s+jT_f+\hat{\tau}_\ell+T_p} r(t)p\left(t - kT_s + jT_f + \hat{\tau}_\ell\right)dt. \tag{4-11}$$

As in the right hand side of equation (4-11), correlation is employed to capture the signal energy by matching the template to L_c delayed versions.

For the case when multi-atom dictionary is used, another configuration has to be considered. The resultant sparse vector, Θ, provides three channel parameters rather than two, the gain $\hat{\alpha}$, the delay $\hat{\tau}_\ell$ and an index of the corresponding pulse shape. The CS-Rake receiver is shown in Figure 4-11. The pulse-shape-selector block utilizes the pulse index received from the channel estimator to provide the appropriate pulse shape.

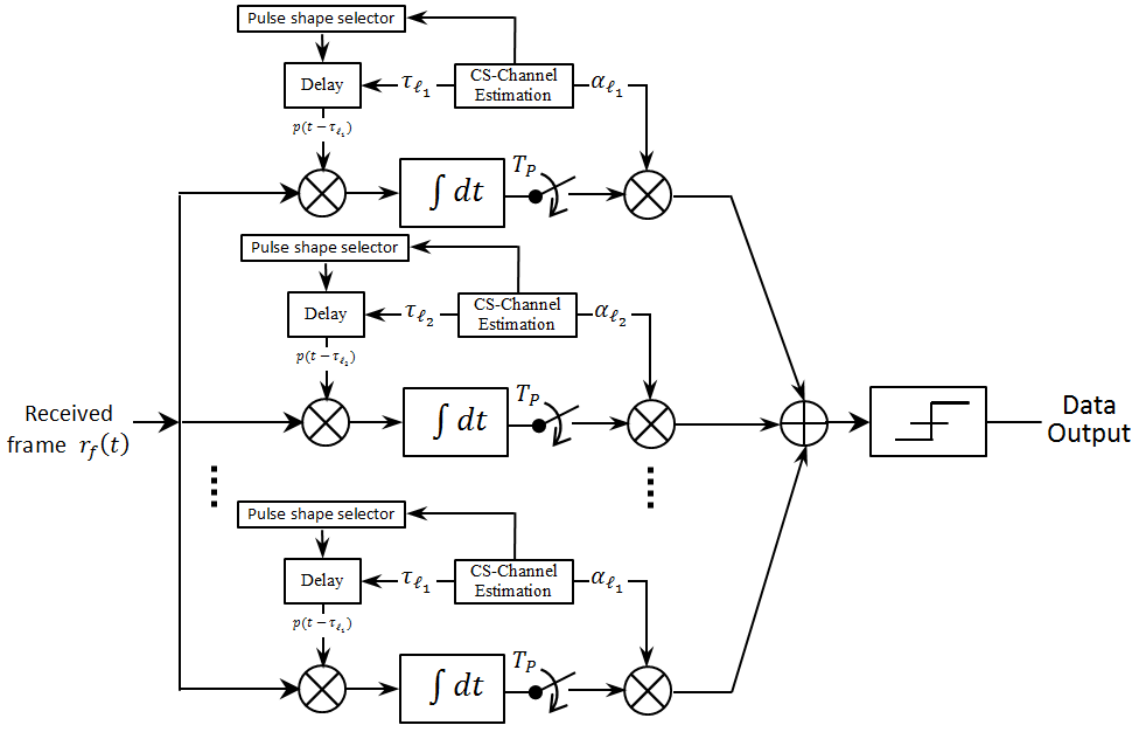

Figure 4-11 CS-Rake Receiver.

Since we are using N_f frames per symbol to convey information, the decision is statically made according to the summation of the MRC outputs for N_f consecutive frames. The estimated bit of the k^{th} information symbol is given as

$$\hat{b}(k) = \begin{cases} 1 & \text{if} \quad \sum_{j=0}^{N_f-1} z_r(k,j) > 0 \\ -1 & \text{if} \quad \sum_{j=0}^{N_f-1} z_r(k,j) \leq 0 \end{cases} . \tag{4-12}$$

Practically, the number of fingers is a design parameter and it is usually chosen as a tradeoff between the complexity of the design and the performance of the receiver. Since the energy is concentrated in the strongest paths, the number of fingers in our approach is restricted by the number of the significant paths in UWB channel, i.e. L_c.

Like the CS-FP-correlator, the complexity in this receiver is mainly in the channel estimation stage. Particularly, it depends on the number of iterations in the MP algorithm. If we consider the maximum number of iteration, the complexity of MP algorithm is approximated to $\mathcal{O}(CL_CT_0)$, where T_0 is the number of MP iterations and C is a constant depends on the dictionary size [Par07b]. However, we do not need to run MP for T_0 iterations. To find the L_c strongest paths, the number of iterations has to be equal to the number of Rake's fingers. The complexity of UWB channels estimation via CS increases linearly with the number of Rake fingers.

4.4 Performance Analysis

Having described CS-channel estimation techniques, this section evaluates these techniques in presence of AWGN. Simulation results are presented to show the level reliability of CS in practical UWB signal detection. The IEEE 802.15.4a channel model is involved for a comparison purpose. As has been proven in Section 3.5, the directional channel model of UWB in [Muq10] well-simulates the measured profiles, thus, the noiseless practical profiles will be generated by the directional model in [Muq10].

The performance of the proposed dictionaries is examined for the CS-FP-Correlator and the CS-Rake receivers. We have selected the first derivative of the Gaussian pulse as the transmitted pulse waveform, $p(t)$, that has been normalized to have unit energy and a pulse duration of 0.34. All dictionary atoms have unit energy likewise.

The transmitted information was modulated using binary-PAM where the information bits, $b(k)$, are independent binary symbols with equal probability. Moreover, the frame

time parameter in equations, (4-10) and (4-11) are set to $T_f = 100$ ns to guarantee no overlapping between consecutive frames. The number of symbols that are used to estimate the channel is $N_f = 25$. All IEEE based profiles and Gaussian reference pulse were sampled before the projection stage by rate of 50 GHz which is higher than the Nyquist rate, meaning, the continuous-time signals are simulated with time resolution of 20 ps. The channel taps are normalized to unit energy for fair comparison.

The performance of our approaches is evaluated over 200 channel realization. For each channel realization 10 000 symbols are transmitted, out of these transmitted symbol $N_p = 2$ symbols are used to estimate the channel parameters. Each pilot symbol is randomly projected and sampled by low rate ADC. The output pilot projections are averaged by N_p and passed to MP algorithm to produce the estimated channel response using one of dictionaries defined in Section 3.4.2. The remaining information symbols $10\,000 - N_p$ are then demodulated by the estimated channel response. Eventually, we average out the obtained 200 BER readings to determine the BER for the considered channel. The evaluation criterion is the average bit error rate as a function of the SNR.

The termination criterion of MP algorithm is set as explained in Section 2.3. The maximum number of MP iterations in CS-FP-Correlator is set to 400 iterations and the target residual energy is set to 1.3 percent of the energy left in the averaged of the projected pilot signals. Since CS-Rake rake receiver utilizes few paths (the strongest ones), it requires less iterations to recover the first strongest paths. The MP algorithm is reset to produce the sparse vector,Θ, after 30 iterations. The MP algorithm is executed once per channel estimation period for both CS-FP-Correlator and CS-Rake receivers.

Figure 4-12 depicts the BER performance of the proposed directional dictionaries. The IEEE profiles generated for indoor residential environment with LOS propagation (CM1). The sampling frequency has been reduced to 30% of the original sampling frequency to be 15 GHz. The number of fingers for CS-Rake is set to 30 fingers. Two pilot symbols are used for channel estimation.

As can be seen in Figure 4-12, the performance of CS-FP-Correlator is optimum for IEEE channel model. CS-Rake has few number of MP iterations in contrast to the CS-FP-Correlator; however its performance is very close to CS-FP-Correlator.

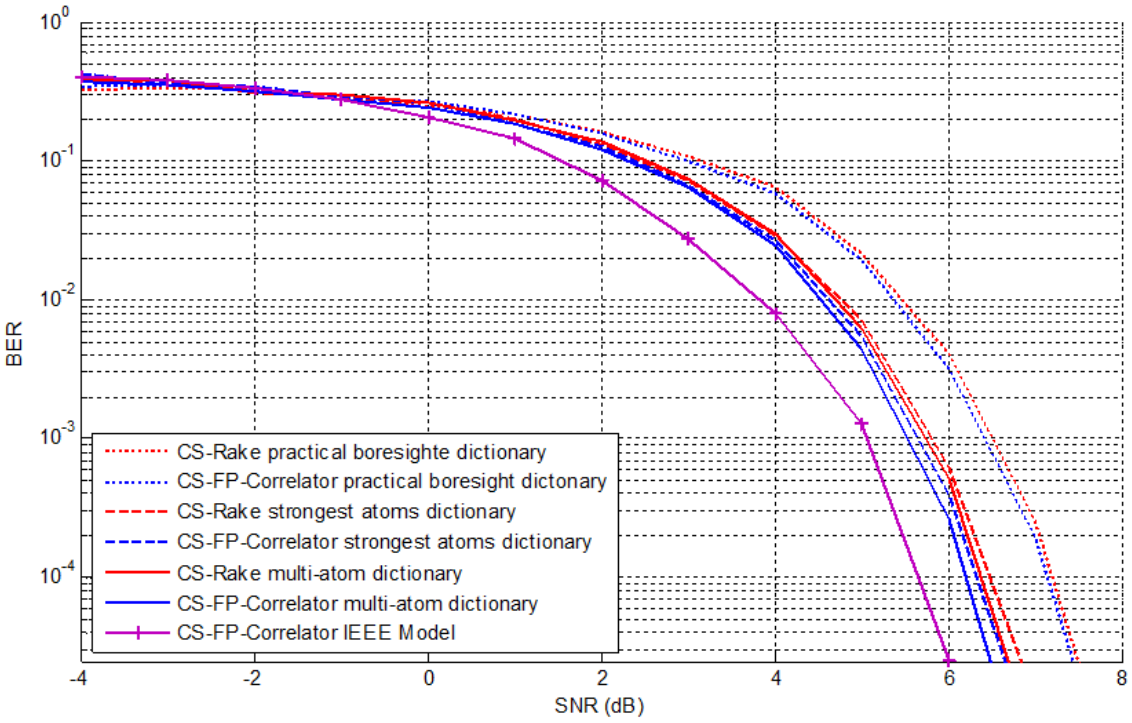

Figure 4-12 Performance of the proposed dictionaries in CS-FP-Correlator and CS-Rake receiver.

The practical channel resulted in about 2 dB degradation in the BER performance as can be seen when comparing the performance of the CS-FP-Correlator over IEEE channel with its performance over a practical channel. About 1 dB can be recovered by using the multi-atom dictionary at the cost of added complexity.

Though it has less complexity in contrast to the multi-atom dictionary, the strongest atom dictionary has a very comparable performance. The strongest atoms dictionary is a trade-off between the relatively-low performance of the boresight dictionary and the complexity of the multi-atom one.

4.5 Chapter summary

In this chapter, we have employed the proposed dictionaries in UWB channel estimation. Two receivers were implemented as depicted in Figure 4-13, the major difference between the CS-FP-Correlator receiver and the Rake receiver is that number of iterations, T_0. In CS-Rake concentrates on only the strongest paths, L_c, and makes use of their energy in the detection stage. The CS-FP-Correlator requires more iteration.

The conclusions of this chapter can be summarized as follows:

- The practical channel resulted in about 2 dB degradation in the BER performance in contrast to IEEE channel model
- About 1 dB can be recovered by using the multi-atom dictionary at the cost of added complexity.
- The strongest atoms dictionary is a trade-off between the relatively-low performance of the boresight dictionary and the complexity of the multi-atom one.

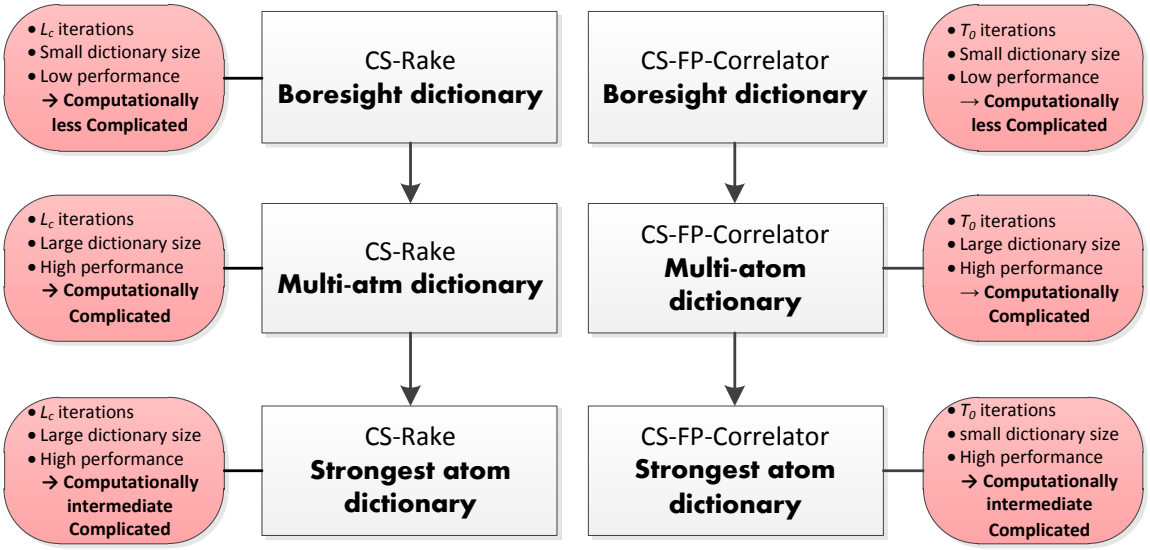

Figure 4-13 Receivers flowchart.

CHAPTER 5

5 CONCLUSION AND FUTURE WORK

This research has shed some light on the implementation of CS to UWB channels and evaluated its performance from a practical point of view. This chapter concludes the work of this thesis and gives an idea about the potential research that could be pursued.

5.1 Conclusion

In this work, we have established new dictionaries in which the practical UWB signals are sparse and have also shown that using such domains enhance the performance of CS for practical channels.

It was shown in Chapter 1 that due to the UWB receiver's demand for a very high sampling rate, its design is challenging, complicated and limits power resources.

In the second chapter, CS was applied to the IEEE 802.15.4a model which allowed a significant reduction in the sampling rate. By means of MP algorithms, the sampling frequency was reduced by factor of 0.3 and we were still able to recover the signal with an error which does not exceed 5 percent of the signal energy. The IEEE model does not account for pulse dispersion and antenna directionality, hence, the performance of CS in the practical channels is not guaranteed.

Chapter 3 aimed at finding a sparsity domain that would include the impact of realistic channel and antenna effects. To do so, we have explored different practical scenarios based on the antenna responses. The measured profiles showed that the realistic UWB signals cannot be considered sparse in time domain. Moreover, building a dictionary based on the transmitted pulse can be misleading. We made use of a boresight signal to build the first practical spare domain. Simulation showed that the signal reconstruction enhanced and the error was reduced by a factor of 0.78 from the Gaussian pulse-based dictionary.

The directivity of the antenna plays an important factor in the synthesis of UWB signals; hence, to guarantee that the antenna effects are included in the sparse domain, we exploited the antenna response at different angles to design a multi atom directional dictionary. This method proved to be more efficient compared to the boresight dictionary. The reconstruction error was less by a factor of 0.8 from the boresight dictionary error.

Complexity is a big concern in multi atom directional dictionary. Since the size of the dictionary is the cause of this problem, we can choose the atoms with the strongest contributions in the dictionary to reduce its size. The strongest atoms dictionary is able to tolerate the changing in pulse shape and also reduces the size of the directional dictionary.

Apart from the pulse shape deformation, a variable-width atoms dictionary accounted for the temporal dispersion. This dictionary has an intermediate performance between those of the directional and boresight dictionaries. The complexity is reduced since the size of the dictionary lessens as the atom widens.

In Chapter 4, we have employed the proposed approaches to estimate the practical UWB channels. CS was used to estimate the practical channels. The estimated channel was used to demodulate the received data within two receivers. CS-FP-correlator demodulates the data by correlating the received frame with the CS-estimated frame. CS-Rake receiver takes advantage MP algorithm to exploit the energy available in the multipath.

In CS-FP-correlator the MP algorithm keeps running for the maximum number of iterations, T_0. In the other hand, CS-Rake concentrates only on the strongest paths, L_c, and makes use of their energy in the detection stage. The reduction in the number of iterations and the processing requirements is achieved at limited reduction in the performance.

The bit error rate performance of the CS based channel estimation for the different proposed dictionaries was evaluated as a function of signal to noise ratio. It is shown that CS based on the strongest atoms has an excellent performance at relatively low complexity.

5.2 Future work

The work we have presented in this thesis is a node with many potential branches. The most important in such branches are:

- Since the directive impulse response of the antenna varies from one antenna to another, different antennas can be examined.
- The reflection of incident wave depends on the reflector materials, and so, an adaptive dictionary can be derived to include more physical effects. Where a specific training symbols can be employed to update the dictionary atoms.

- CS-signal reconstruction can be enhanced by increasing the incoherence between the measurement matrix and the sparsity domain.
- NBI mitigation is a field where UWB receivers encounter various challenges. Since NBI falls in known frequency band, a directional dictionary which jointly mitigates NBI can be designed.
- The impact of varying different parameters like the number of fingers in the Rake receiver can be further examined.

APPENDIX

Table 2 Abbreviations

Abbreviation	Stand for
ADC	Analog to digital converter
AWG	Additive White Gaussian
AWGN	Additive White Gaussian noise
BCS	Bayesian compressive sensing
BER	Bit Error Rate
BP	Basis Pursuit
BPF	Band pass Filter
CM1	Channel Model 1
CM2	Channel Model 2
CS	Compressive Sensing
CS-FP-Correlator	Compressive Sensing Full-Profile Correlator
CS-Rake	Compressive Sensing Rake
DSP	Digital signal processing
FOMP	Fast Orthogonal Matching Pursuit
IEEE	Institute of Electrical and Electronics Engineers
IEEE 802.15.4a	A Standard which specifies the physical layer and media access control for wireless networks
IR-UWB	Impulse Radio Ultra Wideband
LOS	Line of Sight
MC-UWB	Multicarrier Ultra wideband
MP	Matching Pursuit
MRC	Maximum Ratio Combining
MSE	Mean Square Error
NBI	Narrow Band Interference
NLOS	Non Line of Sight
OMP	Orthogonal Matching Pursuit
PAM	Pulse Amplitude Modulation
PAM	Pulse Amplitude Modulation
SNR	Signal to Noise Ratio
TDOA	Time Difference of Arrival
TEM	Transverse Electric and Magnetic
ToA	Time of Arrival
UWB	Ultra Wideband

Table 3 Indicated variables

Variable	Indication
α_ℓ	Tap gain of ℓ^{th}path
B_f	fractional bandwidth
Δ	The amount of shift between consecutive atom in Ψ
ϵ	The ratio of the residual energy to the measurements energy
e_t	Residual in the measurement vector after t iterations
f_C	center frequency
f_H	Upper cutoff frequency
f_l	Lower cutoff frequency
f_s	Sampling Frequency
X	Signal to be reconstructed
$h(.)$	The impulse response of the channel
k	Number of the binary information (Symbol)
L	Number of the propagation paths
L_c	Number of the strongest paths
L_r	Number of fingers in Rake receiver
M	The number of measurements.
$\sim N(0,1)$	Generate a random number by normal distribution
N	Number of samples in UWB signal
N_b	Number of symbol per frame
N_f	Number of pulses in one symbol
N_p	Number of pilot symbols
N_s	Number of symbols where the channel is invariant during them
N_w	Number of the pilot frames
$p(t)$	Monocycle Gaussian Pulse
$p(t)$	Transmitted Pulse

Variable	Indication
Φ	Measurement (Sensing) Matrix
ψ_n	The n^{th} column in Ψ
Ψ	Dictionary where the UWB signal supposed to be sparse in, has dimensions of $M \times N$.
r_x'	Reconstructed Received Signal
r_x	Received UWB Signal
T_0	Maximum number of iteration in MP algorithm
τ_l	Tap delay of ℓ^{th}path
T_f	Frame time
Θ	The sparse vector that represent the signal in Ψ
T_p	Pulse duration: $T_p \ll T_f$
T_s	Symbol duration
T_w	Time duration of the tailor waveforms
V	Holographic dictionary
y	Measurements vector

REFERENCES

[Ahm04] A. Bayram, *A Study of Indoor Ultra-wideband Propagation Measurement and Characterization*. Virginia Polytechnic Institute and State University, Master Thesis, 2004.

[Alo99] M. .-S. Alouini and M. K. Simon, "Performance of coherent receivers with hybrid SC/MRC over Nakagami-m ," *Vehicular Technology, IEEE Transactions on*, vol. 48, pp. 1155-1164, Jul. 1999.

[Bar07] R. G. Baraniuk, "Compressive Sensing (lecture notes)," *IEEE SIGNAL PROCESSING MAGAZINE*, p. 4, 2007.

[Ben06] M.-G. D. Benedetto, et al., Eds., *UWB Communication Systems A Cmperhensive Overview*. Hindawi Publishing Corporation, 2006.

[Can06] E. J. Candes, J. Romberg, and T. Tao, "Robust uncertainty principles: exact signal reconstruction from highly incomplete frequency information," *Information Theory, IEEE Transactions on*, vol. 52, no. 2, pp. 489-509, 2006.

[Can08] E. J. Candès and M. B. Wakin, "An Introduction To Compressive Sampling," *IEEE Signal Processing Magazine*, 2008.

[Che99] S. S. Chen, D. L. Donoho, and M. A. Saunders, "Atomic decomposition by basis pursuit," *SIAM Journalon Scientific Computing*, pp. 33-31, 1999.

[Dep11] D. Yang, H. Li, G. D. Peterson, and A. Fathy, "Compressive sensing TDOA for UWB positioning systems," *Radio and Wireless Symposium (RWS),* , pp. 194-197,16-19, Jan. 2011.

[Don06] D. L. Donoho, "Compressed Sensing," *IEEE Transaction on information theory*, vol. 52, pp. 1289-1306, Apr. 2006.

[Dua05] M. F. Duarte, M. B. Wakin, and R. G. Baraniuk, "Fast Reconstruction of Piecewise Smooth Signals from Incoherent Projections," *SPIE Wavelets XI*, 2005.

[Dua05] M. F. Duarte, M. B. Wakin, and R. G. Baraniuk, "Fast Reconstruction of

Piecewise Smooth Signals from Incoherent Projections," *SPIE Wavelets XI*, 2005.

[Guv08] I. Guvenc, S. Gezici, and Z. Sahinoglu, "Ultra-wideband range estimation: Theoretical limits and Practical Algorithms," in *Ultra-Wideband, 2008. ICUWB 2008. IEEE International Conference on*, 2008, pp. 93-96.

[Has93] H. Hashemi, "Impulse response modeling of indoor radio propagation channels," *Selected Areas in Communications, IEEE Journal on*, vol. 11 ,, no. Sep 1993, pp. 967-978, 1993.

[Hir03] W. Hirt and D. Porcino, "Ultra-wideband radio technology: Potential and challenges ahead," vol. 41, no. 7, pp. 66-74, 2003.

[Hua10] H. Yu and S. Guo, "Pre-filtering Ultra-wideband Channel Estimation Based on Compressed Sensing," *International Conference on Communications and Mobile Computing (CMC), 2010*, vol. 3, pp. 110-114,12-14, Apr. 2010.

[Krs06] S. Krstulovic and R. Gribonval, "Mptk: Matching Pursuit Made Tractable," *IEEE International Conference on Acoustics, Speech and Signal Processing,*, vol. 3, pp. III,14-19, May 2006.

[La05] C. La and M. Do, "Signal reconstruction using sparse tree representations,," *in Proc. SPIE Wavelets XI,*, 2005.

[Lam10] L. Lampe and K. Witrisal, "Challenges and recent advances in IR-UWB system design," in *Circuits and Systems (ISCAS), Proceedings of 2010 IEEE International Symposium on*, 2010, pp. 3288-3291.

[Law78] R. A. Lawton and A. R. Ondrejka, *Antennas and Associated Time Domain Range Measurement of Impulsive Fields*. NBS Technical Note 1008, Boulder, Colorado 80303,: U.S. Department of Commerce/ National Bureau of Standards,, 1978.

[Le10] T. N. Le, J. Kim, and Y. Shin, "An improved ToA estimation in compressed sensing-based UWB systems," in *Communication Systems (ICCS), 2010 IEEE International Conference on*, 2010, pp. 249-253.

[Lei10] L. Shi, Z. Zhou, L. Tang, H. Yao, and J. Zhang, "Ultra-wideband channel

estimation based on Bayesian compressive sensing," *International Symposium on Communications and Information Technologies (ISCIT)*, pp. 779-782,26-29, Oct. 2010.

[Lic04] S. Licul, *Ultra-wideband Antenna characterization and Mesurements* . Blacksburg, Virginia : Ph.D. dissertation, , 2004.

[Liu04b] L. Yang and G. B. Giannakis, "Optimal Pilot Waveform Assisted Modulation for Ultrawideband Communications," *IEEE Transactions on Wireless Communications*, vol. 3, pp. 1236-1249, Jul. 2004.

[Lot02] V. Lottici, A. D'Andrea, and U. Mengali, "Channel estimation for ultra-wideband communications," *Selected Areas in Communications, IEEE Journal on*, vol. 20, 2002.

[May11] R. A. M. Company. (2011, Nov.) RAMayes . [Online]. http://www.ramayes.com/Snap_Mount_Antennas.htm

[Mdu05] M. W. a. R. B. M. Duarte, "Fast reconstruction of piecewise smooth signals from random projections,"," *Available: http://spars05.irisa.fr/ACTES/TS5-3.pdf* , 2005.

[Men09] J. Meng, et al., "Sampling rate reduction for 60 GHz UWB communication using compressive sensing," in *Conference Record of the Forty-Third Asilomar Conference on Signals, Systems and Computers*, 2009, pp. 1125-1129.

[Mol04] A. F. Molisch, K. Balakrishnan, C.-C. Chong, S. Emami, and Andrew Fort, "IEEE 802.15.4a Channel Model—Final Repor," Available: http://www.ieee802.org/15/pub/TG4a.html, 2004.

[Mol06] A. F. Molisch, et al., "A Comprehensive Standardized Model for Ultrawideband Propagation Channels," *Antennas and Propagation, IEEE Transactions on* ,, vol. 54, pp. 3151-3166, Nov. 2006.

[Muq02] A. Muqaibel, A. Safaai-Jazi, B. Woerner, and S. Riad, "UWB Channel Impulse Response Characterization Using Deconvolution Techniques," *Circuits and Systems, MWSCAS*, vol. 3, pp. 605-608, Aug. 2002.

[Muq03] A. H. Muqaibel, *Characterization of Ultra Wideband Communication*

Channels, PhD Dissertation. Vrginia Tech: Depatment of Electrical and Computer Engineering, 2003.

[Muq06] A. Muqaibel, A. Safaai-Jazi, A. Attiya, B. Woerner, and S. Riad, "Path-loss and time dispersion parameters for indoor UWB propagation,," *Wireless Communications, IEEE Transactions on*, vol. 5, pp. 550-559, Mar. 2006.

[Muq07] A. H. Muqaibel and U. M. Johar, "UWB Multipath Simulator based on TEM Horn Antenna," *The 2nd International Conference on Wireless Broadband and Ultra Wideband Communications*, pp. 27-30, Aug. 2007.

[Muq08] A. Muqaibel and A. Safaai-Jazi, "Characterization of wall dispersive and attenuative effects on UWB radar signals,," *Journal of the Franklin Institute,*, vol. 345, pp. 640-658, Sep. 2008.

[Muq10] A. H. Muqaibel, "Directional modelling of ultra wideband communication channels," *Communications, IET*, vol. 4, pp. 51-62, Jan. 2010.

[Oka09] A. Oka and L. Lampe, "A compressed sensing receiver for UWB impulse radio in bursty applications like wireless sensor networks," *Physical Communication 2*, 2009.

[Oka09] A. Oka and L. Lampe, "Compressed Sensing Reception of Bursty UWB Impulse Radio is Robust to Narrow-Band Interference," in *Global Telecommunications Conference, IEEE*, 2009.

[Par07] J. L. Paredes, G. R. Arce, and Z. Wang, "Ultra-Wideband Compressed Sensing: Channel Estimation," *IEEE Journal of Selected Topics in Signal Processing*, vol. 1, pp. 383-396, 2007.

[Par07b] J. L. Paredes, G. R. Arce, and Z. Wang, "Compressed Sensing for Ultrawideband Impulse Radio," in *ICASSP 2007. IEEE International Conference on Acoustics, Speech and Signal Processing*, vol. 3, pp. III-553-III-556,15-20.

[Qiu02] Robert C. Qiu, "A Study of the Ultra-Wideband Wireless Propagation Channel and Optimum UWB Receiver Design," *IEEE JOURNAL ON SELECTED AREAS IN COMMUNICATIONS*, vol. 20, Dec. 2002.

[Qiu05] R. C. Qiu, H. Liu, and X. Shen, "Ultra-wideband for multiple access communications," *Communications Magazine, IEEE* ,, vol. 43, pp. 80-87, Feb. 2005.

[Ree05] J. H. Reed , et al., *An Introduction to Ultra Wideband Communication Systems*, J. H. Reed , Ed. Prentice Hall PTR, 2005.

[Sal87] A. A. M. Saleh and R. Valenzuela, "A Statistical Model for Indoor Multipath Propagation," *Selected Areas in Communications, IEEE Journal on*, vol. 5, pp. 128-137.

[Shi08] G. Shi, et al., "UWB Echo Signal Detection With Ultra-Low Rate Sampling Based on Compressed Sensing," *IEEE Transactions on Circuits and Systems II: Express Briefs*, vol. 4, no. 55, pp. 379-383, Apr. 2008.

[Spe00] S. Q., J. B., J. M., and S. A., "Modelingthe statistical time and angle of arrival characteristics of an indoor multipath channel," *IEEE J. Sel. Areas Commun.*, p. 347–360, 2000.

[Tro07] J. Tropp and A. C. Gilbert, "Signal recovery from partial information via orthogonalmatching pursuit," *IEEE Trans. Inform. Theory*, pp. 4655-4666, 2007.

[Tro07b] J. A. Tropp and A. C. Gilbert, "Signal Recovery From Random Measurements Via Orthogonal Matching Pursuit," *Information Theory, IEEE Transactions on*, vol. 53, pp. 4655-4666,, Dec. 2007.

[Wan07] Z. Wang, G. R. Arce, J. L. Paredes, and B. M. Sadler, "Compressed Detection For Ultra-wideband Impulse Radio," in *Acoustics, Speech and Signal Processing, 2007. ICASSP 2007. IEEE International Conference on*, vol. 3, 2007, pp. III-553-III-556.

[Wan07b] Z. Wang , G. R. Arce, B. M. Sadler, B.M. , J. L. Paredes, J.L, and X. Ma, "Compressed Detection for Pilot Assisted Ultra-Wideband Impulse Radio," in *ICUWB 2007. IEEE International Conference on*, 2007, pp. 393-398.

[Wan08] Z. Wang, et al., "Compressed UWB signal detection with narrowband interference mitigation," in *Ultra-Wideband, 2008. ICUWB 2008. IEEE*

International Conference on, 2008, pp. 157-160,10-12.

[Woo08] S. Wood and R. Aiello, *Essintial of UWB*. Cambridge University Press, 2008.

[Wu06] L. Wu, X. Wu, and Z. Tian, "Asymptotically optimal UWB receivers with noisy templates: design and comparison with RAKE," *Selected Areas in Communications, IEEE Journal on*, vol. 24, pp. 808-814, Apr. 2006.

[Yan04] L. Yang and G. B. Giannakis, "Ultra-Wideband Communications An Idea Whose Time Has Come," *IEEE Signal processing Magazine*, pp. 26-54, Nov. 2004.

[Zha10] Z. Xian-yu, L. Yu-lin, Z. Jian-xin, H. Ji-wei, and W. Kai, "Random filter based Ultra-wideband channel estimation," *International Conference on Future Computer and Communication (ICFCC)*, pp. V2-399-V2-403, May 2010.

[Zha93] S. Mallat and Z. Zhang, "Matching pursuits with time-frequency dictionaries," *IEEE Trans. Signal Process*, vol. 41, p. 3397–3415, Dec. 1993.

VITAE

- Mohammad Tamim Alkhodary.
- Born in Taif, Saudi Arabia on November 1985.
- Revived Bachelor degree in Communication Engineering from University of science and Technology, Sana'a, Yemen, in August 2008.
- Joined the Electrical Engineering Department as a Research Assistant at King Fahd University of Petroleum and Minerals in February, 2009.
- Email: mtamim@kfupm.edu.sa

  mohamd2020@hotmail.com


الحمد لله رب العالمين